Elsevier Editorial System(tm) for Quaternary Science Reviews

Manuscript Draft

Manuscript Number: JQSR-D-16-00430R1

Title: Geomorphic and shallow-acoustic investigation of an Antarctic Peninsula fjord system using high-resolution ROV and shipboard geophysical observations: ice dynamics and behaviour since the Last Glacial Maximum

Article Type: Research paper

Keywords: Antarctic Peninsula; Fjord systems; Last Glacial Maximum; Glacial sedimentary processes; Geomorphology; ROV-derived bathymetry

Corresponding Author: Dr. Marga Garcia,

Corresponding Author's Institution: Instituto Andaluz de Ciencias de la Tierra (CSIC-UGR)

First Author: Marga Garcia

Order of Authors: Marga Garcia; Julian A Dowdeswell; Riko Noormets; Kelly A Hogan; Jeffrey Evans; Colm Ó Cofaigh; Robert D Larter

Abstract: Detailed bathymetric and sub-bottom acoustic observations in Bourgeois Fjord (Marguerite Bay, Antarctic Peninsula) provide evidence on sedimentary processes and glacier dynamics during the last glacial cycle. Submarine landforms observed in the 50 km-long fjord, from the margins of modern tidewater glaciers to the now ice-distal Marguerite Bay, are described and interpreted. The landforms are grouped into four morpho-sedimentary systems: (i) glacial advance and full-glacial; (ii) subglacial and ice-marginal meltwater; (iii) glacial retreat and neoglaciation; and (iv) Holocene mass-wasting. These morpho-sedimentary systems have been integrated with morphological studies of the Marguerite Bay continental shelf and analysed in terms of the specific sedimentary processes and/or stages of the glacial cycle. They demonstrate the action of an ice-sheet outlet glacier that produced drumlins and crag-and-tail features in the main and outer fjord. Meltwater processes eroded bedrock channels and ponds infilled by fine-grained sediments. Following the last deglaciation of the fjord at about 9 000 yr BP, subsequent Holocene neoglacial activity involved minor readvances of a tidewater glacier terminus in Blind Bay. Recent stillstands and/or minor readvances are inferred from the presence of a major transverse moraine that indicates grounded ice stabilization, probably during the Little Ice Age, and a series of smaller landforms that reveal intermittent minor readvances. Mass-wasting processes also affected the walls of the fjord and produced scars and fan-shaped deposits during the Holocene. Glacier-terminus changes during the last six decades, derived from satellite images and aerial photographs, reveal variable behaviour of adjacent tidewater glaciers. The smaller glaciers show the most marked recent retreat, influenced by regional physiography and catchment-area size.

Granada, 21th October 2016

Quaternary Science Reviews
Editorial Office

Dear Editors,

Please find enclosed the revised manuscript and figures for the Research Paper: *Geomorphic and shallow-acoustic investigation of an Antarctic Peninsula fjord system using high-resolution ROV and shipboard geophysical observations: ice dynamics and behaviour since the Last Glacial Maximum*, by Marga Garcia, Julian A. Dowdeswell, Riko Noormets, Kelly A. Hogan, Jeffrey Evans, Colm Ó Cofaigh and Rob D. Larter.

We enclose:

- JQSR-D-16-00430_Revision_Notes.docx
- JQSR-D-16-00430_ReviewedManuscript_ChangesMarked.docx
- JQSR-D-16-00430_ReviewedManuscript.docx
- Figures 1 and 7 (TIF format)

  Should the manuscript be accepted, all figures should be printed in greyscale.

We acknowledge the kind comments of the Reviewers and all their corrections and suggestions and we hope the revised article is worth publishing in Quaternary Science Reviews.

Yours sincerely,

Marga García

Instituto Andaluz de Ciencias de la Tierra (CSIC-UGR)

Geomorphic and shallow-acoustic investigation of an Antarctic Peninsula fjord system using high-resolution ROV and shipboard geophysical observations: ice dynamics and behaviour since the Last Glacial Maximum

Marga García[1,2*], J.A. Dowdeswell[2], R. Noormets[3], K.A. Hogan[1,4], J. Evans[5], C. Ó Cofaigh[6], R.D. Larter[4]

[1] Instituto Andaluz de Ciencias de la Tierra, CSIC-University of Granada. Avda. de las Palmeras, 4. 18100, Armilla, Spain.

[2] Scott Polar Research Institute, University of Cambridge, Lensfield Road, Cambridge CB2 1ER, UK

[3] Departments of Arctic Geology and Arctic Geophysics, University Centre in Svalbard, 9170 Longyearbyen, Norway

[4] British Antarctic Survey, Natural Environment Research Council, High Cross, Madingley Road, Cambridge CB3 0ET, UK

[5] Department of Geography, University of Loughborough, Loughborough LE11 3TU, UK

[6] Department of Geography, Durham University, Durham DH1 3LE, UK

[*] Corresponding author. Email address: m.garcia@csic.es; marguita.garcia@gmail.com.

ABSTRACT

Detailed bathymetric and sub-bottom acoustic observations in Bourgeois Fjord (Marguerite Bay, Antarctic Peninsula) provide evidence on sedimentary processes and glacier dynamics during the last glacial cycle. Submarine landforms observed in the 50 km-long fjord, from the margins of modern tidewater glaciers to the now ice-distal Marguerite Bay, are described and interpreted. The landforms are grouped into four morpho-sedimentary systems: (i) glacial advance and full-glacial; (ii) subglacial and ice-marginal meltwater; (iii) glacial retreat and neoglaciation; and (iv) Holocene mass-wasting. These morpho-sedimentary systems have been integrated with morphological studies of the Marguerite Bay continental shelf and analysed in terms of the specific sedimentary processes and/or stages of the glacial cycle. They demonstrate the action of an ice-sheet outlet glacier that produced drumlins and crag-and-tail features in the main and outer fjord. Meltwater processes eroded bedrock channels and ponds infilled by fine-grained sediments. Following the last deglaciation of the fjord at about 9 000 yr BP, subsequent Holocene neoglacial activity involved minor readvances of a tidewater glacier terminus in Blind Bay. Recent stillstands and/or minor readvances are inferred from the presence of a major transverse moraine that indicates grounded ice stabilization, probably during the Little Ice Age, and a series of smaller

landforms that reveal intermittent minor readvances. Mass-wasting processes also affected the walls of the fjord and produced scars and fan-shaped deposits during the Holocene. Glacier-terminus changes during the last six decades, derived from satellite images and aerial photographs, reveal variable behaviour of adjacent tidewater glaciers. The smaller glaciers show the most marked recent retreat, influenced by regional physiography and catchment-area size.

Keywords: Antarctic Peninsula; Fjord systems; Last Glacial Maximum; Glacial sedimentary processes; Geomorphology; ROV-derived bathymetry.

1. Introduction

The geomorphology of glaciated continental margins contains records of environmental history and of the geological processes shaping the seafloor (e.g. Anderson, 1999; Ó Cofaigh et al., 2002; Ottesen et al., 2005). The increasing resolution of geophysical and geological datasets acquired from high-latitude shelves and fjords is providing new insights into the major processes occurring during the last full-glacial and deglacial periods in particular (Dowdeswell and Ó Cofaigh, 2002; Jakobsson et al., 2008). The high sensitivity of the Antarctic Peninsula Ice Sheet (APIS) results from the regional amplification of global warming (Vaughan et al., 2003), and the response mechanisms involve factors such as oceanography, atmospheric circulation and regional air-sea-ice feedback (Bentley et al., 2010). The Antarctic Peninsula has experienced rapid warming in the last 600 years, and an unusually high warming trend over the past century, resulting in ice-shelf vulnerability along the Peninsula with its potential impact on global climate (Mulvaney et al., 2012). The assessment of models for predicting the future evolution of ice masses requires a knowledge of past ice dynamics and, in particular, studies of the styles of deglaciation for the last glacial cycle, that depend on a complex interplay between global and local factors (Livingstone et al., 2012). Mass balance models for outlet glaciers highlight the influence of glacier dynamics on climate and global sea-level (Kaser et al., 2006) and, in the case of tidewater glaciers, processes involving iceberg discharge are particularly important but poorly known contributors to mass loss from ice caps (Dowdeswell et al., 2008a; Radić and Hock, 2011).

The complexity of glacial-marine systems has been revealed by numerous investigations of the geomorphology and shallow stratigraphy of Arctic fjords (e.g. Griffith and Anderson, 1989; Domack and Ishman, 1993; Gilbert et al., 2002; Ottesen and Dowdeswell, 2006, 2009; Ottesen et al., 2007, 2008), allowing detailed palaeoenvironmental reconstructions of the last glacial cycle, whereas high-resolution studies from Antarctic fjords are still relatively scarce (Griffith and Anderson, 1989; Anderson, 1999; Rodrigo et al., 2016). In Marguerite Bay, western Antarctic Peninsula, research has focused on past ice-stream dynamics along a glacial trough that occupies almost 400 km across the continental shelf

(Dowdeswell et al., 2004a; Ó Cofaigh et al., 2005; Livingstone et al., 2013, 2016). However, a detailed study of the most proximal areas is still needed in order to understand the complete system and, in particular, the transition from the outlet glaciers near the coast to the large ice-streams on the continental shelf. This paper investigates the submarine landform record in Bourgeois Fjord, providing evidence for the glacial dynamics in the area from the termini of tidewater glaciers to the more open marine environment of Marguerite Bay. The area is characterized today by the presence of relatively small outlet glaciers draining Graham Land, but was covered by an extensive APIS with grounding lines reaching the continental-shelf edge during the Last Glacial Maximum (LGM) (e.g. Pudsey et al., 1994; Bentley and Anderson, 1998; Anderson, 1999; Anderson et al., 2002; Dowdeswell et al., 2004a; Ó Cofaigh et al., 2014). The paper is focused on the processes and patterns shaping the seafloor during the last glacial cycle in order to analyse the glacial and deglacial dynamics and the factors influencing them, and to provide an integrated view of the processes affecting the complete system, from the fjord to the outer continental shelf. This work analyses sedimentary processes at different spatial and temporal scales: the last glacial cycle affecting the entire system from the fjord to the continental shelf-edge, the Little Ice Age (LIA) event recorded in the inner areas of Bourgeois Fjord (Blind Bay), and recent patterns of tidewater glaciers retreat caused by rapid regional warming during the last century.

2. Geological and ice-sheet chronological framework

Bourgeois Fjord is one of the many relatively narrow and steep-sided fjords that connect tidewater glaciers draining from the APIS in Graham Land with Marguerite Bay and the Pacific Southern Ocean margin (Kennedy and Anderson, 1989; Anderson, 1999) (Fig. 1). The Antarctic Ice Sheet expanded across continental shelves all around the Antarctic Peninsula during the LGM and grew to fill Bourgeois Fjord and spread across the Marguerite Bay continental shelf with fast-flowing ice streams reaching the shelf edge (Pudsey et al., 1994; Bentley and Anderson, 1998; Anderson et al., 2002; Dowdeswell et al., 2004a; Amblas et al., 2006). Evidence of the last glacial ice stream dynamics has been described along the Marguerite Trough which drained the Marguerite Bay palaeo-ice stream across the continental shelf. Large isolated basins in the inner shelf are characterized by crag-and-tails in areas with exposed bedrock that have similar dimensions and orientations to mega-scale glacial lineations (MSGLs) identified in the neighbouring areas (Livingstone et al., 2013, 2016). On the middle shelf, a basinward succession of landforms has been identified, from deep roughly parallel gouges and subglacial meltwater channels incised into crystalline bedrock, to streamlined hills, whalebacks and MSGLs (Livingstone et al., 2013, 2016). The mid-outer shelf displays streamlined bedrock outcrops and GZWs (Ó Cofaigh et al., 2005). The outer shelf is characterized by MGSLs with a N-NW trend that are overprinted by iceberg ploughmarks close to the continental-shelf edge (Dowdeswell et al., 2004a; Ó Cofaigh et al., 2005;

Livingstone et al., 2013, 2016). Numerous gullies occur on the upper slope. Those located on the sides of the palaeo-ice stream mouth are incised directly at the shelf edge whereas those offshore of the trough mouth are incised on the upper continental slope (Dowdeswell et al., 2004a; Noormets et al., 2009; Livingstone et al., 2013).

Morphological, sedimentological and geochronological analysis of the landforms identified on the continental shelf has revealed that the LGM occurred around 18 000 yr BP (e.g. Kennedy and Anderson, 1989; Heroy and Anderson, 2007; Ó Cofaigh et al., 2014) and ice-sheet retreat began on the outer shelf of Marguerite Bay by 14 000 cal yr BP (Bentley et al., 2005; Heroy and Anderson, 2007; Kilfeather et al, 2011; Ó Cofaigh et al., 2014). A first stage of rapid retreat coincided with the sea-level rise of Meltwater Pulse 1a (Heroy and Anderson, 2007; Kilfeather et al., 2011). The ice sheet remained grounded on the inner shelf and an ice shelf formed beyond the grounding-zone at that time. Retreat then became more episodic (Ó Cofaigh et al., 2014); the ice shelf broke-up and the calving front retreated slowly from ca. 13.2 to 12.5 ka B.P. across the outer and mid-shelf, probably linked to an incursion of Weddell Sea Transitional Water onto the shelf. Finally, ice retreated into the inner bay from 9.3 ka B.P. (Kilfeather et al, 2011), and this retreat is interpreted to have been rapid (Allen et al., 2010; Ó Cofaigh et al., 2014). A two-step deglacial model in Marguerite Bay has been proposed, with a first stage related to rapid sea-level rise during Meltwater Pulse 1-a at 14.2 ka BP, when grounded ice retreated to the area coincident with the transition from crystalline bedrock to soft sedimentary substrate, and a second phase shortly before 9.6 ka, when the intrusion of Circumpolar Deep Water provoked the rapid thinning of the ice cover (Bentley et al., 2011). During the Holocene sedimentation in Marguerite Bay has been linked to oceanographic variability (Peck et al., 2015). During the early Holocene incursions of the warm upper circumpolar deep water (UCDW) led to extensive glacial melt and limited sea ice, from 9.7 to 7.0 ka BP. The influence of this water mass decreased through the mid Holocene, with seasons of persistent sea ice by 4.2 ka BP followed by a succession of episodic incursions of UCDW during the late Holocene (Peck et al., 2015). Open-marine conditions existed between 8 000 and 2 700 14C yr BP, with a climatic optimum between 4 200 and 2 700 yr BP in Lallemand Fjord, 16 km north of Bourgeois Fjord (Fig. 1B; Shevenell et al., 1996). A modest glacier advance between 2 850 and 2 500 cal. yr BP has been described in Neny Fjord, which drains into Marguerite Bay south of Bourgeois Fjord (Fig. 1B; Allen et al., 2010). The Little Ice Age has been recorded in several areas of the Antarctic Peninsula. Neoglacial cold events associated with the LIA produced an ice-shelf advance approximately 400 years ago in Lallemand Fjord (Shevenell et al., 1996). Sedimentological studies in Barilari Bay (Graham Land) constrained this event to ca. 730-82 cal. yr B.P. by, and its effect has been compared with other records, showing that the LIA was regionally synchronous in the Pacific and Atlantic southern sectors (Christ et al., 2014). Recently, grounded ice

cover in the Marguerite Bay region has experienced a general retreat since the late 1920s with the largest observed changes from glaciers with small drainage basins (Fox and Cooper, 1998). This general retreat is related to the 'recent rapid regional warming' described for the Antarctic Peninsula over the past half-century (Vaughan et al., 2003).

3. Datasets and methodology

Datasets for this study were acquired during cruise JR-157 of RRS *James Clark Ross* (JCR) in 2007 (Fig. 1). They include observations from both a Remotely-Operated Vehicle (ROV), *Isis*, and from hull-mounted instruments on the JCR. The ROV was configured to deploy several types of instrument. An MS-2000 multibeam swath-bathymetry system was fitted to the *Isis* ROV and flown about 20 m above the seafloor at speeds of less than 0.5 knots, giving a swath width of about 60 m. The multibeam system operated at a frequency of 200 kHz, with an equidistant beam configuration of 128 beams giving a swath width of 120°. Horizontal resolution is better than 0.5 m (Dowdeswell et al., 2008b). An *Isis* ROV dive was carried out along a transect close to the tidewater ice cliffs of Forel Glacier in Blind Bay at the head of the main Bourgeois Fjord (Fig. 1). Three parallel navigation lines were acquired, resulting in a high-resolution bathymetric mosaic of approximately 0.6 km-width. During the *Isis* dive, video records and high-resolution photographs of the seafloor were taken using *Pegasus* and *Scorpio* cameras, when the ROV was flown at about 0.6 m above the seafloor at a speed of approximately 20 cm s^{-1}. 10 cm-spaced laser beams were used in all cases to provide a scale for the imagery.

Hull–mounted equipment on board the JCR included an EM-120 *Kongsberg-Simrad* multibeam swath-bathymetry system with 191 beams displaying a maximum swath width of 150°, operating at frequencies between 11.25 and 12.75 kHz and enabling generation of grids with a horizontal resolution averaging 20 m. Navigation data were obtained from GPS and data processing and production of maps were performed with *Caris*, *Mirone* and *Fledermaus* software. The TOPAS PS 018 system operated with a primary frequency of 18 kHz and a secondary frequency in the range of 0.5-5 kHz was used to obtain sub-bottom profiles. It provides a vertical resolution better than 1 m. Data were processed with TOPAS software.

Glacier-terminus change information and glacier-catchment areas were calculated using data made available by the USGS Coastal-Change and Glaciological Maps of Antarctica project (Williams et al., 1995; Fretwell et al., 2013; Cook et al, 2014) and from LIMA mosaics provided by the USGS EROS Data Center and constructed using Landsat images gathered between 1999 and 2002.

4. Results

4.1. Echo-type description, distribution and interpretation

Three echo-types were identified in Bourgeois Fjord and Blind Bay from the analysis of sub-bottom profiler records. The description, distribution and interpretation of echo-types are shown in Figure 2, integrating the classical criteria of Damuth (1980), Kuhn and Weber (1993) and Droz et al. (2001) for echo-facies characterization and the seismic facies attributes, such as the acoustic amplitude, lateral continuity, geometry and internal configuration of reflections on parametric profiles (Payton, 1977; Veeken, 2007). A non-penetrative echo-type (I) is dominant in the study area and represents irregular surfaces of outcropping bedrock, coarse deposits and/or high gradients that prevent the penetration of the acoustic signal. It includes two subtypes. Echo-type IA represents a very irregular, non-penetrative seafloor reflection and is the predominant type in the main and outer fjord. Echo-type IB represents a smooth non-penetrative seafloor reflection and is present mostly close to the fjord walls and on the seafloor of Blind Bay (Fig. 2). A transparent-chaotic echo-type (II) occurs only locally, forming patches on the seafloor of both relatively shallow and deep areas of the fjord. It consists of transparent deposits of an irregular, mounded-shaped geometry, or thin packages of transparent-chaotic reflections. Echo-type III is stratified and represents smooth distinct parallel-layered reflections with relatively high acoustic amplitude. It occurs locally in deep, flat areas of the main and outer fjord and results from fine-layered sedimentation (Fig. 2).

4.2. Physiography of Bourgeois Fjord

Multibeam swath-bathymetric mapping allows the physiography of Bourgeois Fjord and Blind Bay to be mapped in detail (Fig. 1). The fjord system includes a central, main fjord, north of 67° 37'S, which terminates in Blind Bay at its northeastern end. The main fjord is separated by a relatively shallow 300 m deep sill from a narrower outer fjord that opens westwards into Marguerite Bay (Fig. 1). The main fjord is a 90 km^2 semi-closed basin up to 665 m deep that receives direct meltwater and iceberg input from several tidewater glaciers. Lliboutry, Perutz and Bader glaciers as well as part of the ice fed from Heim Glacier drain into the main fjord today, and Forel and Barnes glaciers have calving fronts in Blind Bay (Fig. 1).

The main fjord is 455-665 m deep and displays a U-shaped cross-profile (Fig. 1). The eastern sector has a NNE-SSW-orientation and is about 3 km wide. It displays a relatively flat floor at depths of 530-540 m. The central sector of the main fjord is E-W oriented and 4.5 km wide on average, with a more irregular seafloor at depths ranging from 445-560 m. A prominent SE-NW-oriented high, up to 2.2 km wide, occurs in the SE part of the basin, off the mouth of Perutz Glacier. The western sector of the main fjord is NE-SW oriented, with an average width of 4.2 km and a maximum depth of 665 m. The main Bourgeois

Fjord connects with Marguerite Bay through an outer fjord that consists of a relatively narrow NE-SW-oriented channel between Pourquoi Pas Island and Ridge Island (Fig. 1). The outer fjord is 450-680 m deep, about 35 km long and 1-3 km wide. It presents a markedly irregular seafloor with numerous topographic highs.

4.3. Fjord Seafloor Landforms

4.3.1. Bourgeois Fjord

The main Bourgeois Fjord presents a typical U-shaped cross profile, with steep fjord walls and a relatively flat deep seafloor and can be divided into three sectors - proximal, central and distal – each with distinct morphological and physiographic characteristics (Fig. 3). The *proximal sector* is NNE-SSW-oriented and is approximately 7 km long and 3 km wide. The seafloor is relatively flat at depths of 520-550 m and presents smooth-floored elongate basins that parallel the fjord trend with a stratified echo-type (III), suggesting a fine-laminated sedimentary bed, and a weak ridge-and-valley topography (Figs. 3B and 3D) characterized by irregular non-penetrative echo-type, implying a mainly rock bed.

The *central sector* is E-W-orientated and is 7 km long and 5 km wide (Fig. 3). The seafloor is 450-570 m deep and markedly irregular. The northern wall presents numerous arcuate scarps. Here the fjord floor presents smaller flat basins, delimited by N-S to NW-SE-oriented escarpments (Fig. 3B). A NW-SE-oriented prominent morphological high occurs off the terminus of Perutz Glacier and displays some elongate ESE-WNW-oriented features on its top. To the west the seafloor is characterized by irregular morphological highs displaying non-penetrative echo-type (IA). Morphological highs become more elongate and crag-and-tail shaped towards the distal zone (elongation ratio - length:width - of 2:1 to 3:1). Small, irregular channels with a dendritic convergent pattern and small flat basins occur between the morphological highs (Figs. 3B and 3E).

The *distal sector* is NE-SW-oriented, about 8 km long and 5 km wide (Fig. 3D). A shallow area connects the terminus of Lliboutry Glacier with the main fjord and displays NE-SW-oriented morphological highs that delimit deep elongate basins off the glacier front. The main fjord floor in the distal sector is characterized by elongate, crag-and-tails (elongation ratios of 2:1 to 4:1), channels and low relief lineations with irregular non-penetrative echo-type (IA) suggesting bedrock cropping out at the seafloor (Figs. 3B and 3F). A flat basin occupies the distal area at depths averaging 660 m and is of stratified echo-type (III), implying fine-layered sedimentation (Fig. 2).

The outer fjord connects the main Bourgeois Fjord with Marguerite Bay (Figs. 1 and 4). Arcuate scarps occur on the steep fjord walls, where the predominant echo-type is irregular, non-penetrative (IA) (Fig.

2). The sector between Pourquoi Pas and Ridge islands is characterized by streamlined features with high elongation ratios of 2:1 to 5:1 (Figs. 4D and 4E) and channels oriented parallel to the fjord long-axis (Fig. 4E). To the SW some minor crag-and-tail features and weak lineations are observed and the seafloor is markedly irregular, with some morphological highs and relatively flat basins with stratified echo-type (III) and scarcer and smaller elongate features (Figs. 2 and 4). Together this implies small basins filled with fine-layered sediments separated by bedrock highs.

4.3.2. Blind Bay

The inner 4 km of Blind Bay has been mapped at high-resolution using a combination of *Isis* and *JCR* multibeam data (Figs. 5 and 6), and a transect of photographs acquired by the *Isis* ROV has been used for characterizing the seafloor (Fig. 7). The submarine landform assemblage of inner Blind Bay includes a large transverse ridge at its ice-distal end (Fig. 5). Inside this ridge, arcuate-shaped and longitudinal ridges, finger-like ridges with straight lineations, transverse escarpments and channel-like features are present (Fig. 5). The dimensions of these landforms and their main characteristics are given in Table I.

The distal transverse ridge occupies the entire width of the bay at about 4 km from the front of Forel Glacier (Fig. 5). It is responsible for the step-like, landward-deepening profile of the inner sector of Blind Bay. The ridge is markedly asymmetric, with a gentle ice-proximal face and a steeper ice-distal face (up to 25º, 40-70 m high; Fig. 5D). TOPAS profiles show smooth non-penetrative echo-type IB along the inner sector, reflecting coarse surficial sediment, and stratified echo-type (III) suggesting layered sedimentation in the proximal part of the outer sector (at the foot of the ridge) that becomes non-penetrative seawards (Fig. 5D).

Three crescent-shaped ridges are identified in the inner sector of Blind Bay (Fig. 5), where the seafloor is generally characterized by the irregular non-penetrative echo-type IA (Figs. 2 and 5D). The largest arcuate ridge is up to 25 m high and 500 m wide and occupies the central part of the Blind Bay inner sector, delimiting a relatively flat basin floor. The ridge is asymmetric with a steeper, convex-downstream ice-distal face and straight lateral flanks parallel to the bay limits (Figs. 5B and 5C). Two crescent-shaped ridges of similar morphological characteristics but smaller in size occur at more ice-proximal positions (Fig. 5). The middle ridge is displaced to the eastern fjord flank, whereas the most ice-proximal one is located about 1 km from the Forel Glacier front at depths of 280-290m. Longitudinal ridges are identified along lateral positions in the inner sector of Blind Bay (Fig. 5). Overall, the eastern ridges are higher (up to 10 m high), with a consistent NE-SW trend slightly oblique to the fjord walls. To the west, ridges are smaller (up to 2 m high) and their trend is NNE-SSW.

Finger-like ridges are identified in the high-resolution *Isis* swath-bathymetric mosaics and occur within the flat area delimited by the distal crescent-shaped ridge, at depths of 245-270 m (Figs. 5 and 6). They are up to 1 km long and relatively narrow (5-50 m wide). They are generally asymmetric with steeper eastern flanks (up to 22º) that delimit relatively flat areas (Fig. 6). Their orientations vary between 320º and 350º and they display highly variable shapes in a complex overlapping pattern. The proximal irregular ridges are markedly elongate and display arcuate, concave-eastward shapes, slightly oblique to the regional gradient. In contrast, the more distal ridges are much more irregular and display arcuate, finger-shape trends with concave-landward distal fronts up to 5 m high. Lineations have been identified on the *Isis* high-resolution swath-bathymetry data at depths of 240-280m (Fig. 6). They present sharp terminations toward the ridges, to which they are parallel to oblique in orientation. Lineations are straight with consistent orientations varying basinward from 330º to 310º (parallel to the basin trend) and are spaced 3-20 m apart. They are up to 20 m long and less than 1 m high with slope gradients of up to 5º.

The most ice-proximal part of the bay presents an irregular topography (Fig. 5) with an irregular non-penetrative echo-type IA (Fig. 2). There is a series of NW-SE-oriented transverse escarpments which are up to 10 m high and asymmetric, with smoother ice-proximal flanks (5-10º steep) and steeper (up to 18º) distal fronts (Figs. 5A and 5B). A network of diverging channel-like features occurs on the NW fjord wall, approximately 500 m from the Forel Glacier front (Figs. 5A and 5B). The system is about 500 m long, and individual channels are up to 80 m wide and 35 m deep.

A longitudinal transect of photographs was acquired by the *Isis* ROV along inner Blind Bay (Fig. 7). The photographs show a transition in seafloor character between about 1 and 3 km from the modern ice front (Fig. 7B). There is a progressive change from a predominance of relatively small clastclasts with angular shapes, little or no fine sediment drape and weak colonization by benthic organisms (Fig. 7B, Photo 1), to a wider range of sizes and shapes of clasts, including relatively large ones, a thicker and widespread sediment drape that covers completely the seafloor at the most distal positions, and a higher abundance of benthic organisms (Fig. 7B, Photos 2 and 3). Individual or grouped clasts on the floor of Blind Bay display striated surfaces and sub-rounded faces, but most clasts have faceted and angular shapes. The upper surfaces of many clasts are covered by a thin layer of sediment, and they are weakly colonized by benthic organisms (Fig. 7B, Photos 2 and 3). Photographs from the proximal areas show the presence of eroded bedrock on the inner fjord wall (Fig. 7C, Photo 4). The area with irregular ridges shows clasts of heterogeneous size, but of larger dimensions, than those in the surrounding areas covered by a thin sediment drape and is poorly colonized by benthic organisms (Fig. 7C, Photos 5 and 6).

5. Discussion

5.1. Interpretation and distribution of landforms

The interpretation of the landforms in Bourgeois Fjord identified in this work can be integrated with a compilation of morphological and geophysical studies of the continental shelf of Marguerite Trough in order to obtain a complete understanding of the system (Fig. 8). The inner shelf offshore of Bourgeois Fjord is characterized by crag-and-tails in areas of mixed bedrock and unconsolidated sediment (Livingstone et al., 2013, 2016). Further seawards, a succession of landforms with increased elongation ratios (parallel gouges, streamlined hills and bedrock outcrops, whalebacks, drumlins and MSGLs) on the mid-shelf marks the transition from crystalline bedrock, where subglacial meltwater channels are also incised, to sedimentary bedrock (Ó Cofaigh et al., 2005; Anderson and Fretwell, 2008; Livingstone et al., 2013, 2016). The middle to outer shelf is characterized mainly by the presence of streamlined bedrock outcrops, drumlins and MSGLs and by a series of grounding-zone wedges and scarps (Ó Cofaigh et al., 2005). The outer shelf displays MSGLs and, in relatively shallower water iceberg ploughmarks proximal to the shelf edge, into which numerous short gullies are incised (Dowdeswell et al., 2004a; Ó Cofaigh et al., 2005; Livingstone et al., 2013, 2016).

The morphological and acoustic characterization and the environmental and geological setting of the submarine landforms in Bourgeois Fjord and the continental shelf of Marguerite Trough allows the differentiation of four major morpho-sedimentary systems that reflect different stages of the last glacial cycle through the Bourgeois Fjord and Blind Bay system, involving specific sedimentary processes: 1) Glacial advance, full-glacial and early deglacial system; 2) Subglacial and ice-marginal meltwater system; 3) Glacial retreat system (APIS retreat and Little Ice Age re-advance and retreat); and 4) Holocene mass-wasting system (Fig. 9). The detailed interpretations of each of the landform types described above is given in Table I.

5.1.1. Glacial advance, full-glacial system and early deglaciation

The flow of ice through the Bourgeois Fjord system during the last full-glacial, when the APIS advanced to the shelf edge and an ice stream was present in Marguerite Bay (e.g. Anderson et al., 2002; Heroy and Anderson, 2007; Livingstone et al., 2013, 2016; Ó Cofaigh et al., 2014), is indicated by the broad-scale physiography and the landform assemblage in the main and outer Bourgeois Fjord areas (Fig. 9A). The main and outer fjord are characterized by bedrock landforms that increase in their elongation ratio down-fjord (from 2:1 to 5:1) and have crag-and-tail morphologies indicating westward ice flow towards Marguerite Bay (Figs. 3 and 4). Similar progressive elongation of whalebacks in the inner and middle shelf of Marguerite Bay (2:1-4:1 to 18:1; Livingstone et al., 2013) and the transition to more elongate morphologies (drumlins, MSGLs) towards more distal areas of the shelf (Fig. 8; Ó Cofaigh et al, 2014;

Livingstone et al., 2013, 2016) suggest that processes forming the landforms in the main and outer Bourgeois Fjord are similar to those that acted in Marguerite Bay, and that they reflect the subglacial erosion and sculpting action typical of an accelerating ice stream (e.g. Wellner et al., 2006; Graham et al., 2009). Streamlining is assumed to result from subglacial erosion of bedrock (e.g. bedrock lineations, whaleback features), or from the shaping of till and/or bedrock by subglacial erosion and/or deposition (e.g. drumlins, crag-and-tail features) (Bradwell et al., 2008; Ottesen et al., 2008; Livingstone et al., 2013). In Bourgeois Fjord, these landforms appear to evolve from irregular erosional crystalline bedrock highs characterized by a hard, irregular sea-floor with no acoustic penetration (acoustic facies IA; Fig. 2) into elongate, more streamlined landforms (Fig. 8). This suggests an increasing sedimentary component of the substrate (e.g. Wellner et al., 2006; Graham et al., 2009; Livingstone et al., 2012). It is important to note that landforms sculpted in bedrock may reflect the cumulative activity of fast-flowing ice over successive glacial cycles, not simply during the LGM (Graham et al., 2009; Smith et al., 2009; Livingstone et al., 2013; Krabbendam et al., 2016). Lineations in Bourgeois Fjord appear to result from the action of rapid ice flow on bedrock with a relatively thin sedimentary cover, as revealed by the TOPAS record and submarine photographs (Figs. 2 and 7) and are therefore not as well-developed as the sets of MSGLs found on the sedimentary floor of many Antarctic cross-shelf troughs, including those in Marguerite Bay, that reflect a greater thickness of deformable sedimentary substrate (e.g Dowdeswell et al., 2004b; Ó Cofaigh et al., 2005; Spagnolo et al., 2016).

Flow acceleration, probably in combination with the change in the substrate, may also be responsible for the increased elongation of glacial landforms with distance down Bourgeois Fjord. Ice flow may have been accelerated due to the convergence of flows from a number of drainage basins that merged into the fjord as the ice sheet over Graham Land grew towards it maximum LGM extent and thickness (Figs. 1, 8 and 9A) (e.g. Anderson and Fretwell, 2008; Larter et al., 2009).

The relatively deep elongate basins offshore of Lliboutry Glacier (Fig. 3A) probably record the activity of advancing ice fed from Lliboutry and probably from Heim glaciers, the latter reaching Bourgeois Fjord through the channel north of Blaiklock Island (Fig. 1). The basins form perched platforms at varying depths that seem to be delimited by NE-SW-trending highs. Transverse bedrock escarpments (Figs. 3B, 5B) indicate subglacial quarrying or plucking by the advancing ice sheet on bedrock with differential resistance to erosion in the most proximal area of the main fjord and also in Blind Bay (Dünhforth et al., 2010). The orientation of the escarpments appears to reflect structural control by the NE-SW and NW-SE-oriented regional tectonic fabric related to the NW-SE-oriented fault zones developed during extension in the Marguerite Bay area before about 20 Ma ago (Johnson, 1997), which may have been related to movement on the West Antarctic Rift System (Eagles et al., 2009).

5.1.2. Subglacial and ice-marginal meltwater system

The meltwater system includes channels and small flat basins in the deeper areas of Bourgeois Fjord and on the lower fjord wall in the inner sector of Blind Bay (Fig. 9B). Channels in the main and outer Bourgeois Fjord (Figs. 3 and 4) are interpreted as subglacial meltwater channels eroded into crystalline bedrock, which are common features in many high-latitude inner-shelf and fjord areas, especially where crystalline bedrock predominates (e.g. Lowe and Anderson, 2002; Domack et al., 2006; Anderson and Fretwell, 2008; Smith et al., 2009; Nitsche et al., 2013; Hogan et al., 2016). Similarly to other bedrock erosional glacial landforms, they may record erosion through multiple glaciations (Ó Cofaigh et al., 2002; Graham et al., 2009; Smith et al., 2009; Krabbendam et al., 2016). The more distal channels in the main and outer Bourgeois Fjord are interconnected with small basins limited by morphological highs and tend to open to large basins further down-fjord (Figs 3B and 4B). Smaller channels in inner Blind Bay are related directly to the present-day location of the tidewater terminus of Forel Glacier (Fig. 5B) and, although they may have formed subglacially, provide a continuing conduit for dense underflows of mixed seawater and fresh meltwater loaded with subglacially-derived suspended sediment released directly from the terminus of the glacier (Gales et al., 2013). The channels in Bourgeois Fjord form an isolated drainage network due to the shallowing of the seafloor towards the outer fjord, which impedes a connection with the meltwater channels network in the Marguerite Bay inner- and mid- continental shelf (Ó Cofaigh et al., 2005; Livingstone et al., 2013; Hogan et al., 2016; Fig. 8).

Areas of flat seafloor, with stratified reflections on sub-bottom profiles (Fig. 2), suggest sedimentation by glacimarine processes after deglaciation (e.g. Smith et al., 2009; Ó Cofaigh et al., 2016). A number of processes may be involved, such as tidal pumping of the grounding lines that generate sorted, laminated sediment (Domack et al., 1999; Evans et al., 2005**;** Kilfeather et al., 2011), or marine derived detritus supplied from the grounding line. Furthermore, meltwater plumes containing fine-grained suspended sediments exiting the glacier terminus from a basal drainage system may also produce debris rain-out that would infill the small basins (Powell, 1990; Cowan, 2001; Lowe and Anderson, 2002; Domack et al., 2006; Mugford and Dowdeswell, 2011; Dowdeswell et al., 2014, 2015; Ó Cofaigh et al., 2016). The easternmost NE-SW-oriented basins would have received sediment input from Blind Bay, whereas the westernmost ones would include suspended sediment delivered from Lliboutry Glacier. These acoustically-stratified sedimentary deposits are separated by morphological highs of irregular bedrock in the middle reaches of Bourgeois Fjord (Fig. 4B).

5.1.3. Glacial retreat and neoglaciation system

There are few signs of transverse-to-ice-flow depositional ridges in the outer and main parts of Bourgeois Fjord (Figs. 4 and 5), such as grounding-zone wedges or large retreat moraines (e.g. Batchelor and Dowdeswell, 2015), that could be associated with still-stands during deglacial ice-sheet retreat. An implication of this is that ice-sheet retreat through Bourgois Fjord probably took place relatively rapidly once ice had retreated from the shelf and Marguerite Bay at or shortly after 9,000 years ago (Kilfeather et al., 2011). The fjord system appears, therefore, to have been influenced mainly by glacimarine processes during the Holocene. The glacial retreat system we have mapped is restricted to relatively small-scale morainic landforms identified in the inner sector of Blind Bay, including the distal transverse ridge, the crescent-shaped and longitudinal ridges and the finger-like ridges associated with lineations (Figs. 5B and 9C). The well-preserved appearance of these features indicates that they have not been over-ridden by a subsequent glacier advance and may well be relatively recent features relating to the final post-glacial retreat or to recent neoglacial fluctuations of a few kilometres in the position of the glacier termini in Blind Bay (Fig. 9C). We suggest that these neoglacial cold events are associated with the LIA that has been recorded in neighbouring areas of the Antarctic Peninsula, such as Lallemand Fjord where an ice-shelf advance occurred approximately 400 years ago (Shevenell et al., 1996), probably in relation to the exclusion of Circumpolar Deep Water from the fjord (Domack et al., 1995), or Rothera Point, that experienced a glacial advance between 671 and 317 cal yr. BP (Guglielmin et al., 2007). Although the LIA cooling phase was not synchronous between sites, it has been widely documented in Antarctica, where temperatures ~2º colder were registered from ice cores from the Ross Sea area at about 1300 to 1850 AD (Bertler et al., 2011), roughly coinciding with temperature estimates 0.52±0.28ºC colder than the last 100-year average at the West Antarctic Ice Sheet divide (Orsi et al., 2012).

The distal transverse ridge in Blind Bay is interpreted as an ice-marginal moraine (Figs. 5B and 9C), based on its echo-type and typical asymmetrical morphology with a steeper ice-distal face (Dowdeswell and Vasquez, 2013). This moraine was deposited at the glacier terminus when the grounding-zone was maintained in a relatively stable position in the middle reaches of Blind Bay (e.g. Ottesen et al., 2005; Dowdeswell et al., 2014). The location suggests stabilization of the ice front probably related to the narrowing of Blind Bay (Jamieson et al., 2012; Rydningen et al., 2013), and/or to the presence of a topographic high that may also have acted as pinning point.

Crescent-shaped and longitudinal ridges in the inner sector of Blind Bay (Fig. 5B) are interpreted as recessional moraines (Fig. 9C). They are sedimentary landforms composed of unsorted clasts and finer sediment (Fig. 7). These features are deposited at the front of glaciers during still-stands or re-advances during a general phase of ice retreat (e.g. Bennett et al., 1999; Ottesen and Dowdeswell, 2006, 2009; Johnson et al., 2013). Their dimensions and location in Blind Bay suggest formation during shorter still

418 stands than those linked to the larger transverse moraine ridge and their presence in inner Blind Bay is
419 probably linked to the progressive recession of the ice front, reflecting a slow ice-retreat pattern (Ottesen
420 and Dowdeswell, 2006; McLachlan et al., 2010; Bjarnadóttir et al., 2014; Batchelor and Dowdeswell,
421 2015). Longitudinal ridges converge towards the centre of the bay (Fig. 5) and probably represent the
422 lateral parts of recessional moraines from which the fronts have been eroded and/or reworked by
423 successive small ice readvances and/or by meltwater flow. Crescent-shaped ridges seem to overlay the
424 longitudinal ridges and are interpreted as the frontal ridges of well-preserved moraines over which no
425 significant reworking by ice readvance has occurred. Blocks and rafts showing signs of glacitectonic
426 erosion are evident in the seafloor photographs that show striated and angular clasts (Fig. 7) suggesting
427 short transportation distances of the material after being incorporated into the moraines by bedrock
428 plucking during grounded ice readvance (Laberg et al., 2009).

429 *Finger-like ridges* delimiting *short straight lineations* (Figs. 5B and 6) are the most striking features
430 identified in ROV-acquired high-resolution bathymetric images. They are interpreted as 'ice-fingerprints',
431 having formed by the pushing or ploughing of sediment by minor readvances of the grounded glacier
432 terminus within inner Blind Bay (e.g. Geirsdottir et al., 2008, 2016; Bjarnadottir et al., 2014). The highly
433 elongate shape and variable size of the finger-like ridges (Fig. 6) suggests a very irregular, non-linear ice
434 margin advancing and retreating during the very last stages of glacial retreat. The pervasive, straight
435 lineations delimited by the ridges suggest deformation of soft sediment by the glacier, and are interpreted
436 as lateral push-ridges formed by a non-linear advancing ice front, overprinted by the finger-like ridges.
437 Ice flow may have been constrained by the relief of the ice-marginal transverse moraine that acted as a
438 morphological threshold buttressing minor readvances of the grounded tidewater glacier (Fig. 9C). These
439 features suggest a depleting ice source being drained by bands of faster flowing ice (e.g. Todd and Shaw,
440 2012) and point to a final ice-mass retreat occurring in episodic events with massive iceberg calving.

441 5.1.4. Holocene mass-wasting system

442 Mass-wasting has taken place in Bourgeois Fjord since ice retreated through the steep-sided fjord system
443 to about its present position <9,000 years ago (Kilfeather et al., 2011). Several *debris lobes* mapped close
444 to the margins of Barnes and Bader glaciers (Fig. 3B) are probably related to the failure and downslope
445 flowage of relatively rapidly deposited debris close to the tidewater termini of these glaciers (e.g. Laberg
446 et al., 2009; Dowdeswell et al., 2015), although the relatively coarse resolution of the JCR multibeam data
447 precludes more detailed analysis. Debris lobes sometimes appear stacked on the lower fjord walls,
448 implying a short displacement that reflects the coarse and unsorted nature of the sediment supplied by
449 subglacial erosion (Garcia et al., 2009). Mass-wasting processes on the walls of Bourgeois Fjord (Fig.

9D), and close to the foci of continuing sediment delivery at tidewater glacier margins (cf. Ottesen and Dowdeswell, 2009; Dowdeswell et al., 2016), have probably been operating throughout the Holocene since ice retreated through the fjord system about 8-9,000 years ago and continue to operate today (Shevenell et al., 1996; Kilfeather et al., 2011).

5.2. Ice dynamics inferred from landform distribution and sedimentary characteristics

Most landforms in Blind Bay and Bourgeois Fjord indicate a glacial origin related to flow of active ice and can be attributed to specific stages of the last glacial cycle (Fig. 9), although streamlined bedrock landforms may have evolved over successive glacials. Landforms of the glacial advance and full-glacial system (Fig. 9A) correspond to the ice-growth, glacial maximum and early deglaciation, in a setting dominated by active ice flowing down-fjord. The morphological evidence in this area reflects the imprint of the grounded ice advance, in a similar manner to the neighbouring area of Gerlache Strait continental shelf, dominated by streamlined subglacial bedforms (Evans et al., 2005; Canals et al., 2016). A full-glacial outlet glacier flowing between the steep fjord walls of Bourgeois Fjord appears to have produced crag-and-tails (Figs. 3B and 4B), whose characteristics and distribution along the fjord suggest a transitional flow towards the development of a fast-flowing ice stream (e.g. Wellner et al., 2001). The latter probably required a deformable sedimentary bed similar to that which occupied the outer part of Marguerite Trough (Ó Cofaigh et al., 2002, 2005, 2008; Dowdeswell et a., 2004a,b; Kilfeather et al., 2011). The convergence of glacier flow into Bourgeois Fjord, implied by the present configuration of tidewater glaciers and their adjacent fjords (Fig. 1), suggests acceleration associated with increasing ice flux, which may also be inferred from the increase in landform elongation downstream (Wellner et al., 2006; Bradwell et al., 2008; Graham et al., 2009). The presence of meltwater channels cut into the bedrock of the fjord floor (Fig. 9B) also implies active ice- and meltwater-flow with a bed at the pressure-melting point of ice. Ice flow from Bourgeois Fjord contributed to the Marguerite Bay palaeo-ice stream, the largest ice stream on the Antarctic Peninsula with an estimated drainage basin size of about 100 000 km^2, which reached the western Peninsula continental shelf edge through the Marguerite Bay cross-shelf trough (Fig. 1B; Livingstone et al., 2012).

The absence of transverse-to-flow sedimentary landforms in the outer and main Bourgeois Fjord suggests that ice retreated from Marguerite Bay into Blind Bay during the last deglaciation (Allen et al., 2010; Kilfeather et al, 2011; Ó Cofaigh et al., 2014) without leaving morphological evidence of any significant stillstand. Evidence for a two-step deglacial model in Marguerite Bay locates grounded ice at the mid-shelf transitional area from crystalline bedrock to soft sedimentary substrate (Bentley et al., 2011), offshore of Bourgeois Fjord. In contrast, landforms in Blind Bay demonstrate that the deglacial/Holocene

history in this inner region has been more complicated. Although precise details of timing are uncertain, other studies in neighbouring areas (i.e., the Larsen continental shelf, eastern Antarctic Peninsula) describe a relatively slow ice-stream recession punctuated by stillstands on the inner shelf, resulting in the deposition of a series of grounding-zone wedges (Evans et al., 2005). Bycontrast, other fjords in the Antarctic Peninsula display morphological features pointing to rapid deglaciation with no sign of retreat features (e.g. Simms et al., 2011; Minzoni et al., 2016). We suggest that grounding-zone wedges on the Marguerite Bay continental shelf (Fig. 8) are related to the same processes and timing, but in contrast the high degree of preservation and the morphological characteristics of glacial-sedimentary landforms in Blind Bay suggests that they may have formed relatively recently. We tentatively propose that the transverse moraines originated during the Little Ice Age, by analogy with similar features identified a few kilometres from modern tidewater glaciers in, for example, Chilean fjords (Dowdeswell and Vasquez, 2013). Transverse moraines have been related to glacier advances during the LIA, when valley glaciers readvanced and deposited ice-cored moraines in the West Antarctic region (Clapperton and Sugden, 1982; Shevenell et al., 1996) and also in the Antarctic Peninsula (Carrivick et al., 2012), and the Northern Hemisphere (Svalbard, Greenland; Ottesen and Dowdeswell, 2009; Funder et al., 2011; Dowdeswell et al., 2014). In summary, we propose early Holocene retreat through the fjord system followed by minor readvances of grounded ice in the inner part of Blind Bay, although the timing of these events needs confirmation.

Contrasting with the relatively complex recent Holocene history of glaciation in Blind Bay, the shallow areas off Lliboutry and Perutz glaciers in the main fjord show a relatively smooth seafloor and the absence of transverse-to-flow landforms, suggesting relatively limited ice-margin fluctuations since retreat to approximately their present position after regional deglaciation from the LGM. The differences in the style of deglaciation and recent fluctuations between adjacent tidewater glaciers can be attributed to local physiographic controls (Heroy and Anderson, 2007; Ó Cofaigh et al., 2008, 2014). The locations of transverse ridges in Blind Bay may have been controlled, in part at least, by the reduction in width of the inner sector of the bay, increasing lateral drag on the tidewater glacier and reducing of the volume of ice required for maintaining a stable grounding-zone (Jamieson et al., 2012, 2014; Rydningen et al., 2013).

5.3. Pattern of retreat of tidewater glaciers during the last Century

Environmental-change studies have revealed a recent warming trend in the Antarctic Peninsula, resulting in a reduction of terrigenous sediment supply from retreating glaciers related to a final abrupt phase of climate amelioration corresponding to the ‘rapid regional warming’ of recent decades (Allen et al., 2010). The pattern of recent retreat of the tidewater glaciers draining into the Bourgeois Fjord system, together

514 with the drainage basin-areas of these glaciers, has been compiled from satellite images, maps and aerial
515 photographs for the period between 1947 and 2011 in order to analyse their recent fluctuations (Fig. 10;
516 Table II). With the exception of Perutz Glacier, the glaciers have all undergone retreat since observations
517 began in 1947 (Fig. 10). This is in agreement with a regional trend of glacier retreat in the Antarctic
518 Peninsula over the past half-century (Cook et al., 2005, 2014). This 'recent rapid regional warming' has
519 been related to a series of mechanisms such as changes in oceanographic and/or atmospheric circulation,
520 or regionally amplified greenhouse warming driven by air-see-ice feedback processes (Vaughan et al.,
521 2003).

522 Observations indicate a general pattern of retreat of the glacier fronts over the last six decades, with the
523 retreat of individual glacier termini occurring in a non-systematic pattern (Fig. 10). Forel Glacier has
524 undergone the maximum retreat (about 2.3 km in 64 years). This is the only glacier that displays a reverse
525 gradient proglacial seafloor, which probably increases the rate of modern iceberg calving through
526 increased buoyancy in progressively deepening water (Benn et al., 2007). An inverse relationship can also
527 be tentatively established between drainage-basin size, glacier-terminus width and variations in terminus
528 behaviour. As basin-size increases, the amount of glacier-terminus retreat is reduced. Thus, Perutz and
529 Lliboutry glaciers, which have the largest drainage areas (Fig. 2), have retreated notably less than the
530 smaller Forel, Barnes and Bader glaciers (Fig. 10). This is consistent with the work of Fox and Cooper
531 (1998), who proposed that recent ice retreat has affected most markedly the extent of smaller ice bodies
532 on the Antarctic Peninsula.

533 **5.4. Controls on recent sedimentation in Bourgeois Fjord**

534 In Bourgeois Fjord the major long-term controlling factor on the sediments and landforms we have
535 observed is the growth and decay of ice in the fjord system, linked to the broader glacial-interglacial
536 cycles that affected the APIS. This has resulted in the predominance of glacial advance/full-glacial
537 landforms in the main and outer Bourgeois Fjord, whereas deglacial landforms, which are most likely late
538 Holocene in age, are restricted to the inner sector of Blind Bay. The start of retreat at 9.3 ka B.P. has been
539 linked to the influence of oceanographic factors, which involved the intrusion of modified Circumpolar
540 Deep Water onto the adjacent continental shelf (Kilfeather et al., 2011). Secondary factors controlling the
541 distribution of landforms in Bourgeois Fjord include the structural setting, the seafloor physiography and
542 oceanographic factors. The structural control is revealed by the relationship between general trends in the
543 direction of past ice-flow and erosion and the orientation of bedrock ridges on the fjord floor, with many
544 NE-SW- and NW-SE-oriented features evident (Johnson, 1997; Anderson and Fretwell, 2008). The
545 regional structural fabric is also reflected by perched terraces or basins in the shallow areas off Llibourty

Glacier that appear to have been controlled by NE-SW-oriented structural features. The physiography of the fjords and adjacent mountains, established long before the last glacial cycle, influences in particular the width of glacier fronts and the size of catchment areas and, through this, exerts an influence on the most recent fluctuations of the tidewater glaciers in Blind Bay. Tidal pumping and deep-water currents are common processes involved in sediment dispersal and redeposition in tidewater-glacier influenced fjords (Syvitski, 1989) and they may have influenced the distribution of stratified sediment along Bourgeois Fjord.

6. Summary and conclusions

This study highlights the complexity of the last glacial retreat phase in Bourgeois Fjord and illustrates the importance of high-resolution geophysical observations for the reconstruction of past ice flow. The main conclusions are summarized as follows.

1. High-resolution geophysical evidence reveals a complex landform assemblage in Bourgeois Fjord that can be integrated with regional morphological studies of Marguerite Trough in order to analyse the complete fjord-to-continental shelf system. It is composed of four major morpho-sedimentary systems that resulted from specific processes and/or phases of the last glacial cycle. (i) A glacial advance and full-glacial system is manifested in the outer and main fjord and is composed mainly of streamlined-bedrock and crag-and-tail features that are genetically related to the landforms identified along the continental shelf. (ii) A meltwater system comprising channels and sediment-filled basins in the outer and main fjord. (iii) A well-preserved glacial retreat system is present in the inner sector of Blind Bay and includes a series of recessional sedimentary landforms. (iv) A Holocene mass-wasting system affects unstable glacial sediments on the walls of the fjord, reflected in the form of slide scars and associated fan-shaped deposits.

2. The glacial advance and full-glacial system was formed subglacially by the action of an active LGM outlet glacier that drained the APIS towards Marguerite Bay. A warm basal thermal regime is suggested by the landform distribution in the outer and main fjord, which includes subglacial channels. Ice flow in Bourgeois Fjord was probably characterized by a down-flow transition towards faster moving ice in the form of an outlet glacier from the LGM ice-sheet interior, as indicated by the progressive elongation of subglacially produced landforms.

3. A relatively rapid deglaciation of Bourgeois Fjord is implied by a lack of transverse-to-flow depositional landforms, in which the ice margin migrated landward to the inner fjords during retreat. Morphological evidence of margin stillstands and/or glacial readvances is found only in the inner sector

of Blind Bay. Here, a major transverse moraine indicates grounded ice stabilization probably during the Little Ice Age, followed by minor readvance episodes.

4. The most recent evolution of the outlet glaciers draining into Bourgeois Fjord during the last six decades is not homogeneous. The range of variation of glacier-terminus fluctuations appears to depend on the physiography of the region, including catchment-area size and changing fjord width.

Acknowledgements

We thank the officers and crew of the RRS *James Clark Ross* and the *Isis* ROV team from the National Oceanography Centre, Southampton, for their help with data acquisition. The research was funded by a UK Natural Environment Research Council grant AFI06/14 (NE/C506372/1) to J.A. Dowdeswell, R.D. Larter and G. Griffiths. M. Garcia's work at the Scott Polar Research Institute, University of Cambridge, was funded by an EU Marie Curie Fellowship. We thank the Editor, Prof. John B. Anderson and another anonymous reviewer for their helpful comments and constructive suggestions to improve the original manuscript.

References

Allen, C., Oakes-Fretwell, L., Anderson, J.B., Hodgson, D., 2010. A record of Holocene glacial and oceanographic variability in Neny Fjord, Antarctic Peninsula. The Holocene 20, 551–564.

Amblas, D., Urgeles, R., Canals, M., Calafat, A.M., Rebesco, M., Camerlenghi, A., Estrada, F., De Batist, M., Hughes-Clarke, J.E., 2006. Relationship between continental rise development and palaeo-ice sheet dynamics, Northern Antarctic Peninsula Pacific margin. Quaternary Science Reviews 25, 993–944.

Anderson, J.B., 1999. Antarctic Marine Geology. Cambridge University Press, Cambridge.

Anderson, J.B., Fretwell, L.O., 2008. Geomorphology of the onset area of a paleo-ice stream, Marguerite Bay, Antarctic Peninsula. Earth Surface Processes and Landforms 33, 503–512. doi: 10.1002/esp1662.

Anderson, J.B., Shipp, S.S., Lowe, A.L., Wellner, J.S., Mosola, A.B., 2002. The Antarctic Ice Sheet during the Last Glacial Maximum and its subsequent retreat history: A review. Quaternary Science Reviews 21, 49–70.

Batchelor, C.L., Dowdeswell, J.A., 2015. Ice-sheet grounding-zone wedges (GZWs) on high-latitude continental margins. Marine Geology 363, 65–92.

Benn, D.I., Warren, C.R., Mottram, R.H., 2007. Calving processes and the dynamics of calving glaciers. Earth-Science Reviews 82, 143–179.

Bennett, M.R., Hambrey, M.J., Huddart, D., Glasser, N.F., Crawford, K., 1999. The landform and sediment assemblage produced by a tidewater glacier surge in Kongsfjorden, Svalbard. Quaternary Science Reviews 18, 1213–1246.

Bentley, M.J., Anderson, J.B., 1998. Glacial and marine geological evidence for the ice sheet configuration in the Weddell Sea–Antarctic Peninsula region during the Last Glacial Maximum. Antarctic Science 10, 309–325.

Bentley, M.J., Hodgson, D.A., Smith, J.A., Ó Cofaigh, C., Domack, E.W., Larter, R.D., Roberts, S.J., Brachfeld, S., Leventer, A., Hjort, C., Hillenbrand, C.-D., Evans, J., 2010. Mechanisms of Holocene palaeoenvironmental change in the Antarctic Peninsula region. The Holocene 19, 51–69.

Bentley, M.J., Hodgson, D.A., Smith, J.A., Cox, N.J., 2005. Relative sea level curves for the South Shetland Islands and Marguerite Bay, Antarctic Peninsula. Quaternary Science Reviews 24, 1203–1216.

Bentley, M.J., Johnson, J.S., Hodgson, D.A., Dunai, T., Freeman, S.P.H.T., Ó Cofaigh, C., 2011. Rapid deglaciation of Marguerite Bay, western Antarctic Peninsula in the Early Holocene. Quaternary Science Reviews 30, 3338–3349.

Bertler, N.A.N., Mayewski, P.A., Carter, L., 2011. Cold conditions in Antarctica during the Little Ice Age – Implications for abrupt climate change mechanisms. Earth and Planetary Science Letters 308, 41–51.

Bjarnadóttir, L.R., Winsborrow, M.C.M., Andreassen, K., 2014. Deglaciation of the central Barents Sea. Quaternary Science Reviews 92, 208–226.

Bradwell, T., Stoker, M., Krabbendam, M., 2008. Megagrooves and streamlined bedrock in NW Scotland: The role of ice streams in landscape evolution. Geomorphology 97, 135–156.

Canals, M., Amblas, D., Domack, E., Lastras, G., Lavoie, C., Casamor, J.L. and Smith, C., 2016. The seafloor imprint of the Gerlache–Boyd ice stream (65º to 62ºS), northern Antarctic Peninsula. In Dowdeswell, J.A., Canals, M., Jakobsson, M., Todd, B.J., Dowdeswell, E.K., Hogan, K.A. et al., (eds), Atlas of Submarine Glacial Landforms: Modern, Quaternary and Ancient. Geological Society, London, Memoirs, 46, 477-484. doi: 10.1144/M46.174.

Carrivick, J.L., Davies, B.J., Glasser, N.F., Nývit, D., Hambrey, M.J., 2012. Late-Holocene changes in character and behavior of land-terminating glaciers on James Ross Island, Antarctica. Journal of Glaciology 58, 1176–1190.

Christ, A.J., Talaia-Murray, M., Elking, N., Domack, E.W., Leventer, A., Lavoie, C., Brachfeld, S., Yoo, K.-C., Gilbert, R., Jeong, S.-M., Petrushak, S., Wellner, J., LARISSA Group, 2014. Late Holocene glacial advance and ice shelf growth in Barilari Bay, Graham Land, west Antarctic Peninsula. Geological Society of America Bulletin 127, 297–315. doi: 10.1130/B31035.1.

Clapperton, C.M., Sugden, D.E., 1982. Late quaternary glacial history of George VI Sound area, West Antarctica. Quaternary Research 18, 243–267.

Cook, A.J., Fox, A.J., Vaughan, D.G., Ferrigno, J.G., 2005. Retreating glacier fronts on the Antarctic Peninsula over the past half-century. Science 308, 541–544. doi: 10.1126/science.1104235.

Cook, A.J., Vaughan, D.G., Luckman, A.J., Murray, T., 2014. A new Antarctic Peninsula glacier basin inventory and observed area changes since the 1940s. Antarctic Science. 26, 614–624.

Cowan, E.A, 2001. Identification of the glacial signal from the Antarctic Peninsula since 3.0 Ma at Site 1011 in a continental rise sediment drift. In: Barker, P.F., Camerlenghi, A., Acton, G.D., Ramsay, A.T.S. (Eds.), Proceedings of the ODP, Scientific Results 178, 1–22.

Damuth, J.E., 1980. Use of high-frequency (3.5-12 kHz) echograms in the study of near-bottom sedimentation processes in the deep-sea: a review. Marine Geology 38, 51–75.

Domack, E., Amblàs, D., Gilbert, R., Brachfeld, S., Camerlenghi, A., Rebesco, M., Canals, M., Urgeles, R., 2006. Subglacial morphology and glacial evolution of the Palmer deep outlet system, Antarctic Peninsula. Geomorphology 75, 125–142.

Domack, E.W., Ishman, S., 1993. Oceanographic and physiographic controls on modern sedimentation within Antarctic fjords. Geological Society of America Bulletin 105, 1175–1189.

Domack, E.W., Ishman, S.C., Stein, A.B., McClennen, C.E., Jull, A.J.T., 1995. Late Holocene advance of the Muller Ice Shelf, Antarctic Peninsula: sedimentological, geochemical and palaeontological evidence. Antarctic Science 7, 159–170.

Domack, E.W., Jacobson, E.A., Shipp, S., Anderson, J.B., 1999. Late Pleistocene-Holocene retreat of the West Antarctic Ice-Sheet system in the Ross Sea: Part 2- Sedimentologic and stratigraphic signature. GSA Bulletin 111, 1517–1536. doi: 10.1130/0016-7606.

Dowdeswell, J.A., Ó Cofaigh, C., 2002. Glacier-influenced sedimentation on high-latitude continental margins: introduction and overview. Geological Society of London, Special Publication 203, 1–9.

667 Dowdeswell, J.A., Vásquez, M., 2013. Submarine landforms in the fjords of southern Chile: Implications
668 for glacimarine processes and sedimentation in a mild glacier-influenced environment. Quaternary
669 Science Reviews 64, 1–19.

670 Dowdeswell, J.A., Ó Cofaigh, C., Pudsey, C.J., 2004a. Continental slope morphology and sedimentary
671 processes at the mouth of an Antarctic palaeo-ice stream. Marine Geology 204, 203–214.

672 Dowdeswell, J.A., Ó Cofaigh, C., Pudsey, C.J., 2004b. Thickness and extent f the subglacial till layer
673 beneath an Antarctic paleo-ice stream. Geology 32, 13–16.

674 Dowdeswell, J.A., Benham, T.J., Strozzi, T., Hagen, J.O., 2008a. Iceberg calving flux and mass balance
675 of the Austfonna ice cap on Nordaustlandet, Svalbard. Journal of Geophysical Research. Earth Surface
676 113, 1–12.

677 Dowdeswell, J.A., Noormets, R., Evans, J., Griffiths, G., Larter, R.D., Ó Cofaigh, C., 2008b. A
678 comparison of swath-bathymetric imagery from high-latitude glacier-influenced fjords derived from
679 AUV, ROV and shipboard systems. In: Collins, K., Griffiths, G. (eds.), Workshop on AUV science in
680 extreme environments: collaborative Autosub science in extreme environments. Proceedings of the
681 international science workshop, Cambridge, April 2007, London, Society for Underwater Technology,
682 pp. 47–54.

683 Dowdeswell, J.A., Hogan, K.A., Ó Cofaigh, C., Fugelli, E.M.G., Evans, J., Noormets, R., 2014. Late
684 Quaternary ice flow in a West Greenland fjord and cross-shelf trough system: submarine landforms
685 from Rink Isbrae to Uummannaq shelf and slope. Quaternary Science Reviews 92, 292–309.

686 Dowdeswell, J.A., Hogan, K.A., Arnold, N.S., Mugford, R.I., Wells, M., Hirst, J.P.P., Decalf, C., 2015.
687 Sediment-rich meltwater plumes and ice-proximal fans at the margins of modern and ancient tidewater
688 glaciers: observations and modelling. Sedimentology, 62, 1665–1692,

689 Dowdeswell, J.A., Ottesen, D., Noormets, R., 2016. Submarine slides from the walls of
690 Smeerenburgfjorden, NW Svalbard. In Dowdeswell, J.A., Canals, M., Jakobsson, M., Todd, B.J.,
691 Dowdeswell, E.K., Hogan, K.A., (Eds), Atlas of Submarine Glacial Landforms: Modern, Quaternary
692 and Ancient. Geological Society, London, Memoirs, 46, 105-106. doi:10.1144/M46.21.

693 Droz, L., Kergoat, R., Cochonat, P., Berné, S., 2001. Recent sedimentary events in the western Gulf of
694 Lions (Western Mediterranean). Marine Geology 176, 23–37.

695 Eagles, G., Larter, R.D., Gohl, K., Vaughan, A.P.M., 2009. West Antarctic Rift System in the Antarctic
696 Peninsula. Geophysical Research Letters 36, doi:10.1029/2009GL040721, 2009.

697 Evans, J., Pudsey, C.J., Ó Cofaigh, C., Morris, P., Domack, E., 2005. Late Quaternary glacial history,
698 flow dynamics and sedimentation along the eastern margin of the Antarctic Peninsula Ice Sheet.
699 Quaternary Science Reviews 24, 741–774.

700 Fretwell, L.O. and 55 others, 2013. Bedmap2: improved ice bed, surface and thickness datasets for
701 Antarctica. The Cryosphere 7, 375–393.

702 Fox, A.J., Cooper, A.P.R., 1998. Climate-change indicators from archival aerial photography of the
703 Antarctic Peninsula. Annals of Glaciology 27, 636–642.

704 Funder, S., Kjeldsen, K.K., Kjaer, K.H., Ó Cofaigh, C., 2011. Chapter 50. The Greenland Ice Sheet
705 during the past 300,000 years: a review. Developments in Quaternary Sciences 15, 699–713.

706 Gales, J.A., Larter, R.D., Mitchell, N.C., Dowdeswell, J.A., 2013. Geomorphic signature of Antarctic
707 submarine gullies: Implications for continental slope processes. Marine Geology 337, 112–124.

708 García, M., Ercilla, G., Alonso, B., 2009. Morphology and sedimentary systems in the Central Bransfield
709 Basin, Antarctic Peninsula: sedimentary dynamics from shelf to basin. Basin Research 21,: 295–314.

710

711 Geirsdóttir, Á., Miller, G.H., Wattrus, N.J., Björnsson, H., Thors, K., 2008. Stabilization of glaciers
712 terminating in closed water bodies: Evidence and broader implications. Geophysical Research Letters
713 35, L17502, doi:10.1029/2008GL034432.

714 Geirsdottir, A., Miller, G.H., Larsen, D.J., 2016. Landforms in Hvitarvatn, central Iceland, produced by
715 recent advances of surging and non-surging glaciers. In Dowdeswell, J.A., Canals, M., Jakobsson, M.,
716 Todd, B.J., Dowdeswell, E.K., Hogan, K.A., (eds), Atlas of Submarine Glacial Landforms: Modern,
717 Quaternary and Ancient. Geological Society, London, Memoirs 46, 143-146. doi:10.1144/M46.108.

718 Gilbert, R., Nielsen, N., Möller, H., Desloges, J., Rasch, M., 2002. Glacimarine sedimentation in
719 Kangerdluk (Disko Fjord), West Greenland, in response to a surging glacier. Marine Geology 191, 1–
720 18.

721 Graham, A.G.C., Larter, R.D., Gohl, K., Hillenbrand, C.D., Smith, J.A., Kuhn, G., 2009. Bedform
722 signature of a West Antarctic palaeo-ice stream reveals a multi-temporal record of flow and substrate
723 control. Quaternary Science Reviews 28, 2774–2793.

724 Griffith, T., Anderson, J.B., 1989. Climatic control of sedimentation in bays and fjords of the northern
725 Antarctic Peninsula. Marine Geology 85, 181–204.

726 Guglielmin, M., Convey, P., Malfasi, F., Cannone, N., 2007. Glacial fluctuations since the Medieval
727 Warm Period at Rothera Point (Western Antarctic Peninsula). The Holocene 17, 1253–1258.

728 Heroy, D.C., Anderson, J.B., 2007. Radiocarbon constraints on Antarctic Peninsula Ice Sheet retreat
729 following the Last Glacial Maximum (LGM). Quaternary Science Reviews 26, 3286–3297.

730 Hogan, K.A., Dowdeswell, J.A., Larter, R.D., Ó Cofaigh, C. and Bartholomew, I., 2016. Subglacial
731 meltwater channels in Marguerite Trough, western Antarctic Peninsula. In Dowdeswell, J.A., Canals,
732 M., Jakobsson, M., Todd, B.J., Dowdeswell, E.K., Hogan, K.A. (eds), Atlas of Submarine Glacial
733 Landforms: Modern, Quaternary and Ancient. Geological Society, London, Memoirs, 46, 215-216.
734 doi:10.1144/M46.178.

735 Jakobsson, M., Macnab, R., Mayer, L., Anderson, R., Edwards, M., Hatzky, J., Werner Schenke, H.,
736 Johnson, P., 2008. An improved bathymetric portrayal of the Arctic Ocean: Implications for ocean
737 modeling and geological, geophysical and oceanographic analyses. Geophysical Research Letters 35,
738 doi:10.1029/2008GL033520.

739 Jamieson, S.S.R., Vieli, A., Livingstone, S.J., Ó Cofaigh, C., Stokes, C.R., Hillenbrand, C.-D. and
740 Dowdeswell, J.A., 2012. Ice stream grounding-line stability on a reverse bed slope. Nature
741 Geoscience, 5, 799–802.

742 Jamieson, S.S.R., Vieli, A., Cofaigh, C.Ó., Stokes, C.R., Livingstone, S.J., Hillenbrand, C.D., 2014.
743 Understanding controls on rapid ice-stream retreat during the last deglaciation of Marguerite Bay,
744 Antarctica, using a numerical model. Journal of Geophysical Research. Earth Surface 119, 247–263.

745 Johnson, A.C., 1997. Cenozoic tectonic evolution of the Marguerite Bay area, Antarctic Peninsula,
746 interpreted from geophysical data. Antarctic Science 9, 268–280.

747 Johnson, M.D., Benediktsson, Í.Ö., Björklund, L., 2013. The Ledsjö end moraine-a subaquatic push
748 moraine composed of glaciomarine clay in central Sweden. Proceedings of the Geological Association
749 124, 738–752.

750 Kaser, G., Cogley, J.G., Dyurgerov, M.B., Meier, M.F., Ohmura, A., 2006. Mass balance of glaciers and
751 ice caps: Consensus estimates for 1961–2004. Geophysical Research Letters 33,
752 doi:10.1029/2006GL027511

753 Kennedy, D.S., Anderson, J.B., 1989. Glacial-marine sedimentation and Quaternary glacial history of
754 Marguerite Bay, Antarctic Peninsula. Quaternary Research 31, 255–276.

755 Kilfeather, A.A., Cofaigh, C.Ó., Lloyd, J.M., Dowdeswell, J.A., Xu, S., Moreton, S.G., 2011. Ice-stream
756 retreat and ice-shelf history in Marguerite Trough, Antarctic Peninsula: Sedimentological and
757 foraminiferal signatures. Bulletin of the Geological Society of America. 123, 997–1015.

758 Krabbendam, M., Eyles, N., Putkinen, N., Bradwell, T., Arbelaez-Moreno, L., 2016. Streamlined hard
759 beds formed by palaeo-ice streams: A review. Sedimentary Geology, 338, 24–50. doi:
760 10.1016/j.sedgeo.2015.12.007.

761 Kuhn, G., Weber, M.E., 1993. Acoustical characterization of sediments by Parasound and 3.5 kHz
762 systems: Related sedimentary processes on the southeastern Weddell Sea continental slope, Antarctica.
763 Marine Geology 113, 201–217.

764 Laberg, J.S., Eilertsen, R.S., Vorren, T.O., 2009. The paleo-ice stream in Vestfjorden, north Norway, over
765 the last 35 k.y.: Glacial erosion and sediment yield. Geological Society of America Bulletin 121, 434–
766 447.

767 Larter, R.D., Graham, A.G.C., Gohl, K., Kuhn, G., Hillenbrand, C.D., Smith, J.A., Deen, T.J., Livermore,
768 R.A., Schenke, H.W., 2009. Subglacial bedforms reveal complex basal regime in a zone of paleo-ice
769 stream convergence, Amundsen Sea embayment, West Antarctica. Geology 37, 411–414.

770 Livingstone, S.J., Ó Cofaigh, C., Hogan, K.A. and Dowdeswell, J.A., 2016. Submarine glacial-landform
771 distribution along an Antarctic Peninsula palaeo-ice stream: a shelf-slope transect through the
772 Marguerite Bay system (66° to 70°S). In Dowdeswell, J.A., Canals, M., Jakobsson, M., Todd, B.J.,
773 Dowdeswell, E.K., Hogan, K.A., (eds), Atlas of Submarine Glacial Landforms: Modern, Quaternary
774 and Ancient. Geological Society, London, Memoirs, 46, 485-492. doi:10.1144/M46.180.

775 Livingstone, S.J., Cofaigh, C.Ó., Stokes, C.R., Hillenbrand, C.-D., Vieli, A., Jamieson, S.S.R., 2013.
776 Glacial geomorphology of Marguerite Bay Palaeo-Ice stream, western Antarctic Peninsula. Journal of
777 Maps 9, 558–572.

778 Livingstone, S.J., Ó Cofaigh, C., Stokes, C.R., Hillenbrand, C.D., Vieli, A., Jamieson, S.S.R., 2012.
779 Antarctic palaeo-ice streams. Earth-Science Reviews 111, 90–128.

780 Lowe, A.L., Anderson, J.B., 2002. Reconstruction of the West Antarctic ice sheet in Pine Island Bay
781 during the Last Glacial Maximum and its subsequent retreat history. Quaternary Science Reviews 21,
782 1879–1897.

McLachlan, S.E., Howe, J.A., Vardy, M.E., 2010. Morphodynamic evolution of Kongsfjorden, Svalbard, during the Late Weichselian and Holocene. In: Fowe, J.A., Austin, W.E.N., Forwick, M., Paetzel, M. (Eds.), Fjord Systems and Archives. Geological Society, London, Special Publications 344, 195–205.

Minzoni, R.T., Anderson, J.B., Fernandez, R., Wellner, J.S., 2015. Marine record of Holocene climate, ocean, and cryosphere interactions: Herbert Sound, James Ross Island, Antarctica. Quaternary Science Reviews 129, 239–259.

Mugford, R.I., Dowdeswell, J. A., 2011. Modeling glacial meltwater plume dynamics and sedimentation in high-latitude fjords. Journal of Geophysical Research. Earth Surface 116, 1–20.

Mulvaney, R., Abram, N.J., Hindmarsh, R.C.A., Arrowsmith, C., Fleet, L., Triest, J., Sime, L.C., Alemany, O, Foord, S., 2012. Recent Antarctica Peninsula warming relative to Holocene climate and ice-shelf history. Nature 489, 141–145. doi:10.1038/nature11391.

Nitsche, F.O., Gohl, K., Larter, R.D., Hillenbrand, C.-D., Kuhn, G., Smith, J.A., Jacobs, S., Anderson, J.B., Jakobsson, M., 2013. Paleo ice flow and subglacial meltwater dynamics in Pine Island Bay, West Antarctica. The Cryosphere 7, 249–262.

Noormets, R., Dowdeswell, J.A., Larter, R.D., Ó Cofaigh, C., Evans, J., 2009. Morphology of the upper continental slope in the Bellingshausen and Amundsen Seas – Implications for sedimentary processes at the shelf edge of West Antarctica. Marine Geoloy 258, 100–114.

Ó Cofaigh, C., Hogan, K.A., Dowdeswell, J.A., Strueff, K. 2016. Stratified glacimarine basin-fills in West Greenland fjords. In: Dowdeswell, J.A., Canals, M., Jakobsson, M., Todd, B.J., Dowdeswell, E.K., Hogan, K.A. (Eds), Atlas of Submarine Glacial Landforms: Modern, Quaternary and Ancient. Geological Society, London, Memoirs, 46, 99–100. doi:10.1144/M46.83.

Ó Cofaigh, C., Davies, B.J., Livingstone, S.J., Smith, J.A., Johnson, J.S., Hocking, E.P., Hodgson, D.A., Anderson, J.B., Bentley, M.J., Canals, M., Domack, E., Dowdeswell, J.A., Evans, J., Glasser, N.F., Hillenbrand, C.D., Larter, R.D., Roberts, S.J., Simms, A.R., 2014. Reconstruction of ice-sheet changes in the Antarctic Peninsula since the Last Glacial Maximum. Quaternary Science Reviews 100, 87–110.

Ó Cofaigh, C., Dowdeswell, J. A., Allen, C.S., Hiemstra, J.F., Pudsey, C.J., Evans, J., Evans, D.J.A, 2005. Flow dynamics and till genesis associated with a marine-based Antarctic palaeo-ice stream. Quaternary Science Reviews 24, 709–740.

Ó Cofaigh, C., Dowdeswell, J.A., Evans, J., Larter, R.D., 2008. Geological constraints on Antarctic palaeo-ice-stream retreat. Earth Surface Processes and Landforms 33, 513–525.

Ó Cofaigh, C., Taylor, J., Dowdeswell, J.A., Rosell-Melé, A., Kenyon, N.H., Evans, J., Mienert, J., 2002. Sediment reworking on high-latitude continental margins and its implications for palaeoceanographic studies: insights from the Norwegian-Greenland Sea. Geological Society of London, Special Publications 203, 325–348.

Orsi, A. J., Cornuelle, B. D., Severinghaus, J. P., 2012. Little Ice Age cold interval in West Antarctica: Evidence from borehole temperature at the West Antarctic Ice Sheet (WAIS) Divide. Geophys. Res. Lett., 39, doi:10.1029/2012GL051260.

Ottesen, D., Dowdeswell, J.A., 2006. Assemblages of submarine landforms produced by tidewater glaciers in Svalbard. Journal of Geophysical Research. Earth Surface 111, 1–16. doi:10.1029/2005JF000330

Ottesen, D., Dowdeswell, J. A., 2009. An inter-ice-stream glaciated margin: Submarine landforms and a geomorphic model based on marine-geophysical data from Svalbard. Bulletin of the Geological Society of America 121, 1647–1665.

Ottesen, D., Dowdeswell, J.A., Benn, D.I., Kristensen, L., Christiansen, H.H., Christensen, O., Hansen, L., Lebesbye, E., Forwick, M., Vorren, T.O., 2008. Submarine landforms characteristic of glacier surges in two Spitsbergen fjords. Quaternary Science Reviews 27, 1583–1599.

Ottesen, D., Dowdeswell, J.A., Landvik, J.Y., Mienert, J., 2007. Dynamics of the Late Weichselian ice sheet on Svalbard inferred from high-resolution sea-floor morphology. Boreas 36, 286–306.

Ottesen, D., Rise, L., Knies, J., Olsen, L., Henriksen, S., 2005. The Vestfjorden-Traenadjupet palaeo-ice stream drainage system, mid-Norwegian continental shelf. Marine Geology 218, 175–189.

Payton, C.E., 1977. Seismic Stratigraphy: application to hydrocarbon exploration, AAPG-Memoir 26, AAPG, Tulsa.

Peck, V.L., Allen, C.S., Kender, S., McClymont, E.L., Hodgson, D.A., 2015. Oceanographic variability on the West Antarctic Peninsula during the Holocene and the influence of upper circumpolar deep water. Quaternary Science Reviews 119, 54–65.

Powell, R.D., 1990. Glacimarine processes at grounding-line fans and their growth to ice-contact deltas. Geological Society of London, Special Publication 53, 53–73.

Pudsey, C.J., Barker, P.F., Larter, R.D., 1994. Ice sheet retreat from the Antarctic Peninsula shelf. Continental Shelf Research 14, 1647–1675.

Radić, V., Hock, R., 2011. Regionally differentiated contribution of mountain glaciers and ice caps to future sea-level rise. Nature Geoscience 4, 91–94.

Rodrigo, C., Giglio,S., Varas, A., 2016. Glacier sediment plumes in small bays on the Danco Coast, Antarctic Peninsula. Antarctic Science 28, 395–404. doi:10.1017/S0954102016000237.

Rydningen, T.A., Vorren, T.O., Laberg, J.S., Kolstad, V., 2013. The marine-based NW Fennoscandian ice sheet: Glacial and deglacial dynamics as reconstructed from submarine landforms. Quaternary Science Reviews 68, 126–141.

Shevenell, A., Domack, E.W., Kernan, G., 1996. Record of Holocene paleoclimate change along the Antarctic Peninsula: evidence from glacial marine sediments, Lallemand Fjord. Papers and Proceedings of the Royal Society of Tasmania. 130, 55–64.

Simms, A.R., Milliken, K., Anderson, J.B., Wellner, J.S., 2011. The marine record of deglaciation of the South Shetland Islands, Antarctica since the Last Glacial Maximum. Quaternary Science Reviews 30, 1583–1601.

Smith, J.A., Hillenbrand, C.D., Larter, R.D., Graham, A.G.C., Kuhn, G., 2009. The sediment infill of subglacial meltwater channels on the West Antarctic continental shelf. Quaternary Research 71, 190–200.

Spagnolo, M., Phillips, E., Piotrowski, J.A., Rea, B.R., Clark, C.D., Stokes, C.R., Carr, S.J., Ely, J.C., Ribolini, A., Wysota, W., Szuman, I., 2016. Ice stream motion facilitated by a shallow-deforming accreting bed. Nature Communications, doi: 10.1038/ncomms10723.

Syvitski, J.P.M., 1989. On the deposition of sediment within glacier-influenced fjords: oceanographic controls. Marine Geology 85, 301–329.

Todd, B.J., Shaw, J., 2012. Laurentide Ice Sheet dynamics in the Bay of Fundy, Canada, revealed through multibeam sonar mapping of glacial landsystems. Quaternary Science Reviews 58, 83–103.

Vaughan, D., Marshall, G., Connolley, W.M., Parkinson, C., Mulvaney, R., Hodgson, D.A., King, J.C., Pudsey, C.J., Turner, J., 2003. Recent Rapid Regional Climate Warming on the Antarctic Peninsula. Climatic Change 243–274.

Veeken, P.C.H., 2007. Seismic Stratigraphy, Basin Analysis and Reservoir Characterisation Elsevier, Amsterdam.

Wellner, J.S., Heroy, D.C., Anderson, J.B., 2006. The death mask of the Antarctic ice sheet: Comparison of glacial geomorphic features across the continental shelf. Geomorphology 75, 157–171.

Wellner, J.S., Lowe, A.L., Shipp, S.S., Anderson, J.B., 2001. Distribution of glacial geomorphic features on the Antarctic continental shelf and correlation with substrate: Implications for ice behavior. J. Glaciology 47, 397–411.

Williams, R.S., Ferrigno, J.G., Swithinbank, C., Lucchitta, B.K., Seekins, B.A., 1995. Coastal-change and glaciological maps of Antarctica. Annals of Glaciology 21, 284–290.

Figures and Tables captions

Figure 1. Study area, in Marguerite Bay, Antarctic Peninsula (A). (B) Palaeo-ice streams of the Antarctic Ice Sheet during the last glacial period around the Antarctic Peninsula, from Livingstone et al. (2012). MB P-IS: Marguerite Bay palaeo-ice stream; (C) Regional topographic map of Marguerite Bay (data from the Marine Geoscience Data System; http://www.marine-geo.org). Neny and Lallemand Fjords, located in neighbouring areas of the Antarctic Peninsula are shown. (D) Bathymetry of Bourgeois Fjord on the Pacific side of the Antarctic Peninsula. The limits of glaciers on Graham Land and the islands have been mapped from the LIMA satellite-image mosaic provided by the USGS EROS Center. The map shows the location of the *Isis* ROV dive in Blind Bay, off Forel Glacier and the bathymetry of the main and outer Bourgeois Fjord from our multibeam data.

Figure 2. Acoustic facies characterization, distribution and interpretation. Selected TOPAS profiles are shown to illustrate the acoustic character of each echo-type: non-penetrative, transparent-chaotic and stratified. Descriptions and interpretations are given, and follow the criteria first proposed by Damuth (1980) and further developed by Kuhn and Weber (1993) and Droz et al. (2001).

Figure 3. Morphological characterization of the main Bourgeois Fjord and shallow areas off the tidewater glaciers draining into it. (A) Multibeam bathymetry. (B) Distribution of submarine landforms. (C) Bathymetric profile along the main fjord illustrating the seafloor relief along the proximal, central and distal sectors. (D) Transverse escarpments and basins. (E). Smooth sedimentary basins and bedrock channels. (F) Elongate features and streamlined lineations.

Figure 4. Morphological characterization of outer Bourgeois Fjord. (A) Location map. (B) Distribution of submarine landforms inferred from multibeam bathymetry data. (C) to (E) Detailed bathymetric mosaics illustrating the morphological characteristics of channels, streamlined features and smooth basins identified in the outer fjord (located in B).

Figure 5. Morphological characterization of the inner sector of Blind Bay, showing the distribution of submarine landforms based multibeam bathymetry data. (A) Swath-bathymetric mosaic of Blind Bay. (B) Landform distribution, including channels, transverse ridges and distal wedges. (C) Oblique view of inner Blind Bay with landforms labeled. (D) TOPAS sub-bottom acoustic profile along the inner sector of Blind Bay (located in B).

Figure 6. Morphological characterization of the inner sector of Blind Bay, based on the *Isis* ROV high-resolution multibeam imagery. (A) Bathymetric mosaic and interpretation (located in Fig. 6A). (B) and (C) Detailed sections showing the bathymetry, gradient-slope direction and gradient of the area characterized by finger-like ridges and lineations. (D) Bathymetric profiles displaying the morphology of the ridges and lineations (axes in m).

Figure 7. ROV-acquired photographs of the seafloor along a transect in the inner sector of Blind Bay (locations of photographs shown in A). (B) Photographic transect from ice-proximal (Photo 1) to distal positions (Photo 3) along the inner part of Blind Bay. (C) Photographs illustrating the erosional character of the proximal area (Photo 4) and the morphological crests in the distal area representing finger-like ridges and lineations (Photos 5 and 6).

Figure 8. (A) Regional map of Marguerite Bay showing the landforms assemblage as discussed in this work, integrated with the results from Dowdeswell et al. (2004), Ó Cofaigh et al. (2005) and Livingstone et al. (2013). (B) to (H) Greyscale seafloor bathymetric models (see location in (A)) showing the detailed characteristics and distribution of the landforms. Regional bathymetric data have been obtained from the Marine Geoscience Data System (http://www.marine-geo.org).

930

931 Figure 9. Spatial distribution of the submarine landforms composing the four morpho-sedimentary
932 systems in Bourgeois Fjord. (A) Glacial advance and full-glacial; (B) Subglacial and ice-marginal
933 meltwater ; (C) Glacial retreat and neoglaciation; and (D) Holocene mass-wasting.

934

935 Figure 10. Variations in the locations of tidewater-glacier margins between 1947 to 2011, inferred from
936 maps, aerial photographs and satellite images. The figure illustrates the different trends in terminus
937 fluctuations different tidewater glaciers draining into Bourgeois Fjord.

938

939 Table I. Morphological characteristics and interpretations of the landforms observed in Bourgeois Fjord.

940

941 Table II. Morphological and physiographic parameters of the tidewater glaciers draining into Bourgeois
942 Fjord (located in Figure 1).

Geomorphic and shallow-acoustic investigation of an Antarctic Peninsula fjord system using high-resolution ROV and shipboard geophysical observations: ice dynamics and behaviour since the Last Glacial Maximum

Marga García[1,2*], J.A. Dowdeswell[2], R. Noormets[3], K.A. Hogan[1,4], J. Evans[5], C. Ó Cofaigh[6], R.D. Larter[4]

[1] Instituto Andaluz de Ciencias de la Tierra, CSIC-University of Granada. Avda. de las Palmeras, 4. 18100, Armilla, Spain.
[2] Scott Polar Research Institute, University of Cambridge, Lensfield Road, Cambridge CB2 1ER, UK
[3] Departments of Arctic Geology and Arctic Geophysics, University Centre in Svalbard, 9170 Longyearbyen, Norway
[4] British Antarctic Survey, Natural Environment Research Council, High Cross, Madingley Road, Cambridge CB3 0ET, UK
[5] Department of Geography, University of Loughborough, Loughborough LE11 3TU, UK
[6] Department of Geography, Durham University, Durham DH1 3LE, UK

[*] Corresponding author. Email address: m.garcia@csic.es; marguita.garcia@gmail.com.

Formatted: Not Superscript/ Subscript

ABSTRACT

Detailed bathymetric and sub-bottom acoustic observations in Bourgeois Fjord (Marguerite Bay, Antarctic Peninsula) provide evidence on sedimentary processes and glacier dynamics during the last glacial cycle. Submarine landforms observed in the 50 km-long fjord, from the margins of modern tidewater glaciers to the now ice-distal Marguerite Bay, are described and interpreted. The landforms are grouped into four morpho-sedimentary systems: (i) glacial advance and full-glacial; (ii) subglacial and ice-marginal meltwater; (iii) glacial retreat and neoglaciation; and (iv) Holocene mass-wasting. These morpho-sedimentary systems have been integrated with morphological studies of the Marguerite Bay continental shelf and analysed in terms of the specific sedimentary processes and/or stages of the glacial cycle. They demonstrate the action of an ice-sheet outlet glacier that produced drumlins and crag-and-tail features in the main and outer fjord. Meltwater processes eroded bedrock channels and ponds infilled by fine-grained sediments. Following the last deglaciation of the fjord at about 9,000 yr BP, subsequent Holocene neoglacial activity involved minor readvances of a tidewater glacier terminus in Blind Bay. Recent stillstands and/or minor readvances are inferred from the presence of a major transverse moraine that indicates grounded ice stabilization, probably during the Little Ice Age, and a series of smaller

landforms that reveal intermittent minor readvances. Mass-wasting processes also affected the walls of the fjord and produced scars and fan-shaped deposits during the Holocene. Glacier-terminus changes during the last six decades, derived from satellite images and aerial photographs, reveal variable behaviour of adjacent tidewater glaciers. The smaller glaciers show the most marked recent retreat, influenced by regional physiography and catchment-area size.

Keywords: Antarctic Peninsula; Fjord systems; Last Glacial Maximum; Glacial sedimentary processes; Geomorphology; ROV-derived bathymetry.

1. Introduction

The geomorphology of glaciated continental margins contains records of environmental history and of the geological processes shaping the seafloor (e.g. Anderson, 1999; Ó Cofaigh et al., 2002; Ottesen et al., 2005). The increasing resolution of geophysical and geological datasets acquired from high-latitude shelves and fjords is providing new insights into the major processes occurring during the last full-glacial and deglacial periods in particular (Dowdeswell and Ó Cofaigh, 2002; Jakobsson et al., 2008). The high sensitivity of the Antarctic Peninsula Ice Sheet (APIS) results from the regional amplification of global warming (Vaughan et al., 2003), and the response mechanisms involve factors such as oceanography, atmospheric circulation and regional air-sea-ice feedback (Bentley et al., 2010). The Antarctic Peninsula has experienced rapid warming in the last 600 years, and an unusually high warming trend over the past century, resulting in ice-shelf vulnerability along the Peninsula with its potential impact on global climate (Mulvaney et al., 2012). The assessment of models for predicting the future evolution of ice masses requires a knowledge of past ice dynamics and, in particular, studies of the styles of deglaciation for the last glacial cycle, that depend on a complex interplay between global and local factors (Livingstone et al., 2012). Mass balance models for outlet glaciers highlight the influence of glacier dynamics on climate and global sea-level (Kaser et al., 2006) and, in the case of tidewater glaciers, processes involving iceberg discharge are particularly important but poorly known contributors to mass loss from ice caps (Dowdeswell et al., 2008aa; Radić and Hock, 2011).

Formatted: Font color: Text 2

The complexity of glacial-marine systems has been revealed by numerous investigations of the geomorphology and shallow stratigraphy of Arctic fjords (e.g. Griffith and Anderson, 1989; Domack and Ishman, 1993; Gilbert et al., 2002; Ottesen and Dowdeswell, 2006, 2009; Ottesen et al., 2007, 2008), allowing detailed palaeoenvironmental reconstructions of the last glacial cycle, whereas high-resolution studies from Antarctic fjords are still relatively scarce (Griffith and Anderson, 1989; Anderson, 1999; Rodrigo et al., 2016). In Marguerite Bay, ~~Western~~ western Antarctic Peninsula, research has focused on past ice-stream dynamics along a glacial trough that occupies almost 400 km across the continental shelf

(Dowdeswell et al., 2004a; Ó Cofaigh et al., 2005; Livingstone et al., 2013, 2016). However, a detailed study of the most proximal areas is still needed in order to understand the complete system and, in particular, the transition from the outlet glaciers near the coast to the large ice-streams on the continental shelf. This paper investigates the submarine landform record in Bourgeois Fjord, providing evidence for the glacial dynamics in the area from the termini of tidewater glaciers to the more open marine environment of Marguerite Bay. The area is characterized today by the presence of relatively small outlet glaciers draining Graham Land, but was covered by an extensive APIS with grounding lines reaching the continental-shelf edge during the Last Glacial Maximum (LGM) (e.g. Pudsey et al., 1994; Bentley and Anderson, 1998; Anderson, 1999; Anderson et al., 2002; Dowdeswell et al., 2004a; Ó Cofaigh et al., 2014). The paper is focused on the processes and patterns shaping the seafloor during the last glacial cycle in order to analyse the glacial and deglacial dynamics and the factors influencing them, and to provide an integrated view of the processes affecting the complete system, from the fjord to the outer continental shelf. This work analyses sedimentary processes at different spatial and temporal scales: the last glacial cycle affecting the entire system from the fjord to the continental shelf-edge, the Little Ice Age (LIA) event recorded in the inner areas of Bourgeois Fjord (Blind Bay), and recent ~~retreat~~ patterns of tidewater glaciers retreat caused by rapid regional warming during the last century.

2. Geological and ice-sheet chronological framework

Bourgeois Fjord is one of the many relatively narrow and steep-sided fjords that connect tidewater glaciers draining from the APIS in Graham Land with Marguerite Bay and the Pacific Southern Ocean margin (Kennedy and Anderson, 1989; Anderson, 1999) (Fig. 1). The Antarctic Ice Sheet expanded across continental shelves all around the Antarctic Peninsula during the LGM and grew to fill Bourgeois Fjord and spread across the Marguerite Bay continental shelf with fast-flowing ice streams reaching the shelf edge (Pudsey et al., 1994; Bentley and Anderson, 1998; Anderson et al., 2002; Dowdeswell et al., 2004a; ~~Amblás~~ Amblas et al., 2006). Evidence of the last glacial ice stream dynamics has been described along the Marguerite Trough which drained the Marguerite Bay palaeo-ice stream across the continental shelf. Large isolated basins in the inner shelf are characterized by crag-and-tails in areas with exposed bedrock that have similar dimensions and orientations to mega-scale glacial lineations (MSGLs) identified in the neighbouring areas (Livingstone et al., 2013, 2016). On the middle shelf, a basinward succession of landforms has been identified, from deep roughly parallel gouges and subglacial meltwater channels incised into crystalline bedrock, to streamlined hills, whalebacks and MSGLs (Livingstone et al., 2013, 2016). The mid-outer shelf displays streamlined bedrock outcrops and GZWs (Ó Cofaigh et al., 2005). The outer shelf is characterized by MGSLs with a N-NW trend that are overprinted by iceberg ploughmarks close to the continental-shelf edge (Dowdeswell et al., 2004a; Ó Cofaigh et al., 2005;

Livingstone et al., 2013, 2016). Numerous gullies occur on the upper slope. Those located on the sides of the palaeo-ice stream mouth are incised directly at the shelf edge whereas those offshore of the trough mouth are incised on the upper continental slope (Dowdeswell et al., 2004a; Noormets et al., 2009; Livingstone et al., 2013).

Morphological, ~~and~~ sedimentological and geochronological analysis of the landforms identified on the continental shelf has revealed that the LGM occurred around 18 000 yr BP (e.g. Kennedy and Anderson, 1989; Heroy and Anderson, 2007; Ó Cofaigh et al., 2014) and ice-sheet retreat began on the outer shelf of Marguerite Bay by 14 000 cal yr BP (Bentley et al., 2005; Heroy and Anderson, 2007; Kilfeather et al, 2011; Ó Cofaigh et al., 2014). A first stage of rapid retreat coincided with the sea-level rise of Meltwater Pulse 1a (Heroy and Anderson, 2007; Kilfeather et al., 2011). The ice sheet remained grounded on the inner shelf and an ice shelf formed beyond the grounding-zone at that time. Retreat then became more episodic (Ó Cofaigh et al., 2014); the ice shelf broke-up and the calving front retreated slowly from ca. 13.2 to 12.5 ka B.P. across the outer and mid-shelf, probably linked to an incursion of Weddell Sea Transitional Water onto the shelf. Finally, ice retreated into the inner bay from 9.3 ka B.P. (Kilfeather et al, 2011), and this retreat is interpreted to have been rapid (Allen et al., 2010; Ó Cofaigh et al., 2014). A two-step deglacial model in Marguerite Bay has been proposed, with a first stage related to rapid sea-level rise during ~~meltwater~~ Meltwater ~~pulse~~ Pulse 1-a at ~~9.6~~14.2 ka BP, when grounded ice retreated to the area coincident with the transition from crystalline bedrock to soft sedimentary substrate, and a second phase shortly before 9.6 ka, when the intrusion of Circumpolar Deep Water provoked the rapid thinning of the ice cover (Bentley et al., 2011). During the Holocene sedimentation in Marguerite Bay has been linked to oceanographic variability (Peck et al., 2015). During the early Holocene incursions of the warm upper circumpolar deep water (UCDW) led to extensive glacial melt and limited sea ice, from 9.7 to 7.0 ka BP. The influence of this water mass decreased through the mid Holocene, with seasons of persistent sea ice by 4.2 ka BP followed by a succession of episodic incursions of UCDW during the late Holocene (Peck et al., 2015). ~~o~~Open-marine conditions existed between 8 000 and 2 700 14C yr BP, with a climatic optimum between 4 200 and 2 700 yr BP in Lallemand Fjord, 16 km north of Bourgeois Fjord (Fig. 1B; Shevenell et al., 1996). A modest glacier advance between 2 850 and 2 500 cal. yr BP has been described in Neny Fjord, which drains into Marguerite Bay south of Bourgeois Fjord (Fig. 1B; Allen et al., 2010). The Little Ice Age has been recorded in several areas of the Antarctic Peninsula. Neoglacial cold events associated with the LIA produced an ice-shelf advance approximately 400 years ago in Lallemand Fjord (Shevenell et al., 1996). Sedimentological studies in Barilari Bay (Graham Land) constrained this event to ca. 730-82 cal. yr B.P. by, and its effect has been compared with other records, showing that the LIA was regionally synchronous in the Pacific and Atlantic southern sectors (Christ et al., 2014). Recently,

Formatted: Font color: Text 2

Formatted: Font color: Text 2

Formatted: Font color: Text 2

grounded ice cover in the Marguerite Bay region has experienced a general retreat since the late 1920s with the largest observed changes from glaciers with small drainage basins (Fox and Cooper, 1998). This general retreat is related to the 'recent rapid regional warming' described for the Antarctic Peninsula over the past half-century (Vaughan et al., 2003).

Formatted: Font color: Text 2

3. Datasets and methodology

Datasets for this study were acquired during cruise JR-157 of RRS *James Clark Ross* (JCR) in 2007 (Fig. 1). They include observations from both a Remotely-Operated Vehicle (ROV), *Isis*, and from hull-mounted instruments on the JCR. The ROV was configured to deploy several types of instrument. An MS-2000 multibeam swath-bathymetry system was fitted to the *Isis* ROV and flown about 20 m above the seafloor at speeds of less than 0.5 knots, giving a swath width of about 60 m. The multibeam system operated at a frequency of 200 kHz, with an equidistant beam configuration of 128 beams giving a swath width of 120°. Horizontal resolution is better than 0.5 m (Dowdeswell et al., ~~2008b~~2008b). An *Isis* ROV dive was carried out along a transect close to the tidewater ice cliffs of Forel Glacier in Blind Bay at the head of the main Bourgeois Fjord (Fig. 1). Three parallel navigation lines were acquired, resulting in a high-resolution bathymetric mosaic of approximately 0.6 km-width. During the *Isis* dive, video records~~,~~ and high-resolution photographs ~~and digital still images~~ of the seafloor were taken using *Pegasus* and *Scorpio* cameras, when the ROV was flown at about 0.6 m above the seafloor at a speed of approximately 20 cm s^{-1}. ~~A~~ 10 cm-spaced~~wide~~ laser beams ~~was~~were used in all cases to provide a scale for the imagery.

Hull–mounted equipment on board the JCR included an EM-120 *Kongsberg-Simrad* multibeam swath-bathymetry system with 191 beams displaying a maximum swath width of 150°, operating at frequencies between 11.25 and 12.~~6~~ 75 kHz and ~~providing~~ enabling generation of grids with a horizontal resolution averaging 20 m. Navigation data were obtained from ~~D~~GPS and data processing and production of maps were performed with *Caris*, *Mirone* and *Fledermaus* software. The TOPAS PS 018 system operated with a primary frequency of ~~15~~ 18 kHz and a secondary frequency in the range of 0.5-5 kHz was used to obtain sub-bottom profiles. It provides a vertical resolution better than 1 m. Data were processed with TOPAS software.

Glacier-terminus change information and glacier-catchment areas were calculated using data made available by the USGS Coastal-Change and Glaciological Maps of Antarctica project (Williams et al., 1995; Fretwell et al., 2013; Cook et al, 2014) and from LIMA mosaics provided by the USGS EROS Data Center and constructed using Landsat images gathered between 1999 and 2002.

4. Results

4.1. Echo-type description, distribution and interpretation

Three echo-types were identified in Bourgeois Fjord and Blind Bay from the analysis of sub-bottom profiler records. The description, distribution and interpretation of echo-types are shown in Figure 2, integrating the classical criteria of Damuth (1980), Kuhn and Weber (1993) and Droz et al. (2001) for echo-facies characterization and the seismic facies attributes, such as the acoustic amplitude, lateral continuity, geometry and internal configuration of reflections on parametric profiles (Payton, 1977; Veeken, 2007). A non-penetrative echo-type (I) is dominant in the study area and represents irregular surfaces of outcropping bedrock, coarse deposits and/or high gradients that prevent the penetration of the acoustic signal. It includes two subtypes. Echo-type IA represents a very irregular, non-penetrative seafloor reflection and is the predominant type in the main and outer fjord. Echo-type IB represents a smooth non-penetrative seafloor reflection and is present mostly close to the fjord walls and on the seafloor of Blind Bay (Fig. 2). A transparent-chaotic echo-type (II) occurs only locally, forming patches on the seafloor of both relatively shallow and deep areas of the fjord. It consists of transparent deposits of an irregular, mounded-shaped geometry, or thin packages of transparent-chaotic reflections. Echo-type III is stratified and represents smooth distinct parallel-layered reflections with relatively high acoustic amplitude. It occurs locally in deep, flat areas of the main and outer fjord and results from fine-layered sedimentation (Fig. 2).

4.2. Physiography of Bourgeois Fjord

Multibeam swath-bathymetric mapping allows the physiography of Bourgeois Fjord and Blind Bay to be mapped in detail (Fig. 1). The fjord system includes a central, main fjord, north of 67° 37'S, which terminates in Blind Bay at its northeastern end. The main fjord is separated by a relatively shallow 300 m deep sill from a narrower outer fjord that opens westwards into Marguerite Bay (Fig. 1). The main fjord is a 9~~-0~~~~0~~ km^2 semi-closed basin up to 665 m deep that receives direct meltwater and iceberg input from several tidewater glaciers. Lliboutry, Perutz and Bader glaciers as well as part of the ice fed from Heim Glacier drain into the main fjord today, and Forel and Barnes glaciers have calving fronts in Blind Bay (Fig. 1).

The main fjord is 455-665 m deep and displays a U-shaped cross-profile (Fig. 1). The eastern sector has a NNE-SSW-orientation and is about 3 km wide. It displays a relatively flat floor at depths of 530-540 m. The central sector of the main fjord is E-W oriented and 4.5 km wide on average, with a more irregular seafloor at depths ranging from 445-560 m. A prominent SE-NW-oriented high, up to 2.2 km wide, occurs in the SE part of the basin, off the mouth of Perutz Glacier. The western sector of the main fjord is NE-SW oriented, with an average width of 4.2 km and a maximum depth of 665 m. The main Bourgeois

Fjord connects with Marguerite Bay through an outer fjord that consists of a relatively narrow NE-SW-oriented channel between Pourquoi Pas Island and Ridge Island (Fig. 1). The outer fjord is 450-680 m deep, about 35 km long and 1-3 km wide. It presents a markedly irregular seafloor with numerous topographic highs.

4.3. Fjord Seafloor Landforms

4.3.1. Bourgeois Fjord

The main Bourgeois Fjord presents a typical U-shaped cross profile, with steep fjord walls and a relatively flat deep seafloor and can be divided into three sectors - proximal, central and distal – each with distinct morphological and physiographic characteristics (Fig. 3). The *proximal sector* is NNE-SSW-oriented and is approximately 7 km long and 3 km wide. The seafloor is relatively flat at depths of 520-550 m and presents smooth-floored elongate basins that parallel the fjord trend with a stratified echo-type (III), suggesting a fine-laminated sedimentary bed, and a weak ridge-and-valley topography (Figs. 3B and 3D) characterized by irregular non-penetrative echo-type, implying a mainly rock bed.

The *central sector* is E-W-orientated and is 7 km long and 5 km wide (Fig. 3). The seafloor is 450-570 m deep and markedly irregular. The northern wall presents numerous arcuate scarps. Here the fjord floor presents smaller flat basins, delimited by N-S to NW-SE-oriented escarpments (Fig. 3B). A NW-SE-oriented prominent morphological high occurs off the terminus of Perutz Glacier and displays some elongate ESE-WNW-oriented features on its top. To the west the seafloor is characterized by irregular morphological highs displaying non-penetrative echo-type (IA). Morphological highs become more elongate and crag-and-tail shaped towards the distal zone (elongation ratio - length:width - of 2:1 to 3:1). Small, irregular channels with a dendritic convergent pattern and small flat basins occur between the morphological highs (Figs. 3B and 3E).

The *distal sector* is NE-SW-oriented, about 8 km long and 5 km wide (Fig. 3D). A shallow area connects the terminus of Lliboutry Glacier with the main fjord and displays NE-SW-oriented morphological highs that delimit deep elongate basins off the glacier front. The main fjord floor in the distal sector is characterized by elongate, crag-and-tails (elongation ratios of 2:1 to 4:1), channels and low relief lineations with irregular non-penetrative echo-type (IA) suggesting bedrock cropping out at the seafloor (Figs. 3B and 3F). A flat basin occupies the distal area at depths averaging 660 m and is of stratified echo-type (III), implying fine-layered sedimentation (Fig. 2).

The outer fjord connects the main Bourgeois Fjord with Marguerite Bay (Figs. 1 and 4). Arcuate scarps occur on the steep fjord walls, where the predominant echo-type is irregular, non-penetrative (IA) (Fig.

2). The sector between Pourquoi Pas and Ridge islands is characterized by streamlined features with high elongation ratios of 2:1 to 5:1 (Figs. 4D and 4E) and channels oriented parallel to the fjord long-axis (Fig. 4E). To the SW some minor crag-and-tail features and weak lineations are observed and the seafloor is markedly irregular, with some morphological highs and relatively flat basins with stratified echo-type (III) and scarcer and smaller elongate features (Figs. 2 and 4). Together this implies small basins filled with fine-layered sediments separated by bedrock highs.

4.3.2. Blind Bay

The inner 4 km of Blind Bay has been mapped at high-resolution using a combination of *Isis* and *JCR* multibeam data (Figs. 5 and 6), and a transect of photographs acquired by the *Isis* ROV has been used for characterizing the seafloor (Fig. 7). The submarine landform assemblage of inner Blind Bay includes a large transverse ridge at its ice-distal end (Fig. 5). Inside this ridge, arcuate-shaped and longitudinal ridges, finger-like ridges with straight lineations, transverse escarpments and channel-like features are present (Fig. 5). The dimensions of these landforms and their main characteristics are given in Table I.

Formatted: Font: Italic

The distal transverse ridge occupies the entire width of the bay at about 4 km from the front of Forel Glacier (Fig. 5). It is responsible for the step-like, landward-deepening profile of the inner sector of Blind Bay. The ridge is markedly asymmetric, with a gentle ice-proximal face and a steeper ice-distal face (up to 25º, 40-70 m high; Fig. 5D). TOPAS profiles show smooth non-penetrative echo-type IB along the inner sector, reflecting coarse surficial sediment, and stratified echo-type (III) suggesting layered sedimentation in the proximal part of the outer sector (at the foot of the ridge) that becomes non-penetrative seawards (Fig. 5D).

Three crescent-shaped ridges are identified in the inner sector of Blind Bay (Fig. 5), where the seafloor is generally characterized by the irregular non-penetrative echo-type IA (Figs. 2 and 5D). The largest arcuate ridge is up to 25 m high and 500 m wide and occupies the central part of the Blind Bay inner sector, delimiting a relatively flat basin floor. The ridge is asymmetric with a steeper, convex-downstream ice-distal face and straight lateral flanks parallel to the bay limits (Figs. 5B and 5C). Two crescent-shaped ridges of similar morphological characteristics but smaller in size occur at more ice-proximal positions (Fig. 5). The middle ridge is displaced to the eastern fjord flank, whereas the most ice-proximal one is located about 1 km from the Forel Glacier front at depths of 280-290m. Longitudinal ridges are identified along lateral positions in the inner sector of Blind Bay (Fig. 5). Overall, the eastern ridges are higher (up to 10 m high), with a consistent NE-SW trend slightly oblique to the fjord walls. To the west, ridges are smaller (up to 2 m high) and their trend is NNE-SSW.

Finger-like ridges are identified in the high-resolution *Isis* swath-bathymetric mosaics and occur within the flat area delimited by the distal crescent-shaped ridge, at depths of 245-270 m (Figs. 5 and 6). They are up to 1 km long and relatively narrow (5-50 m wide). They are generally asymmetric with steeper eastern flanks (up to 22º) that delimit relatively flat areas (Fig. 6). Their orientations vary between 320º and 350º and they display highly variable shapes in a complex overlapping pattern. The proximal irregular ridges are markedly elongate and display arcuate, concave-eastward shapes, slightly oblique to the regional gradient. In contrast, the more distal ridges are much more irregular and display arcuate, finger-shape trends with concave-landward distal fronts up to 5 m high. Lineations have been identified on the *Isis* high-resolution swath-bathymetry data at depths of 240-280m (Fig. 6). They present sharp terminations toward the ridges, to which they are parallel to oblique in orientation. Lineations are straight with consistent orientations varying basinward from 330º to 310º (parallel to the basin trend) and are spaced 3-20 m apart. They are up to 20 m long and less than 1 m high with slope gradients of up to 5º.

The most ice-proximal part of the bay presents an irregular topography (Fig. 5) with an irregular non-penetrative echo-type IA (Fig. 2). There is a series of NW-SE-oriented transverse escarpments which are up to 10 m high and asymmetric, with smoother ice-proximal flanks (5-10º steep) and steeper (up to 18º) distal fronts (Figs. 5A and 5B). A network of diverging channel-like features occurs on the NW fjord wall, approximately 500 m from the Forel Glacier front (Figs. 5A and 5B). The system is about 500 m long, and individual channels are up to 80 m wide and 35 m deep.

A longitudinal transect of photographs was acquired by the *Isis* ROV along inner Blind Bay (Fig. 7). The photographs show a transition in seafloor character between about 1 and 3 km from the modern ice front (Fig. 7B). There is a progressive change from a predominance of relatively small ~~boulder~~clastclasts with angular shapes, little or no fine sediment drape and weak colonization by benth~~on~~ic organisms (Fig. 7B, Photo 1), to a wider range of sizes and shapes of ~~boulder~~clasts, including relatively large ones, a thicker and widespread sediment drape that covers completely the seafloor at the most distal positions, and a higher abundance of benth~~on~~ic organisms (Fig. 7B, Photos 2 and 3). Individual or grouped ~~boulder~~clasts on the floor of Blind Bay display striated surfaces and sub-rounded faces, but most ~~boulder~~clasts have faceted and angular shapes. The upper surfaces of many ~~boulder~~clasts are covered by a thin layer of sediment, and they are weakly colonized by benth~~on~~ic organisms (Fig. 7B, Photos 2 and 3). Photographs from the proximal areas show the presence of eroded bedrock on the inner fjord wall (Fig. 7C, Photo 4). The area with irregular ridges shows ~~boulder~~clasts of heterogeneous size, but of larger dimensions, than those in the surrounding areas covered by a thin sediment drape and is poorly colonized by benthic organisms (Fig. 7C, Photos 5 and 6).

5. Discussion

5.1. Interpretation and distribution of landforms

The interpretation of the landforms in Bourgeois Fjord identified in this work can be integrated with a compilation of morphological and geophysical studies of the continental shelf of Marguerite Trough in order to obtain a complete understanding of the system (Fig. 8). The inner shelf offshore of Bourgeois Fjord is characterized by crag-and-tails in areas of mixed bedrock and unconsolidated sediment (Livingstone et al., 2013, 2016). Further seawards, a succession of landforms with increased elongation ratios (parallel gouges, streamlined hills and bedrock outcrops, whalebacks, drumlins and MSGLs) on the mid-shelf marks the transition from crystalline bedrock, where subglacial meltwater channels are also incised, to sedimentary bedrock (Ó Cofaigh et al., 2005; Anderson and Fretwell, 2008; Livingstone et al., 2013, 2016). The middle to outer shelf is characterized mainly by the presence of streamlined bedrock outcrops, drumlins and MSGLs and by a series of grounding-zone wedges and scarps (Ó Cofaigh et al., 2005). The outer shelf displays MSGLs and, in relatively shallower water iceberg ploughmarks proximal to the shelf edge, into which numerous short gullies are incised (Dowdeswell et al., 2004a; Ó Cofaigh et al., 2005; Livingstone et al., 2013, 2016).

The morphological and acoustic characterization and the environmental and geological setting of the submarine landforms in Bourgeois Fjord and the continental shelf of Marguerite Trough allows the differentiation of four major morpho-sedimentary systems that reflect different stages of the last glacial cycle through the Bourgeois Fjord and Blind Bay system, involving specific sedimentary processes: 1) Glacial advance, full-glacial and early deglacial system; 2) Subglacial and ice-marginal meltwater system; 3) Glacial retreat system (APIS retreat and Little Ice Age re-advance and retreat); and 4) Holocene mass-wasting system (Fig. 9). The detailed interpretations of each of the landform types described above is given in Table I.

5.1.1. Glacial advance, full-glacial system and early deglaciation

The flow of ice through the Bourgeois Fjord system during the last full-glacial, when the APIS advanced to the shelf edge and an ice stream was present in Marguerite Bay (e.g. Anderson et al., 2002; Heroy and Anderson, 2007; Livingstone et al., 2013, 2016; Ó Cofaigh et al., 2014), is indicated by the broad-scale physiography and the landform assemblage in the main and outer Bourgeois Fjord areas (Fig. 9A). The main and outer fjord are characterized by bedrock landforms that increase in their elongation ratio down-fjord (from 2:1 to 5:1) and have crag-and-tail morphologies indicating westward ice flow towards Marguerite Bay (Figs. 3 and 4). Similar progressive elongation of whalebacks in the inner and middle

shelf of Marguerite Bay (2:1-4:1 to 18:1; Livingstone et al., 2013) and the transition to more elongate morphologies (drumlins, MSGLs) towards more distal areas of the shelf (Fig. 8; Ó Cofaigh et al, ~~2004~~2014; Livingstone et al., 2013~~.~~, 2016) suggest that processes forming the landforms in the main and outer Bourgeois Fjord are similar to those that acted in Marguerite Bay, and that they reflect the subglacial erosion and sculpting action typical of an accelerating ice stream (e.g. Wellner et al., 2006; Graham et al., 2009). Streamlining is assumed to result from subglacial erosion of bedrock (e.g. bedrock lineations, whaleback features), or from the shaping of till and/or bedrock by subglacial erosion and/or deposition (e.g. drumlins, crag-and-tail features) (Bradwell et al., 2008; Ottesen et al., 2008; Livingstone et al., 2013). In Bourgeois Fjord, these landforms appear to evolve from irregular erosional crystalline bedrock highs characterized by a hard, irregular sea-floor with no acoustic penetration (acoustic facies IA; Fig. 2) into elongate, more streamlined landforms (Fig. 8). This suggests an increasing sedimentary component of the substrate (e.g. Wellner et al., 2006; Graham et al., 2009; Livingstone et al., 2012). It is important to note that landforms sculpted in bedrock may reflect the cumulative activity of fast-flowing ice over successive glacial cycles, not simply during the LGM (Graham et al., 2009; Smith et al., 2009; Livingstone et al., 2013; Krabbendam et al., 2016). Lineations in Bourgeois Fjord appear to result from the action of rapid ice flow on bedrock with a relatively thin sedimentary cover, as revealed by the TOPAS record and submarine photographs (Figs. 2 and 7) and are therefore not as well-developed as the sets of MSGLs found on the sedimentary floor of many Antarctic cross-shelf troughs, including those in Marguerite Bay, that reflect ~~an increase in the~~a greater thickness of deformable sedimentary substrate (e.g Dowdeswell et al., 2004b; Ó Cofaigh et al., 2005; Spagnolo et al., 2016).

Flow acceleration, probably in combination with the change in the substrate, may also be responsible for the increased elongation of glacial landforms with distance down Bourgeois Fjord. Ice flow may have been accelerated due to the convergence of flows from a number of drainage basins that merged into the fjord as the ice sheet over Graham Land grew towards it maximum LGM extent and thickness (Figs. 1, 8 and 9A) (e.g. Anderson and Fretwell, 2008; Larter et al., 2009).

The relatively deep elongate basins offshore of Lliboutry Glacier (Fig. 3A) probably record the activity of advancing ice fed from Lliboutry and probably from Heim glaciers, the latter reaching Bourgeois Fjord through the channel north of Blaiklock Island (Fig. 1). The basins form perched platforms at varying depths that seem to be delimited by NE-SW-trending highs. Transverse bedrock escarpments (Figs. 3B, 5B) indicate subglacial quarrying or plucking by the advancing ice sheet on bedrock with differential resistance to erosion in the most proximal area of the main fjord and also in Blind Bay (Dünhforth et al., 2010). The orientation of the escarpments appears to reflect structural control by the NE-SW and NW-SE-oriented regional tectonic fabric related to the NW-SE-oriented fault zones developed during ~~the~~

extension in the Marguerite Bay area before about 20 Ma ago (Johnson, 1997), which may have been related to movement on the West Antarctic Rift System (Eagles et al., 2009).

Formatted: Font color: Text 2

5.1.2. Subglacial and ice-marginal meltwater system

The meltwater system includes channels and small flat basins in the deeper areas of Bourgeois Fjord and on the lower fjord wall in the inner sector of Blind Bay (Fig. 9B). Channels in the main and outer Bourgeois Fjord (Figs. 3 and 4) are interpreted as subglacial meltwater channels eroded into crystalline bedrock, which are common features in many high-latitude inner-shelf and fjord areas, especially where crystalline bedrock predominates (e.g. Lowe and Anderson, 2002; Domack et al., 2006; Anderson and Fretwell, 2008; Smith et al., 2009; Nitsche et al., 2013; Hogan et al., 2016). Similarly to other bedrock erosional glacial landforms, they may record erosion through multiple glaciations (Ó Cofaigh et al., 2002; Graham et al., 2009; Smith et al., 2009; Krabbendam et al., 2016). The more distal channels in the main and outer Bourgeois Fjord are interconnected with small basins limited by morphological highs and tend to open to large basins further down-fjord (Figs 3B and 4B). Smaller channels in inner Blind Bay are related directly to the present-day location of the tidewater terminus of Forel Glacier (Fig. 5B) and, although they may have formed subglacially, provide a continuing conduit for dense underflows of mixed seawater and fresh meltwater ~~and~~ loaded with subglacially-derived suspended sediment released directly from the terminus of the glacier (~~c.f. Powell, 1990~~Gales et al., 2013). The channels in Bourgeois Fjord form an isolated drainage network due to the shallowing of the seafloor towards the outer fjord, which impedes a connection with the meltwater channels network in the Marguerite Bay inner- and mid-continental shelf (Ó Cofaigh et al., 2005; Livingstone et al., 2013; Hogan et al., 2016; Fig. 8).

Areas of flat seafloor, with stratified reflections on sub-bottom profiles (Fig. 2), suggest sedimentation by glacimarine processes after deglaciation (e.g. Smith et al., 2009; Ó Cofaigh et al., ~~In Press a~~2016). A number of processes may be involved, such as tidal pumping of the grounding lines that generate sorted, laminated sediment (Domack et al., 1999; Evans et al., 2005**;** Kilfeather et al., 2011), or marine derived detritus supplied from the grounding line. Furthermore, meltwater plumes containing fine-grained suspended sediments exiting the glacier terminus from a basal drainage system may also produce debris rain-out that would infill the small basins (Powell, 1990; Cowan, 2001; Lowe and Anderson, 2002; Domack et al., 2006; Mugford and Dowdeswell, 2011; Dowdeswell et al., 2014, 2015; Ó Cofaigh et al., ~~In Press~~2016). The easternmost NE-SW-oriented basins would have received sediment input from Blind Bay, whereas the westernmost ones would include suspended sediment delivered from Lliboutry Glacier. These acoustically-stratified sedimentary deposits are separated by morphological highs of irregular bedrock in the middle reaches of Bourgeois Fjord (Fig. 4B).

5.1.3. Glacial retreat and neoglaciation system

There are few signs of transverse-to-ice-flow depositional ridges in the outer and main parts of Bourgeois Fjord (Figs. 4 and 5), such as grounding-zone wedges or large retreat moraines (e.g. Batchelor and Dowdeswell, 2015), that could be associated with still-stands during deglacial ice-sheet retreat. An implication of this is that ice-sheet retreat through Bourgois Fjord probably took place relatively rapidly once ice had retreated from the shelf and Marguerite Bay at or shortly after 9,000 years ago (Kilfeather et al., 2011). The fjord system appears, therefore, to have been influenced mainly by glacimarine processes during the Holocene. The glacial retreat system we have mapped is restricted to relatively small-scale morainic landforms identified in the inner sector of Blind Bay, including the distal transverse ridge, the crescent-shaped and longitudinal ridges and the finger-like ridges associated with lineations (Figs. 5B and 9C). The well-preserved appearance of these features indicates that they have not been over-ridden by a subsequent glacier advance and may well be relatively recent features relating to the final post-glacial retreat or to recent neoglacial fluctuations of a few kilometres in the position of the glacier termini in Blind Bay (Fig. 9C). We suggest that these neoglacial cold events are associated with the LIA that has been recorded in neighbouring areas of the Antarctic Peninsula, such as Lallemand Fjord where an ice-shelf advance occurred approximately 400 years ago (Shevenell et al., 1996), probably in relation to the exclusion of ~~circumpolar~~ Circumpolar ~~deep~~ Deep ~~water~~ Water from the fjord (Domack et al., 1995), or Rothera Point, that experienced a glacial advance between 671 and 317 cal yr. BP (Guglielmin et al., 2007). Although the LIA cooling phase was not synchronous between sites, it has been widely documented in Antarctica, where temperatures ~2º colder were registered from ice cores from the Ross Sea area at about 1300 to 1850 AD (Bertler et al., 2011), roughly coinciding with temperature~~s~~ estimates 0.52±0.28ºC colder than the last 100-year average at the West Antarctic Ice Sheet divide (Orsi et al., 2012).

The distal transverse ridge in Blind Bay is interpreted as an ice-marginal moraine (Figs. 5B and 9C), based on its echo-type and typical asymmetrical morphology with a steeper ice-distal face (Dowdeswell and Vasquez, 2013). This moraine was deposited at the glacier terminus when the grounding-zone was maintained in a relatively stable position in the middle reaches of Blind Bay (e.g. Ottesen et al., 2005; Dowdeswell et al., 2014). The location suggests stabilization of the ice front probably related to the narrowing of Blind Bay (Jamieson et al., 2012; Rydningen et al., 2013), and/or to the presence of a topographic high that may also have acted as pinning point.

Crescent-shaped and longitudinal ridges in the inner sector of Blind Bay (Fig. 5B) are interpreted as recessional moraines (Fig. 9C). They are sedimentary landforms composed of unsorted ~~boulder~~clast~~s~~ and

418 finer sediment (Fig. 7). These features are deposited at the front of glaciers during still-stands or re-
419 advances during a general phase of ice retreat (e.g. Bennett et al., 1999; Ottesen and Dowdeswell, 2006,
420 2009; Johnson et al., 2013). Their dimensions and location in Blind Bay suggest formation during shorter
421 still stands than those linked to the larger transverse moraine ridge and their presence in inner Blind Bay
422 is probably linked to the progressive recession of the ice front, reflecting a slow ice-retreat pattern
423 (Ottesen and Dowdeswell, 2006; McLachlan et al., 2010; Bjarnadóttir et al., 2014; Batchelor and
424 Dowdeswell, 2015). Longitudinal ridges converge towards the centre of the bay (Fig. 5) and probably
425 represent the lateral parts of recessional moraines from which the fronts have been eroded and/or
426 reworked by successive small ice readvances and/or by meltwater flow. Crescent-shaped ridges seem to
427 overlay the longitudinal ridges and are interpreted as the frontal ridges of well-preserved moraines over
428 which no significant reworking by ice readvance has occurred. Blocks and rafts showing signs of
429 glacitectonic erosion are evident in the seafloor photographs that show striated and angular ~~boulder~~clasts
430 (Fig. 7) suggesting short transportation distances of the material after being incorporated into the
431 moraines by bedrock plucking during grounded ice readvance (Laberg et al., ~~2007~~2009).

432 *Finger-like ridges* delimiting *short straight lineations* (Figs. 5B and 6) are the most striking features
433 identified in ROV-acquired high-resolution bathymetric images. They are interpreted as 'ice-fingerprints',
434 having formed by the pushing or ploughing of sediment by minor readvances of the grounded glacier
435 terminus within inner Blind Bay (e.g. Geirsdottir et al., 2008, 2016; Bjarnadottir et al., 2014). The highly
436 elongate shape and variable size of the finger-like ridges (Fig. 6) suggests a very irregular, non-linear ice
437 margin advancing and retreating during the very last stages of glacial retreat. The pervasive, straight
438 lineations delimited by the ridges suggest deformation of soft sediment by the glacier, and are interpreted
439 as lateral push-ridges formed by a non-linear advancing ice front, overprinted by the finger-like ridges.
440 Ice flow may have been constrained by the relief of the ice-marginal transverse moraine that acted as a
441 morphological threshold buttressing minor readvances of the grounded tidewater glacier (Fig. 9C). These
442 features suggest a depleting ice source being drained by bands of faster flowing ice (e.g. Todd and Shaw,
443 2012) and point to a final ice-mass retreat occurring in episodic events with massive iceberg calving.

444 5.1.4. Holocene mass-wasting system

445 Mass-wasting has taken place in Bourgeois Fjord since ice retreated through the steep-sided fjord system
446 to about its present position <9,000 years ago (Kilfeather et al., 2011). Several *debris lobes* mapped close
447 to the margins of Barnes and Bader glaciers (Fig. 3B) are probably related to the failure and downslope
448 flowage of relatively rapidly deposited debris close to the tidewater termini of these glaciers (e.g. Laberg
449 et al., 2009; Dowdeswell et al., 2015), although the relatively coarse resolution of the JCR multibeam data

precludes more detailed analysis. Debris lobes sometimes appear stacked on the lower fjord walls, implying a short displacement that reflects the coarse and unsorted nature of the sediment supplied by subglacial erosion (Garcia et al., 2009). Mass-wasting processes on the walls of Bourgeois Fjord (Fig. 9D), and close to the foci of continuing sediment delivery at tidewater glacier margins (cf. Ottesen and Dowdeswell, 2009; Dowdeswell et al., ~~In Press~~2016), have probably been operating throughout the Holocene since ice retreated through the fjord system about 8-9,000 years ago and continue to operate today (Shevenell et al., 1996; Kilfeather et al., 2011).

5.2. Ice dynamics inferred from landform distribution and sedimentary characteristics

Most landforms in Blind Bay and Bourgeois Fjord indicate a glacial origin related to flow of active ice and can be attributed to specific stages of the last glacial cycle (Fig. 9), although streamlined bedrock landforms may have evolved over successive glacials. Landforms of the glacial advance and full-glacial system (Fig. 9A) correspond to the ice-growth, glacial maximum and early deglaciation, in a setting dominated by active ice flowing down-fjord. The morphological evidence in this area reflects the imprint of the grounded ~~palaeo ice stream~~ice advance, in a similar manner to the neighbouring area of Gerlache Strait continental shelf, dominated by streamlined subglacial bedforms (Evans et al., ~~2004~~2005; Canals et al., 2016). A full-glacial outlet glacier flowing between the steep fjord walls of Bourgeois Fjord appears to have produced crag-and-tails (Figs. 3B and 4B), whose characteristics and distribution along the fjord suggest a transitional flow towards the development of a fast-flowing ice stream (e.g. Wellner et al., 2001). The latter probably required a deformable sedimentary bed similar ~~that~~ to that which occupied the outer part of Marguerite Trough (Ó Cofaigh et al., 2002, 2005, 2008; Dowdeswell et a., 2004a,b; Kilfeather et al., 2011). The convergence of glacier flow into Bourgeois Fjord, implied by the present configuration of tidewater glaciers and their adjacent fjords (Fig. 1), suggests acceleration associated with increasing ice flux, which may also be inferred from the increase in landform elongation downstream (Wellner et al., 2006; Bradwell et al., 2008; Graham et al., 2009). The presence of meltwater channels cut into the bedrock of the fjord floor (Fig. 9B) also implies active ice- and meltwater-flow with a bed at the pressure-melting point of ice. Ice flow from Bourgeois Fjord contributed to the Marguerite Bay palaeo-ice stream, the largest ice stream on the Antarctic Peninsula with an estimated drainage basin size of about 100 000 km^2, which reached the western Peninsula continental shelf edge through the Marguerite Bay cross-shelf trough (Fig. 1B; Livingstone et al., 2012).

The absence of transverse-to-flow sedimentary landforms in the outer and main Bourgeois Fjord suggests that ice retreated from Marguerite Bay into Blind Bay during the last deglaciation (Allen et al., 2010; Kilfeather et al, 2011; Ó Cofaigh et al., 2014) without leaving morphological evidence of any significant

Formatted: Superscript

Formatted: Font color: Green

Formatted: Font color: Text 2

stillstand. Evidence for a two-step deglacial model in Marguerite Bay locates grounded ice at the mid-shelf transitional area from crystalline bedrock to soft sedimentary substrate (Bentley et al., 2011), offshore of Bourgeois Fjord. In contrast, landforms in Blind Bay demonstrate that the deglacial/Holocene history in this inner region has been more complicated. Although precise details of timing are uncertain, other studies in neighbouring areas (i.e., the Larsen continental shelf, eastern Antarctic Peninsula) describe a relatively slow ice-stream recession punctuated by stillstands on the inner shelf, resulting in the deposition of a series of grounding-zone wedges (Evans et al., 2005). By contrast, other fjords in the Antarctic Peninsula display morphological features pointing to rapid deglaciation with no sign of retreat features (e.g. Simms et al., 2011; Minzoni et al., 2016). We suggest that grounding-zone wedges on the Marguerite Bay continental shelf (Fig. 8) are related to the same processes and timing, but in contrast the high degree of preservation and the morphological characteristics of glacial-sedimentary landforms in Blind Bay suggests that they may have formed relatively recently. We tentatively propose that the transverse moraines originated during the Little Ice Age, by analogy with similar features identified a few kilometres from modern tidewater glaciers in, for example, Chilean fjords (Dowdeswell and Vasquez, 2013). Transverse moraines have been related to glacier advances during the LIA, when valley glaciers readvanced and deposited ice-cored moraines in the West Antarctic region (Clapperton and ~~Sudgen~~Sugden, 1982; Shevenell et al., 1996) and also in the Antarctic Peninsula (Carrivick et al., 2012), and the Northern Hemisphere (Svalbard, Greenland; Ottesen and Dowdeswell, 2009; Funder et al., 2011; Dowdeswell et al., 2014). In summary, we propose early Holocene retreat through the fjord system followed by minor readvances of grounded ice in the inner part of Blind Bay, although the timing of these events needs confirmation.

Formatted: Font color: Text 2

Contrasting with the relatively complex recent Holocene history of glaciation in Blind Bay, the shallow areas off Lliboutry and Perutz glaciers in the main fjord show a relatively smooth seafloor and the absence of transverse-to-flow landforms, suggesting relatively limited ice-margin fluctuations since retreat to approximately their present position after regional deglaciation from the LGM. The differences in the style of deglaciation and recent fluctuations between adjacent tidewater glaciers can be attributed to local physiographic controls (Heroy and Anderson, 2007; Ó Cofaigh et al., 2008~~;~~, 2014). The locations of transverse ridges in Blind Bay may have been controlled, in part at least, by the reduction in width of the inner sector of the bay, increasing lateral drag on the tidewater glacier and reducing of the volume of ice required for maintaining a stable grounding-zone (Jamieson et al., 2012, 2014; Rydningen et al., 2013).

5.3. Pattern of retreat of tidewater glaciers during the last Century

Environmental-change studies have revealed a recent warming trend in the Antarctic Peninsula, resulting in a reduction of terrigenous sediment supply from retreating glaciers related to a final abrupt phase of climate amelioration corresponding to the 'rapid regional warming' of recent decades (Allen et al., 2010). The pattern of recent retreat of the tidewater glaciers draining into the Bourgeois Fjord system, together with the drainage basin-areas of these glaciers, has been compiled from satellite images, maps and aerial photographs for the period between 1947 and 2011 in order to analyse their recent fluctuations (Fig. 10; Table II). With the exception of Perutz Glacier, the glaciers have all undergone retreat since observations began in 1947 (Fig. 10). This is in agreement with a regional trend of glacier retreat in the Antarctic Peninsula over the past half-century (Cook et al., 2005, 2014). This 'recent rapid regional warming' has been related to a series of mechanisms such as changes in oceanographic and/or atmospheric circulation, or regionally amplified greenhouse warming driven by air-see-ice feedback processes (Vaughan et al., 2003).

Formatted: Font color: Text 2

Formatted: Font color: Text 2

Observations indicate a general pattern of retreat of the glacier fronts over the last six decades, with the retreat of individual glacier termini occurring in a non-systematic pattern (Fig. 10). Forel Glacier has undergone the maximum retreat (about 2.3 km in 64 years). This is the only glacier that displays a reverse gradient proglacial seafloor, which probably increases the rate of modern iceberg calving through increased buoyancy in progressively deepening water (Benn et al., 2007). An inverse relationship can also be tentatively established between drainage-basin size, glacier-terminus width and variations in terminus behaviour. As basin-size increases, the amount of glacier-terminus retreat is reduced. Thus, Perutz and Lliboutry glaciers, which have the largest drainage areas (Fig. 2), have retreated notably less than the smaller ~~Foral~~Forel, Barnes and Bader glaciers (Fig. 10). This is consistent with the work of Fox and Cooper (1998), who proposed that recent ice retreat has affected most markedly the extent of smaller ice bodies on the Antarctic Peninsula.

5.4. Controls on recent sedimentation in Bourgeois Fjord

In Bourgeois Fjord the major long-term controlling factor on the sediments and landforms we have observed is the growth and decay of ice in the fjord system, linked to the broader glacial-interglacial cycles that affected the APIS. This has resulted in the predominance of glacial advance/full-glacial landforms in the main and outer Bourgeois Fjord, whereas deglacial landforms, which are most likely late Holocene in age, are restricted to the inner sector of Blind Bay. The start of retreat at 9.3 ka B.P. has been linked to the influence of oceanographic factors, which involved the intrusion of modified Circumpolar ~~Warm~~ Deep Water onto the adjacent continental shelf (Kilfeather et al., 2011). Secondary factors controlling the distribution of landforms in Bourgeois Fjord include the structural setting, the seafloor

physiography and oceanographic factors. The structural control is revealed by the relationship between general trends in the direction of past ice-flow and erosion and the orientation of bedrock ridges on the fjord floor, with many NE-SW- and NW-SE-oriented features evident (Johnson, 1997; Anderson and Fretwell, 2008). The regional structural fabric is also reflected by perched terraces or basins in the shallow areas off Llibourty Glacier that appear to have been controlled by NE-SW-oriented structural features. The physiography of the fjords and adjacent mountains, established long before the last glacial cycle, influences in particular the width of glacier fronts and the size of catchment areas and, through this, exerts an influence on the most recent fluctuations of the tidewater glaciers in Blind Bay. Tidal pumping and deep-water currents are common processes involved in sediment dispersal and redeposition in tidewater-glacier influenced fjords (Syvitski, 1989) and they may have influenced the distribution of stratified sediment along Bourgeois Fjord.

6. Summary and conclusions

This study highlights the complexity of the last glacial retreat phase in Bourgeois Fjord and illustrates the importance of high-resolution geophysical observations for the reconstruction of past ice flow. The main conclusions are summarized as follows.

1. High-resolution geophysical evidence reveals a complex landform assemblage in Bourgeois Fjord that can be integrated with regional morphological studies of Marguerite Trough in order to analyse the complete fjord-to-continental shelf system. It is composed of four major morpho-sedimentary systems that resulted from specific processes and/or phases of the last glacial cycle. (i) A glacial advance and full-glacial system is manifested in the outer and main fjord and is composed mainly of streamlined-bedrock and crag-and-tail features that are genetically related to the landforms identified along the continental shelf. (ii) A meltwater system comprising channels and sediment-filled basins in the outer and main fjord. (iii) A well-preserved glacial retreat system is present in the inner sector of Blind Bay and includes a series of recessional sedimentary landforms. (iv) A Holocene mass-wasting system affects unstable glacial sediments on the walls of the fjord, reflected in the form of slide scars and associated fan-shaped deposits.

2. The glacial advance and full-glacial system was formed subglacially by the action of an active LGM outlet glacier that drained the APIS towards Marguerite Bay. A warm basal thermal regime is suggested by the landform distribution in the outer and main fjord, which includes subglacial channels. Ice flow in Bourgeo~~u~~is Fjord was probably characterized by a down-flow transition towards faster moving ice in the form of an outlet glacier from the LGM ice-sheet interior, as indicated by the progressive elongation of subglacially produced landforms.

3. A relatively rapid deglaciation of Bourgeois Fjord is implied by a lack of transverse-to-flow depositional landforms, in which the ice margin migrated landward to the inner fjords during retreat. Morphological evidence of margin stillstands and/or glacial readvances is found only in the inner sector of Blind Bay. Here, a major transverse moraine indicates grounded ice stabilization probably during the Little Ice Age, followed by minor readvance episodes.

4. The most recent evolution of the outlet glaciers draining into Bourgeois Fjord during the last six decades is not homogeneous. The range of variation of glacier-terminus fluctuations appears to depend on the physiography of the region, including catchment-area size and changing fjord width.

Acknowledgements

We thank the officers and crew of the RRS *James Clark Ross* and the *Isis* ROV team from the National Oceanography Centre, Southampton, for their help with data acquisition. The research was funded by a UK Natural Environment Research Council grant AFI06/14 (NE/C506372/1) to J.A. Dowdeswell, R.D. Larter and G. Griffiths. M. Garcia's work at the Scott Polar Research Institute, University of Cambridge, was funded by an EU Marie Curie Fellowship. We thank the Editor, Prof. John B. Anderson and another anonymous reviewer for their helpful comments and constructive suggestions to improve the original manuscript.

References

Allen, C., Oakes-Fretwell, L., Anderson, J.B., Hodgson, D., 2010. A record of Holocene glacial and oceanographic variability in Neny Fjord, Antarctic Peninsula. The Holocene 20, 551–564.

Amblas, D., Urgeles, R., Canals, M., Calafat, A.M., Rebesco, M., Camerlenghi, A., Estrada, F., De Batist, M., Hughes-Clarke, J.E., 2006. Relationship between continental rise development and palaeo-ice sheet dynamics, Northern Antarctic Peninsula Pacific margin. Quaternary Science Reviews 25, 993–944.

Anderson, J.B., 1999. Antarctic Marine Geology. Cambridge University Press, Cambridge.

Anderson, J.B., ~~Oakes-~~Fretwell, L.O., 2008. Geomorphology of the onset area of a paleo-ice stream, Marguerite Bay, Antarctic Peninsula. Earth Surface Processes and Landforms 33, 503–512. ~~Doi~~doi: 10.1002/esp1662.

Anderson, J.B., Shipp, S.S., Lowe, A.L., Wellner, J.S., Mosola, A.B., 2002. The Antarctic Ice Sheet during the Last Glacial Maximum and its subsequent retreat history: A review. Quaternary Science Reviews 21, 49–70.

Batchelor, C.L., Dowdeswell, J.A., 2015. Ice-sheet grounding-zone wedges (GZWs) on high-latitude continental margins. Marine Geology 363, 65–92.

Benn, D.I., Warren, C.R., Mottram, R.H., 2007. Calving processes and the dynamics of calving glaciers. Earth-Science Reviews 82, 143–179.

Bennett, M.R., Hambrey, M.J., Huddart, D., Glasser, N.F., Crawford, K., 1999. The landform and sediment assemblage produced by a tidewater glacier surge in Kongsfjorden, Svalbard. Quaternary Science Reviews 18, 1213–1246.

Bentley, M.J., Anderson, J.B., 1998. Glacial and marine geological evidence for the ice sheet configuration in the Weddell Sea–Antarctic Peninsula region during the Last Glacial Maximum. Antarctic Science 10, 309–325.

Bentley, M.J., Hodgson, D.A., Smith, J.A., Ó Cofaigh, C., Domack, E.W., Larter, R.D., Roberts, S.J., Brachfeld, S., Leventer, A., Hjort, C., Hillenbrand, C.-D., Evans, J., 2010. Mechanisms of Holocene palaeoenvironmental change in the Antarctic Peninsula region. The Holocene 19, 51–69.

Bentley, M.J., Hodgson, D.A., Smith, J.A., Cox, N.J., 2005. Relative sea level curves for the South Shetland Islands and Marguerite Bay, Antarctic Peninsula. Quaternary Science Reviews 24, 1203–1216.

Bentley, M.J., Johnson, J.S., Hodgson, D.A., Dunai, T., Freeman, S.P.H.T., Ó Cofaigh, C., 2011. Rapid deglaciation of Marguerite Bay, western Antarctic Peninsula in the Early Holocene. Quaternary Science Reviews 30, 3338–3349.

Bertler, N.A.N., Mayewski, P.A., Carter, L., 2011. Cold conditions in Antarctica during the Little Ice Age – Implications for abrupt climate change mechanisms. Earth and Planetary Science Letters 308, 41–51.

Bjarnadóttir, L.R., Winsborrow, M.C.M., Andreassen, K., 2014. Deglaciation of the central Barents Sea. Quaternary Science Reviews 92, 208–226.

Bradwell, T., Stoker, M., Krabbendam, M., 2008. Megagrooves and streamlined bedrock in NW Scotland: The role of ice streams in landscape evolution. Geomorphology 97, 135–156.

Canals, M., Amblas, D., Domack, E., Lastras, G., Lavoie, C., Casamor, J.L. and Smith, C., 2016. The seafloor imprint of the Gerlache–Boyd ice stream (65º to 62ºS), northern Antarctic Peninsula. In Dowdeswell, J.A., Canals, M., Jakobsson, M., Todd, B.J., Dowdeswell, E.K., Hogan, K.A. et al., (eds), Atlas of Submarine Glacial Landforms: Modern, Quaternary and Ancient. Geological Society, London, Memoirs, 46, 477-484. doi: 10.1144/M46.174.

~~Canals, M., Amblas, D., Domack, E., Lastras, G., Lavoie, C., Casamor, J.L. and Smith, C., 2016. The seafloor imprint of the Gerlache–Boyd ice stream (65º to 62ºS), northern Antarctic Peninsula. In Dowdeswell, J.A. et al., (eds), Atlas of Submarine Glacial Landforms: Modern, Quaternary and Ancient. Geological Society, London, Memoirs, v. 46.~~

Carrivick, J.L., Davies, B.J., Glasser, N.F., Nývit, D., Hambrey, M.J., 2012. Late-Holocene changes in character and behavior of land-terminating glaciers on James Ross Island, Antarctica. Journal of Glaciology 58, 1176–1190.

Christ, A.J., Talaia-Murray, M., Elking, N., Domack, E.W., Leventer, A., Lavoie, C., Brachfeld, S., Yoo, K.-C., Gilbert, R., Jeong, S.-M., Petrushak, S., Wellner, J., LARISSA Group, 2014. Late Holocene glacial advance and ice shelf growth in Barilari Bay, Graham Land, west Antarctic Peninsula. Geological Society of America Bulletin 127, 297–315. doi: 10.1130/B31035.1.

Clapperton, C.M., Sugden, D.E., 1982. Late quaternary glacial history of George VI Sound area, West Antarctica. Quaternary Research 18, 243–267.

Cook, A.J., Fox, A.J., Vaughan, D.G., Ferrigno, J.G., 2005. Retreating glacier fronts on the Antarctic Peninsula over the past half-century. Science 308, 541–544. doi: 10.1126/science.1104235.

Cook, A.J., Vaughan, D.G., Luckman, A.J., Murray, T., 2014. A new Antarctic Peninsula glacier basin inventory and observed area changes since the 1940s. Antarctic Science. 26, 614–624.

Cowan, E.A, 2001. Identification of the glacial signal from the Antarctic Peninsula since 3.0 Ma at Site 1011 in a continental rise sediment drift. In: Barker, P.F., Camerlenghi, A., Acton, G.D., Ramsay, A.T.S. (Eds.), Proceedings of the ODP, Scientific Results 178, 1–22.

Damuth, J.E., 1980. Use of high-frequency (3.5-12 kHz) echograms in the study of near-bottom sedimentation processes in the deep-sea: a review. Marine Geology 38, 51–75.

~~Rodrigo, C., Giglio, S., Varas, A., 2016. Glacier sediment plumes in small bays on the Danco Coast, Antarctic Peninsula. Antarctic Science doi:10.1017/S0954102016000237.~~

Domack, E., Amblàs, D., Gilbert, R., Brachfeld, S., Camerlenghi, A., Rebesco, M., Canals, M., Urgeles, R., 2006. Subglacial morphology and glacial evolution of the Palmer deep outlet system, Antarctic Peninsula. Geomorphology 75, 125–142.

Domack, E.W., Ishman, S., 1993. Oceanographic and physiographic controls on modern sedimentation within Antarctic fjords. Geological Society of America Bulletin 105, 1175–1189.

Domack, E.W., Ishman, S.C., Stein, A.B., McClennen, C.E., Jull, A.J.T., 1995. Late Holocene advance of the Muller Ice Shelf, Antarctic Peninsula: sedimentological, geochemical and palaeontological evidence. Antarctic Science 7, 159–170.

Domack, E.W., Jacobson, E.A., Shipp, S., Anderson, J.B., 1999. Late Pleistocene-Holocene retreat of the West Antarctic Ice-Sheet system in the Ross Sea: Part 2- Sedimentologic and stratigraphic signature. GSA Bulletin 111, 1517–1536. doi: 10.1130/0016-7606.

~~Domack, E.W., McClennen, C.E. 1996. Accumulation of glacial marine sediments in fjords of the Antarctic Peninsula and their use as Late Holocene paleoenvironmental indicators. Antarctic Research Series 70, 135–154.~~

~~Dowdeswell, J.A., Benham, T.J., Strozzi, T., Hagen, J.O., 2008. Iceberg calving flux and mass balance of the Austfonna ice cap on Nordaustlandet, Svalbard. Journal of Geophysical Research. Earth Surface 113, 1–12.~~

Dowdeswell, J.A., Ó Cofaigh, C., 2002. Glacier-influenced sedimentation on high-latitude continental margins: introduction and overview. Geological Society of London, Special Publication 203, 1–9.

Dowdeswell, J.A., Vásquez, M., 2013. Submarine landforms in the fjords of southern Chile: Implications for glacimarine processes and sedimentation in a mild glacier-influenced environment. Quaternary Science Reviews 64, 1–19.

Dowdeswell, J.A., Ó Cofaigh, C., Pudsey, C.J., 2004a. Continental slope morphology and sedimentary processes at the mouth of an Antarctic palaeo-ice stream. Marine Geology 204, 203–214.

Dowdeswell, J.A., Ó Cofaigh, C., Pudsey, C.J., 2004b. Thickness and extent f the subglacial till layer beneath an Antarctic paleo-ice stream. Geology 32, 13–16.

Dowdeswell, J.A., Benham, T.J., Strozzi, T., Hagen, J.O., 2008a. Iceberg calving flux and mass balance of the Austfonna ice cap on Nordaustlandet, Svalbard. Journal of Geophysical Research. Earth Surface 113, 1–12.

Dowdeswell, J.A., Noormets, R., Evans, J., Griffiths, G., Larter, R.D., Ó Cofaigh, C., 2008b. A comparison of swath-bathymetric imagery from high-latitude glacier-influenced fjords derived from AUV, ROV and shipboard systems. In: Collins, K., Griffiths, G. (eds.), Workshop on AUV science in extreme environments: collaborative Autosub science in extreme environments. Proceedings of the international science workshop, Cambridge, April 2007, London, Society for Underwater Technology, pp. 47–54.

~~Dowdeswell, J.A., Vásquez, M., 2013. Submarine landforms in the fjords of southern Chile: Implications for glacimarine processes and sedimentation in a mild glacier-influenced environment. Quaternary Science Reviews 64, 1–19.~~

Dowdeswell, J.A., Hogan, K.A., Ó Cofaigh, C., Fugelli, E.M.G., Evans, J., Noormets, R., 2014. Late Quaternary ice flow in a West Greenland fjord and cross-shelf trough system: submarine landforms from Rink Isbrae to Uummannaq shelf and slope. Quaternary Science Reviews 92, 292–309.

Dowdeswell, J.A., Hogan, K.A., Arnold, N.S., Mugford, R.I., Wells, M., Hirst, J.P.P., Decalf, C., 2015. Sediment-rich meltwater plumes and ice-proximal fans at the margins of modern and ancient tidewater glaciers: observations and modelling. Sedimentology, 62, 1665–1692,

Dowdeswell, J.A., Ottesen, D., Noormets, R., 2016. Submarine slides from the walls of Smeerenburgfjorden, NW Svalbard. In Dowdeswell, J.A., Canals, M., Jakobsson, M., Todd, B.J., Dowdeswell, E.K., Hogan, K.A., (Eds), Atlas of Submarine Glacial Landforms: Modern, Quaternary and Ancient. Geological Society, London, Memoirs, 46, 105-106. doi:10.1144/M46.21.~~Dowdeswell, J.A., Ottesen, D., Noormets, R., In Press. Submarine slides from the walls of Smeerenburgfjorden,~~

~~NW Spitsbergen. In Dowdeswell, J.A., Canals, M., Jakobsson, M., Todd, B.J., Dowdeswell, E.K., Hogan, K.A., (Eds), Atlas of Submarine Glacial Landforms: Modern, Quaternary and Ancient. Geological Society, London, Memoirs, 46.~~

Droz, L., Kergoat, R., Cochonat, P., Berné, S., 2001. Recent sedimentary events in the western Gulf of Lions (Western Mediterranean). Marine Geology 176, 23–37.

~~Dühnforth, M., Anderson, R.S., Ward, D., Stock, G.M., 2010. Bedrock fracture control of glacial erosion processes and rates. Geology 38, 423–426. doi:10.1130/G30576.1~~

Eagles, G., Larter, R.D., Gohl, K., Vaughan, A.P.M., 2009. West Antarctic Rift System in the Antarctic Peninsula. Geophysical Research Letters 36, doi:10.1029/2009GL040721, 2009.

Evans, J., Pudsey, C.J., Ó Cofaigh, C., Morris, P., Domack, E., 2005. Late Quaternary glacial history, flow dynamics and sedimentation along the eastern margin of the Antarctic Peninsula Ice Sheet. Quaternary Science Reviews 24, 741–774.

Fretwell, L.O. and 55 others, 2013. Bedmap2: improved ice bed, surface and thickness datasets for Antarctica. The Cryosphere 7, 375–393.

Fox, A.J., Cooper, A.P.R., 1998. Climate-change indicators from archival aerial photography of the Antarctic Peninsula. Annals of Glaciology 27, 636–642.

Funder, S., Kjeldsen, K.K., Kjaer, K.H., Ó Cofaigh, C., 2011. Chapter 50. The Greenland Ice Sheet during the past 300,000 years: a review. Developments in Quaternary Sciences 15, 699–713.

Gales, J.A., Larter, R.D., Mitchell, N.C., Dowdeswell, J.A., 2013. Geomorphic signature of Antarctic submarine gullies: Implications for continental slope processes. Marine Geology 337, 112–124.

García, M., Ercilla, G., Alonso, B., 2009. Morphology and sedimentary systems in the Central Bransfield Basin, Antarctic Peninsula: sedimentary dynamics from shelf to basin. Basin Research 21~~(3)~~.: 295–314.

~~Geirsdottir, A., Miller, G.H. and Larsen, D.J., 2016. Landforms in Hvitarvatn, central Iceland, produced by recent advances of surging and non-surging glaciers. In Dowdeswell, J.A. et al., (eds), Atlas of Submarine Glacial Landforms: Modern, Quaternary and Ancient. Geological Society, London, Memoirs, v. 46.~~

Geirsdóttir, Á., Miller, G.H., Wattrus, N.J., Björnsson, H., Thors, K., 2008. Stabilization of glaciers terminating in closed water bodies: Evidence and broader implications. Geophysical Research Letters 35, L17502, doi:10.1029/2008GL034432.

Geirsdottir, A., Miller, G.H., Larsen, D.J., 2016. Landforms in Hvitarvatn, central Iceland, produced by recent advances of surging and non-surging glaciers. In Dowdeswell, J.A., Canals, M., Jakobsson, M., Todd, B.J., Dowdeswell, E.K., Hogan, K.A., (eds), Atlas of Submarine Glacial Landforms: Modern, Quaternary and Ancient. Geological Society, London, Memoirs 46, 143-146. doi:10.1144/M46.108.

Gilbert, R., Nielsen, N., Möller, H., Desloges, J., Rasch, M., 2002. Glacimarine sedimentation in Kangerdluk (Disko Fjord), West Greenland, in response to a surging glacier. Marine Geology 191, 1–18.

Graham, A.G.C., Larter, R.D., Gohl, K., Hillenbrand, C.D., Smith, J.A., Kuhn, G., 2009. Bedform signature of a West Antarctic palaeo-ice stream reveals a multi-temporal record of flow and substrate control. Quaternary Science Reviews 28, 2774–2793.

Formatted: English (United States)

Formatted: English (United States)

Formatted: French (France)

Griffith, T., Anderson, J.B., 1989. Climatic control of sedimentation in bays and fjords of the northern Antarctic Peninsula. Marine Geology 85, 181–204.

Guglielmin, M., Convey, P., Malfasi, F., Cannone, N., 2007. Glacial fluctuations since the Medieval Warm Period at Rothera Point (Western Antarctic Peninsula). The Holocene 17, 1253–1258.

Heroy, D.C., Anderson, J.B., 2007. Radiocarbon constraints on Antarctic Peninsula Ice Sheet retreat following the Last Glacial Maximum (LGM). Quaternary Science Reviews 26, 3286–3297.

Hogan, K.A., Dowdeswell, J.A., Larter, R.D., Ó Cofaigh, C. and Bartholomew, I., 2016. Subglacial meltwater channels in Marguerite Trough, western Antarctic Peninsula. In Dowdeswell, J.A.-, Canals, M., Jakobsson, M., Todd, B.J., Dowdeswell, E.K., Hogan, K.A. (eds), Atlas of Submarine Glacial Landforms: Modern, Quaternary and Ancient. Geological Society, London, Memoirs, 46, 215-216. doi:10.1144/M46.178.et al., (eds), Atlas of Submarine Glacial Landforms: Modern, Quaternary and Ancient. Geological Society, London, Memoirs, v. 46.

Jakobsson, M., Macnab, R., Mayer, L., Anderson, R., Edwards, M., Hatzky, J., Werner Schenke, H., Johnson, P., 2008. An improved bathymetric portrayal of the Arctic Ocean: Implications for ocean modeling and geological, geophysical and oceanographic analyses. Geophysical Research Letters 35, L07602, doi:10.1029/2008GL033520.

Jamieson, S.S.R., Vieli, A., Livingstone, S.J., Ó Cofaigh, C., Stokes, C.R., Hillenbrand, C.-D. and Dowdeswell, J.A., 2012. Ice stream grounding-line stability on a reverse bed slope. Nature Geoscience, 5, 799–802.

Jamieson, S.S.R., Vieli, A., Cofaigh, C.Ó., Stokes, C.R., Livingstone, S.J., Hillenbrand, C.D., 2014. Understanding controls on rapid ice-stream retreat during the last deglaciation of Marguerite Bay, Antarctica, using a numerical model. Journal of Geophysical Research. Earth Surface 119, 247–263.

Johnson, A.C., 1997. Cenozoic tectonic evolution of the Marguerite Bay area, Antarctic Peninsula, interpreted from geophysical data. Antarctic Science 9, 268–280.

Johnson, M.D., Benediktsson, Í.Ö., Björklund, L., 2013. The Ledsjö end moraine-a subaquatic push moraine composed of glaciomarine clay in central Sweden. Proceedings of the Geological Association 124, 738–752.

Kaser, G., Cogley, J.G., Dyurgerov, M.B., Meier, M.F., Ohmura, A., 2006. Mass balance of glaciers and ice caps: Consensus estimates for 1961–2004. Geophysical Research Letters 33, L19501. doi:10.1029/2006GL027511

Kennedy, D.S., Anderson, J.B., 1989. Glacial-marine sedimentation and Quaternary glacial history of Marguerite Bay, Antarctic Peninsula. Quaternary Research 31, 255–276.

Kilfeather, A.A., Cofaigh, C.Ó., Lloyd, J.M., Dowdeswell, J.A., Xu, S., Moreton, S.G., 2011. Ice-stream retreat and ice-shelf history in Marguerite Trough, Antarctic Peninsula: Sedimentological and foraminiferal signatures. Bulletin of the Geological Society of America. 123, 997–1015.

Krabbendam, M., Eyles, N., Putkinen, N., Bradwell, T., Arbelaez-Moreno, L., 2016. Streamlined hard beds formed by palaeo-ice streams: A review. Sedimentary Geology, 338, 24–50. doi: 10.1016/j.sedgeo.2015.12.007.

Kuhn, G., Weber, M.E., 1993. Acoustical characterization of sediments by Parasound and 3.5 kHz systems: Related sedimentary processes on the southeastern Weddell Sea continental slope, Antarctica. Marine Geology 113, 201–217.

Laberg, J.S., Eilertsen, R.S., Vorren, T.O., 2009. The paleo-ice stream in Vestfjorden, north Norway, over the last 35 k.y.: Glacial erosion and sediment yield. Geological Society of America Bulletin 121, 434–447.

~~Salomonsen, G.R., Vorren, T.O., 2007. Submarine push moraine formation during the early Fennoscandian Ice Sheet deglaciation. Quaternary Research 67, 453–462.~~

Larter, R.D., Graham, A.G.C., Gohl, K., Kuhn, G., Hillenbrand, C.D., Smith, J.A., Deen, T.J., Livermore, R.A., Schenke, H.W., 2009. Subglacial bedforms reveal complex basal regime in a zone of paleo-ice stream convergence, Amundsen Sea embayment, West Antarctica. Geology 37, 411–414.

Livingstone, S.J., Ó Cofaigh, C., Hogan, K.A. and Dowdeswell, J.A., 2016. Submarine glacial-landform distribution along an Antarctic Peninsula palaeo-ice stream: a shelf-slope transect through the Marguerite Bay system (66° to 70°S). In Dowdeswell, J.A., Canals, M., Jakobsson, M., Todd, B.J., Dowdeswell, E.K., Hogan, K.A., (eds), Atlas of Submarine Glacial Landforms: Modern, Quaternary and Ancient. Geological Society, London, Memoirs, 46, 485-492. doi:10.1144/M46.180.~~Dowdeswell, J.A. et al., (eds), Atlas of Submarine Glacial Landforms: Modern, Quaternary and Ancient. Geological Society, London, Memoirs, v. 46.~~

Livingstone, S.J., Cofaigh, C.Ó., Stokes, C.R., Hillenbrand, C.-D., Vieli, A., Jamieson, S.S.R., 2013. Glacial geomorphology of Marguerite Bay Palaeo-Ice stream, western Antarctic Peninsula. Journal of Maps 9, 558–572.

Livingstone, S.J., Ó Cofaigh, C., Stokes, C.R., Hillenbrand, C.D., Vieli, A., Jamieson, S.S.R., 2012. Antarctic palaeo-ice streams. Earth-Science Reviews 111, 90–128.

Lowe, A.L., Anderson, J.B., 2002. Reconstruction of the West Antarctic ice sheet in Pine Island Bay during the Last Glacial Maximum and its subsequent retreat history. Quaternary Science Reviews 21, 1879–1897.

McLachlan, S.E., Howe, J.A., Vardy~~-~~, M.E., 2010. Morphodynamic evolution of Kongsfjorden, Svalbard, during the Late Weichselian and Holocene. In: Fowe, J.A., Austin, W.E.N., Forwick, M., Paetzel, M. (Eds.), Fjord Systems and Archives. Geological Society, London, Special Publications 344, 195–205.

Minzoni, R.T., Anderson, J.B., Fernandez, R., Wellner, J.S., 2015. Marine record of Holocene climate, ocean, and cryosphere interactions: Herbert Sound, James Ross Island, Antarctica. Quaternary Science Reviews 129, 239–259.

Mugford, R.I., Dowdeswell, J. A., 2011. Modeling glacial meltwater plume dynamics and sedimentation in high-latitude fjords. Journal of Geophysical Research. Earth Surface 116, 1–20.

Mulvaney, R., Abram, N.J., Hindmarsh, R.C.A., Arrowsmith, C., Fleet, L., Triest, J., Sime, L.C., Alemany, O, Foord, S., 2012. Recent Antarctica Peninsula warming relative to Holocene climate and ice-shelf history. Nature 489, 141–145. doi:10.1038/nature11391.

Nitsche, F.O., Gohl, K., Larter, R.D., Hillenbrand, C.-D., Kuhn, G., Smith, J.A., Jacobs, S., Anderson, J.B., Jakobsson, M., 2013. Paleo ice flow and subglacial meltwater dynamics in Pine Island Bay, West Antarctica. The Cryosphere 7, 249–262.

Noormets, R., Dowdeswell, J.A., Larter, R.D., Ó Cofaigh, C., Evans, J., 2009. Morphology of the upper continental slope in the Bellingshausen and Amundsen Seas – Implications for sedimentary processes at the shelf edge of West Antarctica. Marine Geology 258, 100–114.

Ó Cofaigh, C., Hogan, K.A., Dowdeswell, J.A., Strueff, K. 2016. Stratified glacimarine basin-fills in West Greenland fjords. In: Dowdeswell, J.A., Canals, M., Jakobsson, M., Todd, B.J., Dowdeswell, E.K., Hogan, K.A. (Eds), Atlas of Submarine Glacial Landforms: Modern, Quaternary and Ancient. Geological Society, London, Memoirs, 46, 99–100. doi:10.1144/M46.83.

~~Ó Cofaigh, C., Benetti, S., Dunlop, P. and Monteys, X. (in press). Arcuate moraines on the continental shelf northwest of Ireland. In: Dowdeswell, J.A., Canals, M., Jakobsson, M., Todd, B.J., Dowdeswell, E.K. & Hogan, K.A. (eds), Atlas of Submarine Glacial Landforms: Modern, Quaternary and Ancient. Geological Society, London. The Geological Society of London.~~

Ó Cofaigh, C., Davies, B.J., Livingstone, S.J., Smith, J.A., Johnson, J.S., Hocking, E.P., Hodgson, D.A., Anderson, J.B., Bentley, M.J., Canals, M., Domack, E., Dowdeswell, J.A., Evans, J., Glasser, N.F., Hillenbrand, C.D., Larter, R.D., Roberts, S.J., Simms, A.R., 2014. Reconstruction of ice-sheet changes in the Antarctic Peninsula since the Last Glacial Maximum. Quaternary Science Reviews 100, 87–110.

Ó Cofaigh, C., Dowdeswell, J. A., Allen, C.S., Hiemstra, J.F., Pudsey, C.J., Evans, J., Evans, D.J.A, 2005. Flow dynamics and till genesis associated with a marine-based Antarctic palaeo-ice stream. Quaternary Science Reviews 24, 709–740.

Ó Cofaigh, C., Dowdeswell, J.A., Evans, J., Larter, R.D., 2008. Geological constraints on Antarctic palaeo-ice-stream retreat. Earth Surface Processes and Landforms 33, 513–525.

Ó Cofaigh, C., Taylor, J., Dowdeswell, J.A., Rosell-Melé, A., Kenyon, N.H., Evans, J., Mienert, J., 2002. Sediment reworking on high-latitude continental margins and its implications for palaeoceanographic studies: insights from the Norwegian-Greenland Sea. Geological Society of London, Special Publications 203, 325–348.

~~Ó Cofaigh, C., Hogan, K.A., Dowdeswell, J.A., Strueff, K., 2016. Stratified glacimarine basin-fills in West Greenland fjords. In: Dowdeswell, J.A., Canals, M., Jakobsson, M., Todd, B.J., Dowdeswell, E.K., Hogan, K.A. (Eds), Atlas of Submarine Glacial Landforms: Modern, Quaternary and Ancient. Geological Society, London, Memoirs, 46.~~

Orsi, A. J., Cornuelle, B. D., Severinghaus, J. P., 2012. Little Ice Age cold interval in West Antarctica: Evidence from borehole temperature at the West Antarctic Ice Sheet (WAIS) Divide. Geophys. Res. Lett., 39, ~~L09710,~~ doi:10.1029/2012GL051260.

Ottesen, D., Dowdeswell, J.A., 2006. Assemblages of submarine landforms produced by tidewater glaciers in Svalbard. Journal of Geophysical Research. Earth Surface 111, 1–16. doi:10.1029/2005JF000330

Ottesen, D., Dowdeswell, J. A., 2009. An inter-ice-stream glaciated margin: Submarine landforms and a geomorphic model based on marine-geophysical data from Svalbard. Bulletin of the Geological Society of America 121, 1647–1665.

Ottesen, D., Dowdeswell, J.A., Benn, D.I., Kristensen, L., Christiansen, H.H., Christensen, O., Hansen, L., Lebesbye, E., Forwick, M., Vorren, T.O., 2008. Submarine landforms characteristic of glacier surges in two Spitsbergen fjords. Quaternary Science Reviews 27, 1583–1599.

Ottesen, D., Dowdeswell, J.A., Landvik, J.Y., Mienert, J., 2007. Dynamics of the Late Weichselian ice sheet on Svalbard inferred from high-resolution sea-floor morphology. Boreas 36, 286–306.

Ottesen, D., Rise, L., Knies, J., Olsen, L., Henriksen, S., 2005. The Vestfjorden-Traenadjupet palaeo-ice stream drainage system, mid-Norwegian continental shelf. Marine Geology 218, 175–189.

Payton, C.E., 1977. Seismic Stratigraphy: application to hydrocarbon exploration, AAPG-Memoir 26, AAPG, Tulsa.

Peck, V.L., Allen, C.S., Kender, S., McClymont, E.L., Hodgson, D.A., 2015. Oceanographic variability on the West Antarctic Peninsula during the Holocene and the influence of upper circumpolar deep water. Quaternary Science Reviews 119, 54–65.

Powell, R.D., 1990. Glacimarine processes at grounding-line fans and their growth to ice-contact deltas. Geological Society of London, Special Publication 53, 53–73.

Pudsey, C.J., Barker, P.F., Larter, R.D., 1994. Ice sheet retreat from the Antarctic Peninsula shelf. Continental Shelf Research 14, 1647–1675.

Radić, V., Hock, R., 2011. Regionally differentiated contribution of mountain glaciers and ice caps to future sea-level rise. Nature Geoscience 4, 91–94.

Rodrigo, C., Giglio,S., Varas, A., 2016. Glacier sediment plumes in small bays on the Danco Coast, Antarctic Peninsula. Antarctic Science 28, 395–404. doi:10.1017/S0954102016000237.

Rydningen, T.A., Vorren, T.O., Laberg, J.S., Kolstad, V., 2013. The marine-based NW Fennoscandian ice sheet: Glacial and deglacial dynamics as reconstructed from submarine landforms. Quaternary Science Reviews 68, 126–141.

Shevenell, A., Domack, E.W., Kernan, G., 1996. Record of Holocene paleoclimate change along the Antarctic Peninsula: evidence from glacial marine sediments, Lalle~~a~~mand Fjord. Papers and Proceedings of the Royal Society of Tasmania. 130, 55–64.

Simms, A.R., Milliken, K., Anderson, J.B., Wellner, J.S., 2011. The marine record of deglaciation of the South Shetland Islands, Antarctica since the Last Glacial Maximum. Quaternary Science Reviews 30, 1583–1601.

Smith, J.A., Hillenbrand, C.D., Larter, R.D., Graham, A.G.C., Kuhn, G., 2009. The sediment infill of subglacial meltwater channels on the West Antarctic continental shelf. Quaternary Research 71, 190–200.

Spagnolo, M., Phillips, E., Piotrowski, J.A., Rea, B.R., Clark, C.D., Stokes, C.R., Carr, S.J., Ely, J.C., Ribolini, A., Wysota, W., Szuman, I., 2016. Ice stream motion facilitated by a shallow-deforming accreting bed. Nature Communications, doi: 10.1038/ncomms10723.

Syvitski, J.P.M., 1989. On the deposition of sediment within glacier-influenced fjords: oceanographic controls. Marine Geology 85, 301–329.

Todd, B.J., Shaw, J., 2012. Laurentide Ice Sheet dynamics in the Bay of Fundy, Canada, revealed through multibeam sonar mapping of glacial landsystems. Quaternary Science Reviews 58, 83–103.

Vaughan, D., Marshall, G., Connolley, W.M., Parkinson, C., Mulvaney, R., Hodgson, D.A., King, J.C., Pudsey, C.J., Turner, J., 2003. Recent Rapid Regional Climate Warming on the Antarctic Peninsula. Climatic Change 243–274.

Formatted: Spanish (Spain, International Sort)

Formatted: English (United States)

Veeken, P.C.H., 2007. Seismic Stratigraphy, Basin Analysis and Reservoir ~~characterisation~~ Characterisation Elsevier, Amsterdam.

Wellner, J.S., Heroy, D.C., Anderson, J.B., 2006. The death mask of the ~~antarctic~~ Antarctic ice sheet: Comparison of glacial geomorphic features across the continental shelf. Geomorphology 75, 157–171.

Wellner, J.S., Lowe, A.L., Shipp, S.S., Anderson, J.B., 2001. Distribution of glacial geomorphic features on the Antarctic continental shelf and correlation with substrate: Implications for ice behavior. J. Glaciology 47, 397–411.

Williams, R.S., Ferrigno, J.G., Swithinbank, C., Lucchitta, B.K., Seekins, B.A., 1995. Coastal-change and glaciological maps of Antarctica. Annals of Glaciology 21, 284–290.

Figures and Tables captions

Figure 1. Study area, in Marguerite Bay, Antarctic Peninsula (A). (B) Palaeo-ice streams of the Antarctic Ice Sheet during the last glacial period around the Antarctic Peninsula, from Livingstone et al. (2012). MB P-IS: Marguerite Bay palaeo-ice stream; (~~B~~C) Regional topographic map of Marguerite Bay (data from the Marine Geoscience Data System; http://www.marine-geo.org). Neny and Lallemand Fjords, located in neighbouring areas of the Antarctic Peninsula are shown. (~~C~~D) Bathymetry of Bourgeois Fjord on the Pacific side of the Antarctic Peninsula. The limits of glaciers on Graham Land and the islands have been mapped from the LIMA satellite-image mosaic provided by the USGS EROS Center. The map shows the location of the *Isis* ROV dive in Blind Bay, off Forel Glacier and the bathymetry of the main and outer Bourgeois Fjord from our multibeam data.

Figure 2. Acoustic facies characterization, distribution and interpretation. Selected TOPAS profiles are shown to illustrate the acoustic character of each echo-type: non-penetrative, transparent-chaotic and stratified. Descriptions and interpretations are given, and follow the criteria first proposed by Damuth (1980) and further developed by Kuhn and Weber (1993) and Droz et al. (2001).

Figure 3. Morphological characterization of the main Bourgeois Fjord and shallow areas off the tidewater glaciers draining into it. (A) Multibeam bathymetry. (B) Distribution of submarine landforms. (C) Bathymetric profile along the main fjord illustrating the seafloor relief along the proximal, central and distal sectors. (D) Transverse escarpments and basins. (E). Smooth sedimentary basins and bedrock channels. (F) Elongate features and streamlined lineations.

Figure 4. Morphological characterization of outer Bourgeois Fjord. (A) Location map. (B) Distribution of submarine landforms inferred from multibeam bathymetry data. (C) to (E) Detailed bathymetric mosaics illustrating the morphological characteristics of channels, streamlined features and smooth basins identified in the outer fjord (located in B).

Figure 5. Morphological characterization of the inner sector of Blind Bay, showing the distribution of submarine landforms based multibeam bathymetry data. (A) Swath-bathymetric mosaic of Blind Bay. (B) Landform distribution, including channels, transverse ridges and distal wedges. (C) Oblique view of inner Blind Bay with landforms labeled. (D) TOPAS sub-bottom acoustic profile along the inner sector of Blind Bay (located in B).

Figure 6. Morphological characterization of the inner sector of Blind Bay, based on the *Isis* ROV high-resolution multibeam imagery. (A) Bathymetric mosaic and interpretation (located in Fig. 6A). (B) and (C) Detailed sections showing the bathymetry, gradient-slope direction and gradient of the area characterized by finger-like ridges and lineations. (D) Bathymetric profiles displaying the morphology of the ridges and lineations (axes in m).

Figure 7. ROV-acquired photographs of the seafloor along a transect in the inner sector of Blind Bay (locations of photographs shown in A). (B) Photographic transect from ice-proximal (Photo 1) to distal positions (Photo 3) along the inner part of Blind Bay. (C) Photographs illustrating the erosional character of the proximal area (Photo 4) and the morphological crests in the distal area representing finger-like ridges and lineations (Photos 5 and 6).

Figure 8. (A) Regional map of Marguerite Bay showing the landforms assemblage as discussed in this work, integrated with the results from Dowdeswell et al. (2004), Ó Cofaigh et al. (2005) and Livingstone et al. (2013). (B) to (H) Greyscale seafloor bathymetric models (see location in (A)) showing the detailed characteristics and distribution of the landforms. Regional b~~B~~athymetric data have been obtained from the Marine Geoscience Data System (http://www.marine-geo.org).

Figure 9. Spatial distribution of the submarine landforms composing the four morpho-sedimentary systems in Bourgeois Fjord. (A) Glacial advance and full-glacial; (B) Subglacial and ice-marginal meltwater ; (C) Glacial retreat and neoglaciation; and (D) Holocene mass-wasting.

975 Figure 10. Variations in the locations of tidewater-glacier margins between 1947 to 2011, inferred from
976 maps, aerial photographs and satellite images. The figure illustrates the different trends in terminus
977 fluctuations different tidewater glaciers draining into Bourgeois Fjord.
978
979 Table I. Morphological characteristics and interpretations of the landforms observed in Bourgeois Fjord.
980
981 Table II. Morphological and physiographic parameters of the tidewater glaciers draining into Bourgeois
982 Fjord (located in Figure 1).

Table I. Landforms

Morpho-sedimentary system	Landform (legend in Figures 4 to 6)		Morphology	Maximum size	Distribution	Interpretation
Glacial advance and full-glacial system		Transverse escarpments	N-S- to NW-SE-oriented ridges with steepest north walls	2.5 km long, 10 m high	Inner Blind Bay and main fjord seafloor	Bedrock ridges plucked by advancing ice under the regional tectonic fabric control
		Elongate/ crag-and-tail features	Irregular to elongate highs, parallel to fjord long-axis	5 km long, 1.5 km wide, 80 m high. Elongation ratio increases basinward	Main fjord flat floor and outer fjord	Drumlin-shaped and whaleback bedrock features, eroded by active ice
		Lineations	Elongate ridges parallel to the fjord trend	3 km long, few m wide, 1 m high	Distal main fjord seafloor	Glacial lineations shaped by active ice flow on glacial sediment/ iceberg ploughmarks
Subglacial ice-marginal meltwater system		Near fjord-wall channels	Dendritic pattern of diverging channels	500 m long, 80 m wide, 35 m deep	Near fjord-wall in inner sector of Blind Bay	Channelization of the meltwater from the Forel Glacier front and subglacial meltwater
		Basins	Flat basins with N-S- to NE-SW	5 km long, 1.5 km wide	Blind Bay, main and outer fjord	Sediment-filled basins fed by meltwater channels and sediment rain-out
		Channels	Irregular channels in a dendritic convergent pattern	4 km long, 300 m wide, 35 m deep	Blind Bay, main and outer fjord	Meltwater channels eroded in bedrock
Glacial retreat and neoglaciation system		Distal transverse ridge	Stacked wedges with asymmetric profile	500 m wide (width of the inner bay), step 40-70 m high	Basinward limit of inner sector of Blind Bay	Sedimentary wedges deposited at relatively stable grounding-zone
		Crescent-shaped ridges	Crescent-shape wedge morphology delimiting flat areas	0.5-1.7 km long, 0.3-0.9 km wide, 25 m high	Seafloor of inner sector of Blind Bay	Frontal push moraines ridges, deposited during still-stands or re-advances of a retreating tidewater glacier
		Longitudinal ridges	Straight ridges oblique to the fjord trend	1.2 km long, 10 m high	Seafloor of inner sector of Blind Bay	Lateral push moraines ridges, deposited during still-stands or re-advances of a retreating tidewater glacier
		Finger-like ridges & lineations	Irregular, elongate and finger-shaped ridges with N-S- to NNE-SSW-oriented lineations	1 km long, 5-50 m wide, 5 m high	Seafloor of inner sector of Blind Bay	Push ridges of readvancing filaments of a tidewater glacier terminus
Holocene mass-wasting system		Scarps	Straight to arcuate scarps	0.5 km wide, tens of meters high	Walls of main Bourgeois Fjord	Slide scars resulting from mass-wasting processes from steep fjord walls
		Debris lobes	Elongate lobe-shaped deposits	5-20 m high, 100-200 m wide, 500 m long	Walls of main fjord, off Barnes Glacier front	Mass-wasting deposits from steep fjord walls

Table II. Tidewater glaciers

Glacier	Drainage size (km^2)	Average width (km)	Average pro-glacial area water depth (m)	Average slope of pro-glacial area (º)	Range of coastline variation (km)
Lliboutry	110	2.3	350	4.7	0.6
Perutz	380	3.2	320	7.8	1.0
Bader	35	0.9	620	15	1.3
Barnes	150	1.4	500	12	1.5
Forel	55	1.9	250	-0.2 (reverse)	2.7

Fig 1. Study Area and methods

Click here to download high resolution image

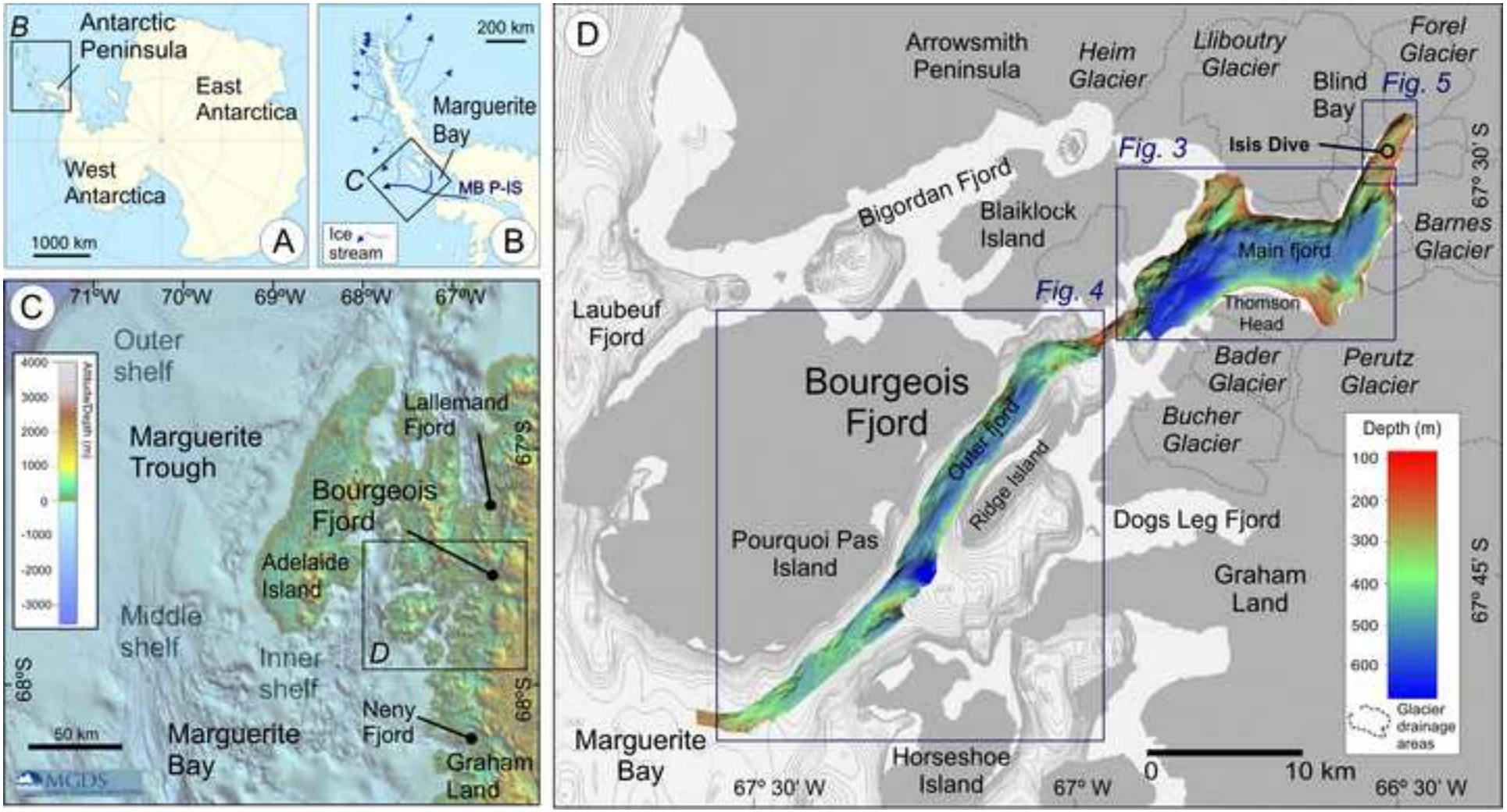

Figure 2. Echotypes

Click here to download high resolution image

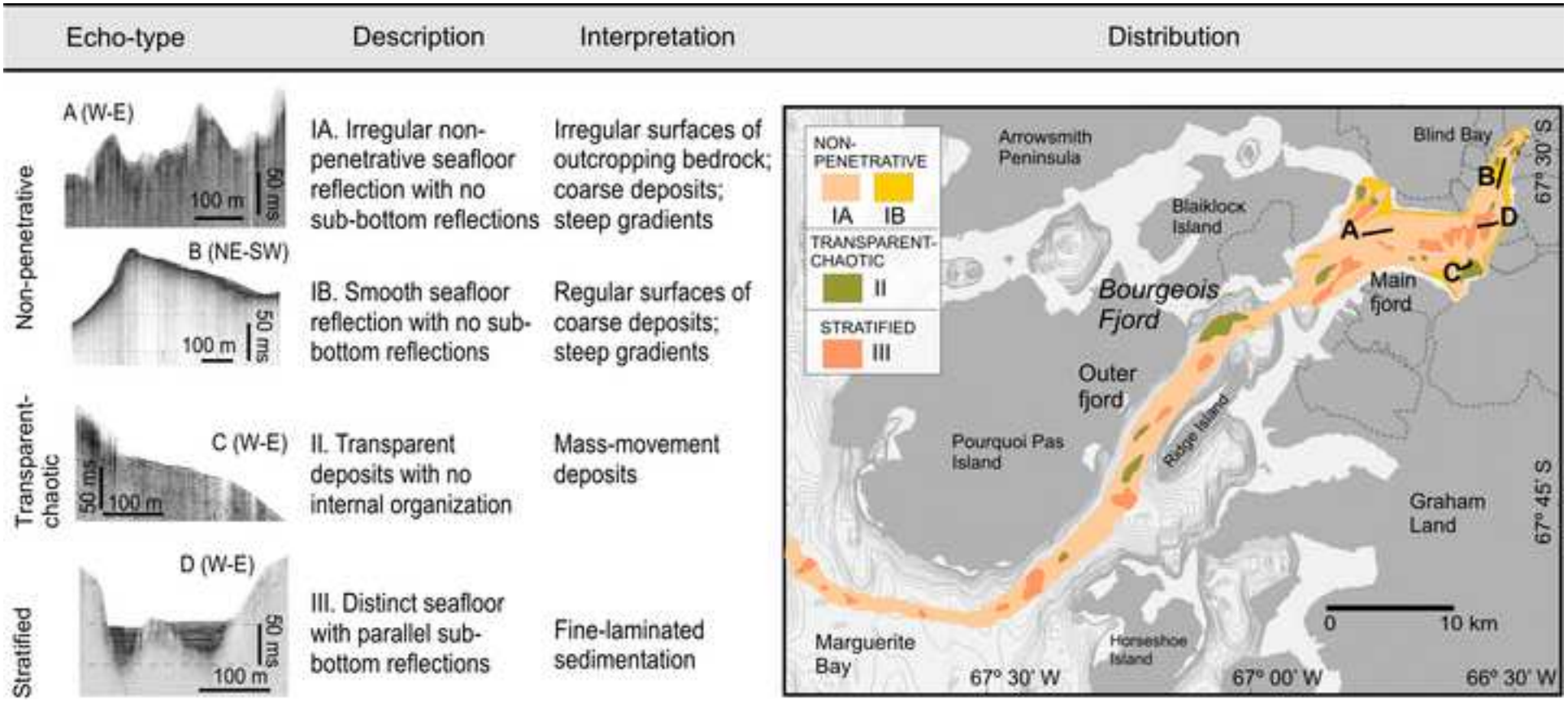

Figure 3. Main fjord

Click here to download high resolution image

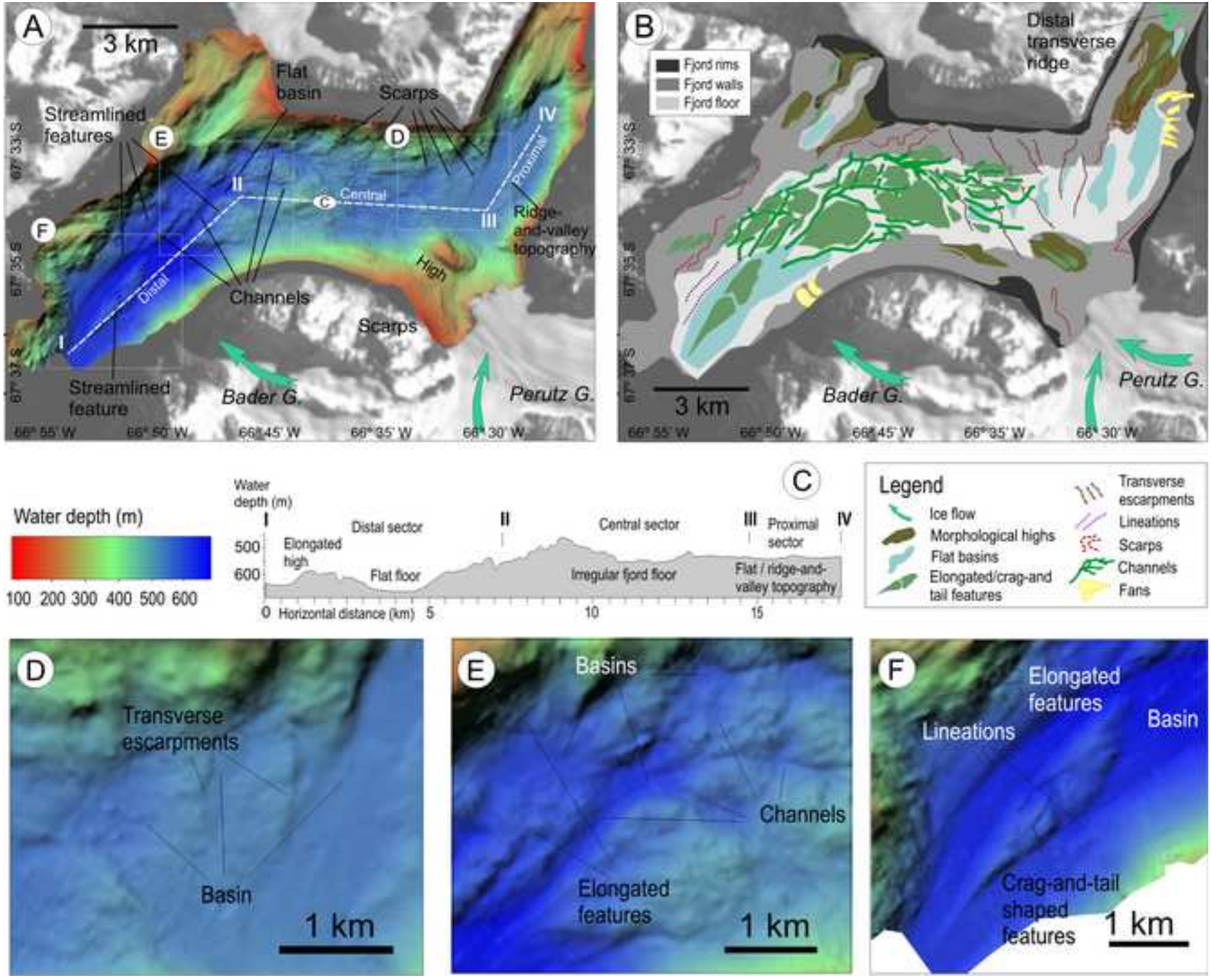

Figure 4. Outer fjord

Click here to download high resolution image

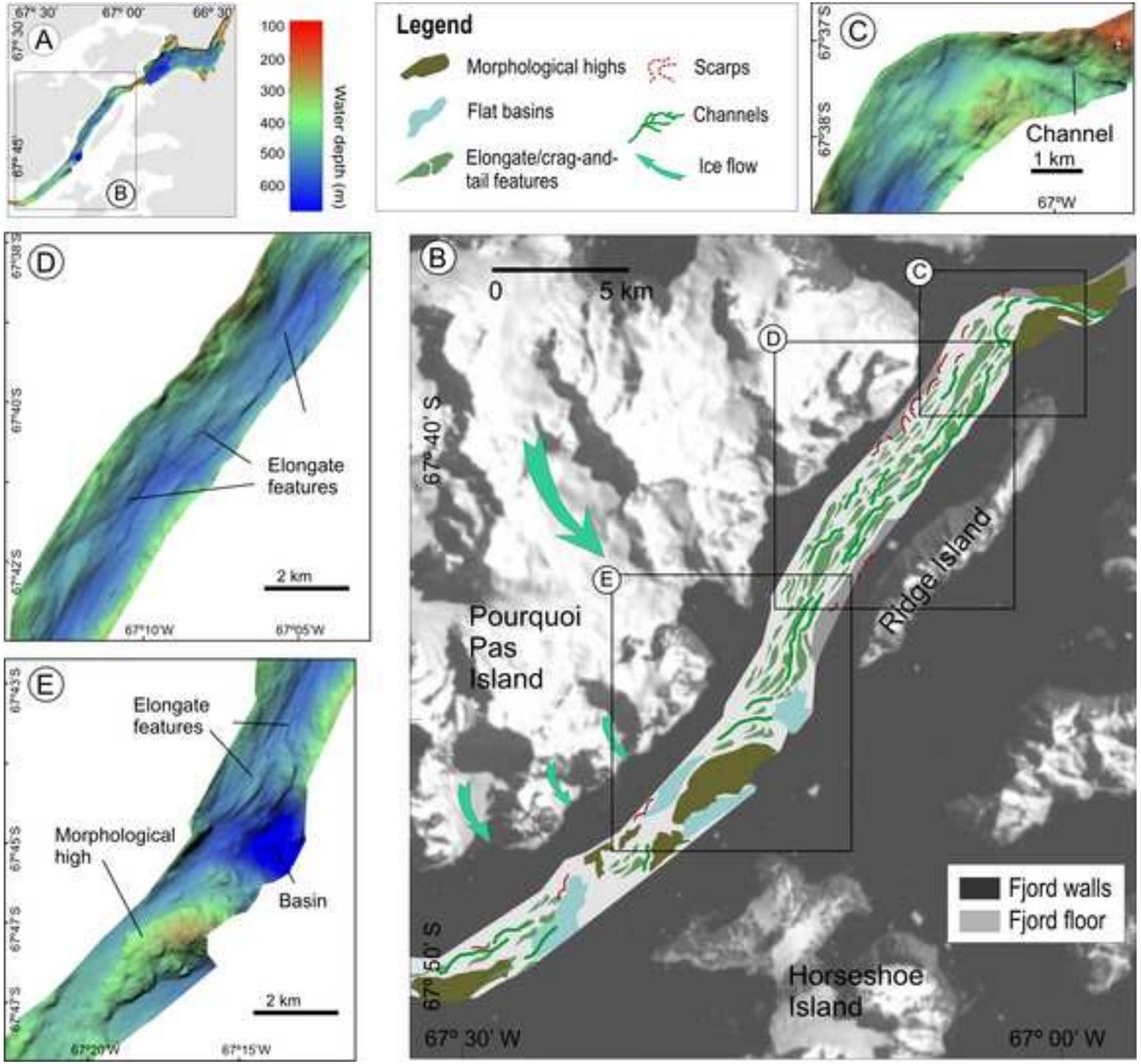

Figure 5. Morphology of Blind Bay

Click here to download high resolution image

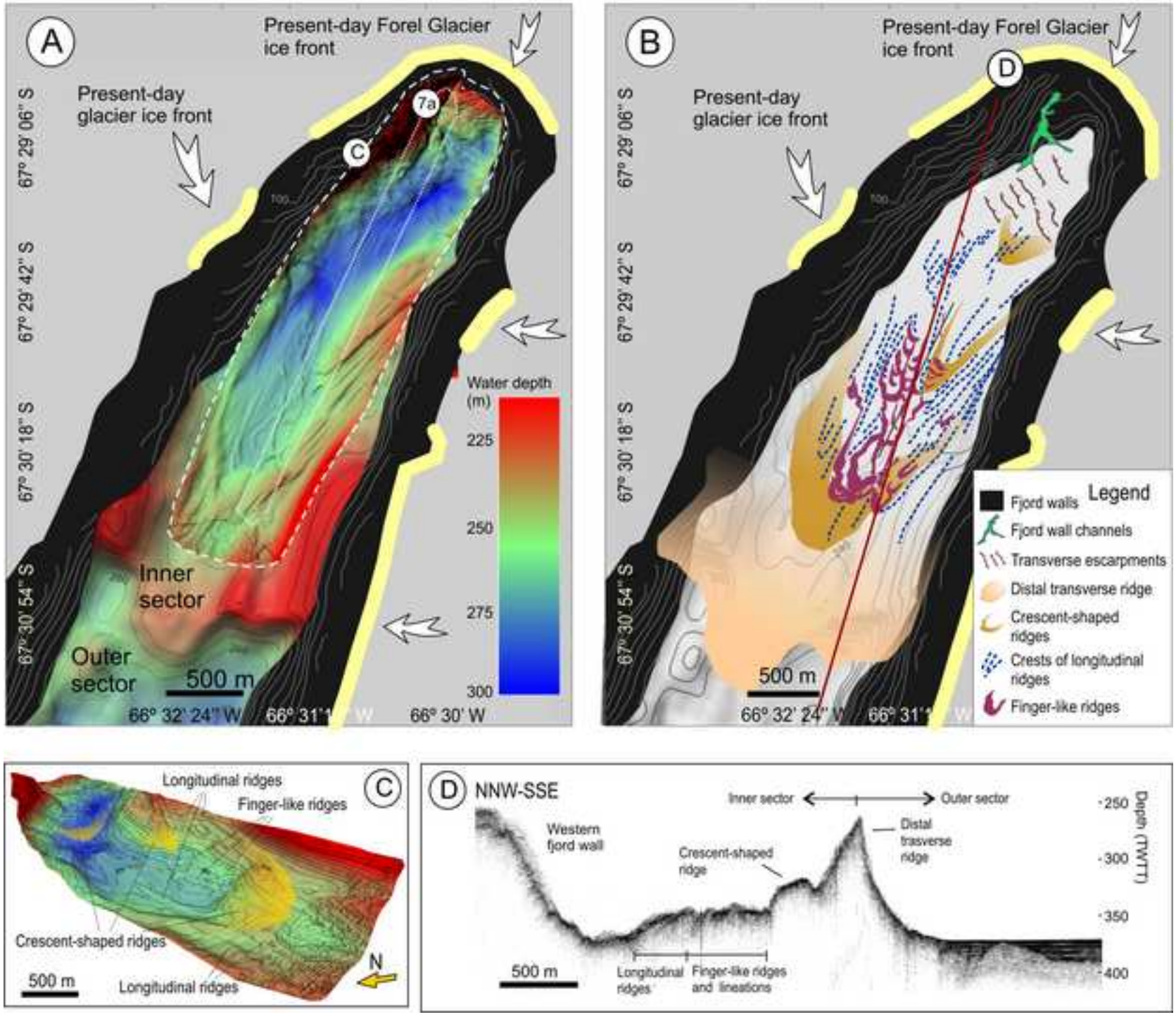

Figure 6. Lineations and ridges in Blind Bay
Click here to download high resolution image

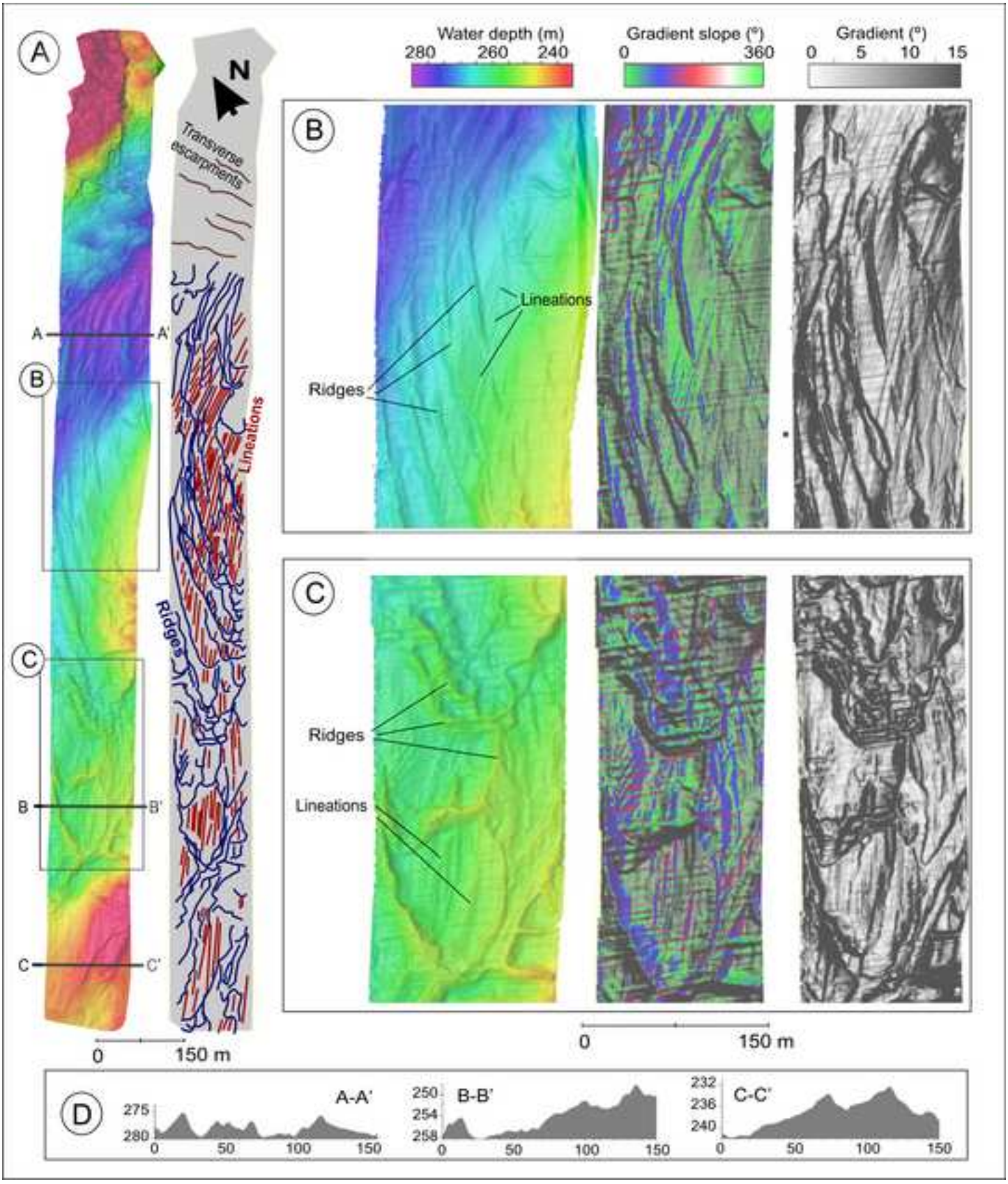

Fig 7. Photos

Click here to download high resolution image

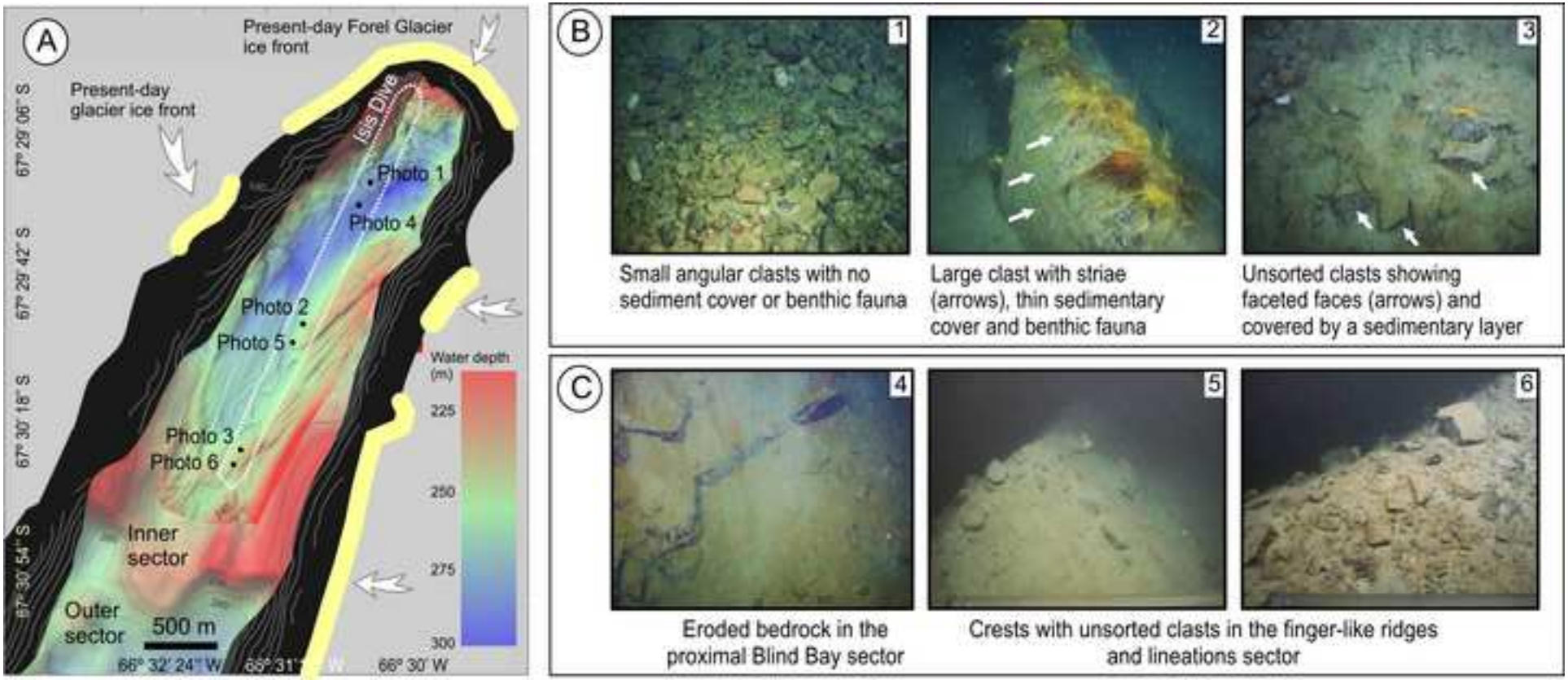

Figure 8. Landforms in Marguerite Bay
Click here to download high resolution image

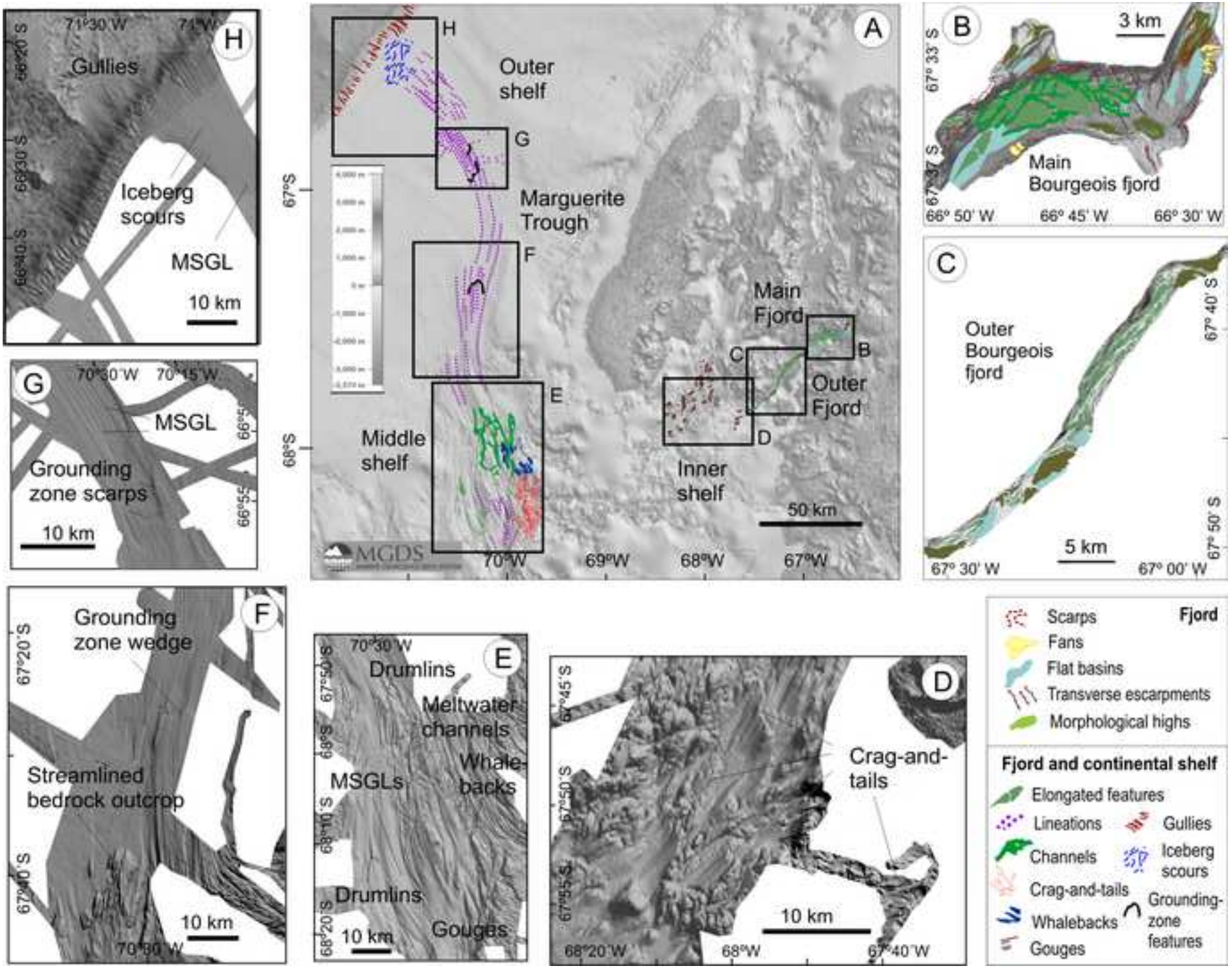

Figure 9. Morphosedimentary systems
Click here to download high resolution image

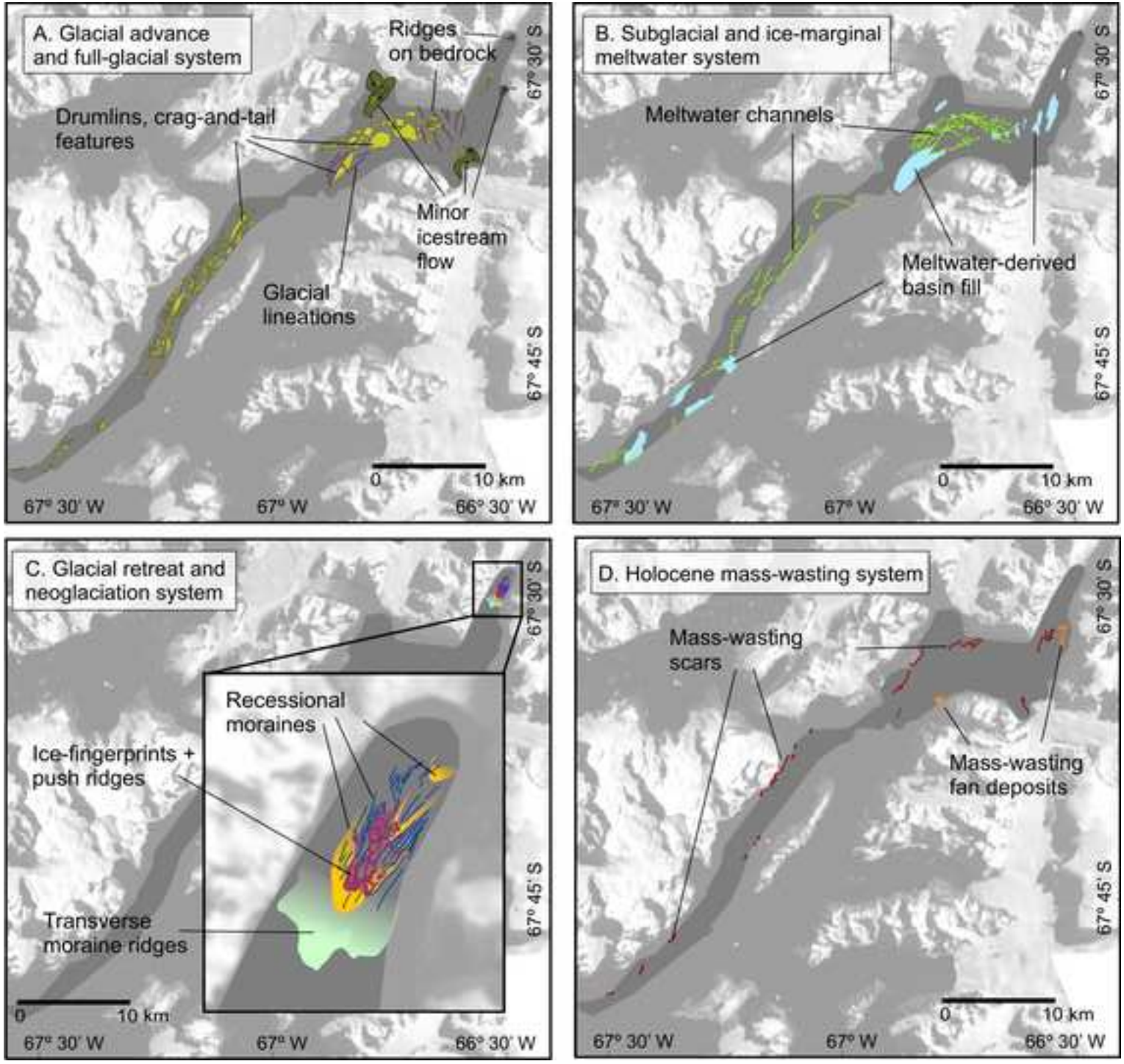

Figure 10. Tidewater glaciers coastlines
Click here to download high resolution image

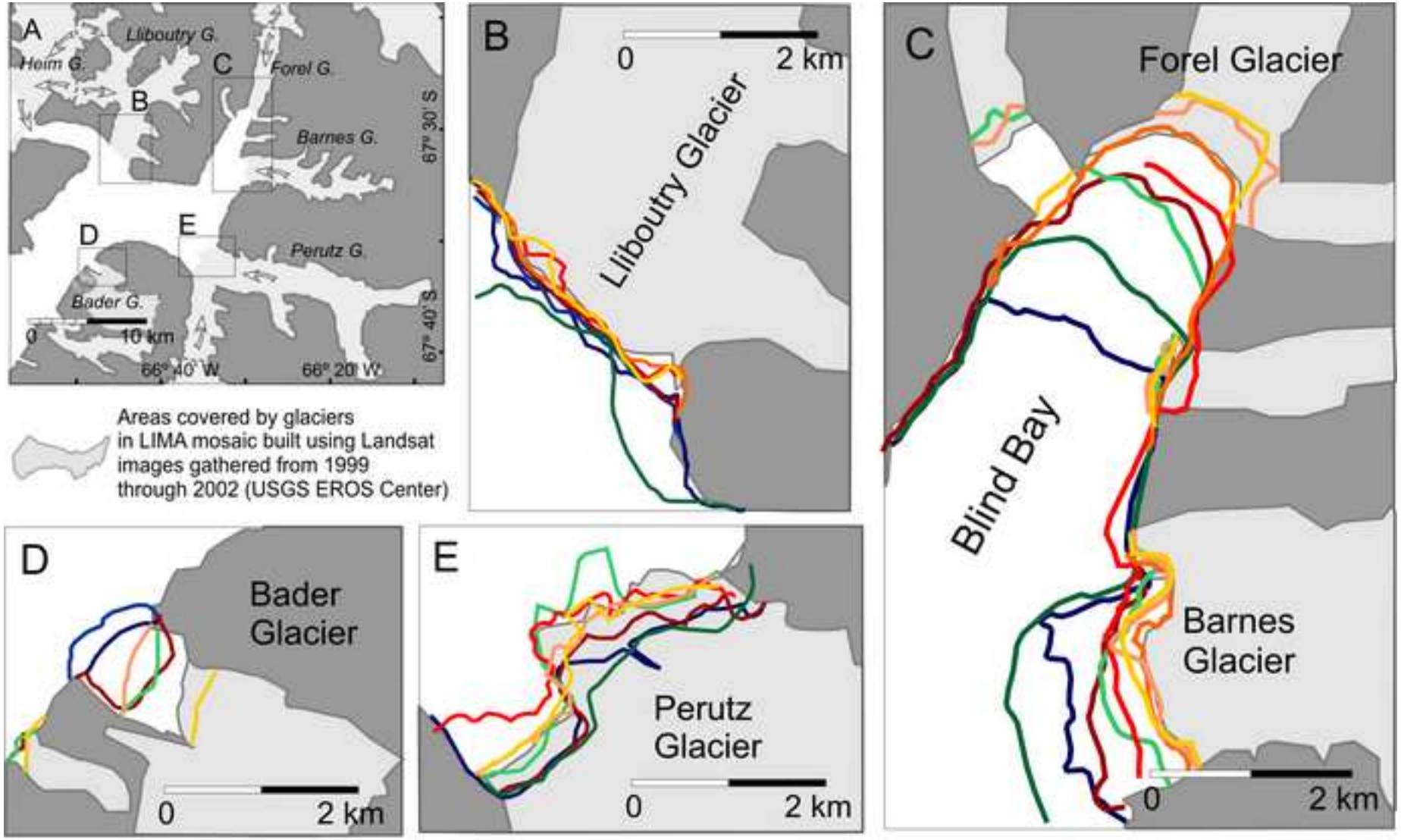

	Drainage size (km^2)	Range of coastline variation (m)
Perutz Glacier	380	1000
Barnes Glacier	150	1500
Lliboutry Glacier	110	600
Forel Glacier	55	2700
Bader Glacier	35	1300

HIGHLIGHTS

Paper Title: Geomorphic and shallow-acoustic investigation of an Antarctic Peninsula fjord system using high-resolution ROV and shipboard geophysical observations: ice dynamics and behavior since the Last Glacial Maximum

Marga García et al.

- We present a detailed study of landforms from Bourgeois Fjord to Marguerite Bay
- Landforms from the inner fjord (Blind Bay) to the shelf-edge are genetically linked
- The outer and main fjord underwent a relatively rapid and continuous deglaciation
- Blind Bay records recent glacial readvances, probably related to the Little Ice Age
- Tidewater glaciers have generally retreated in the last decades, but not homogeneously

Re manuscript: JQSR-D-16-00430

Title: Geomorphic and shallow-acoustic investigation of an Antarctic Peninsula fjord system using high-resolution ROV and shipboard geophysical observations: ice dynamics and behavior since the Last Glacial Maximum

Authors: Marga Garcia; Julian A. Dowdeswell, Riko Noormets, Kelly A. Hogan, Jeffrey Evans, Colm Ó Cofaigh, Rob D. Larter

Corresponding author: Dr. Marga Garcia. m.garcia@csic.es; marguita.garcia@gmail.com

General Comments to Editors and Reviewers

We acknowledge the kind comments of the editor and reviewers, and their suggestions which have contributed to improve the manuscript, regarding the clarity, scientific content and bibliographic references.

After the corrections and suggestions of the Editor and Reviewers we have revised the manuscript and figures. We are attaching the following documents:

- Revision Notes
- Marked manuscript
- A clean version of the revised manuscript.
- New versions of Figures 1 and 7.

We explain the changes we have made to the revised manuscript using the line numbers from the *revised version with changes marked*. We have also had a chance to revise and update the Reference List.

We also would like to add one more co-author, R.D. Larter (British Antarctic Survey). He was not included in the original list by a mistake. He was one of the PIs on the original AUV Grant, which allowed the execution of the JR-157 of RRS James Clark Ross cruise. He was involved in the data acquisition and processing and has contributed to the discussions included in this manuscript.

Comments to Reviewer 1 (Prof. J.B. Anderson)

1. *I found the following statement in the Discussion to be confusing. "The morphological evidence in this area reflects the imprint of the palaeo-ice stream advance, in a similar manner to the neighbour area of Gerlache Strait continental shelf, dominated by streamlined subglacial bedforms (Evans et al., 2004; Canals et al., 2016)."*
   I don't think that the authors are implying that an ice stream filled the fjord, but it sounds this way. I recommend clarification by stating that this is an outlet glacier that may have contributed

to an ice stream, but even that is not clear. It appears to me that it drained into two different systems. I think it might be good to discuss regional drainage a bit more, perhaps even include a figure of the Livingstone et al. drainage map for the area showing how the study area fits into the bigger glacial drainage system.

We have modified the text to avoid confusion between ice stream and grounded ice (Line 462). We have included a reference to the larger scheme of glacial drainage in Marguerite Bay at the end of the paragraph (Lines 475-478), and modified Figure 1 to illustrate the drainage areas, after Livingstone et al. (2012) (Lines 921-923; Figures and Tables captions).

2. *The authors imply that the rapid deglaciation of the fjord is unusual. I would argue that it is the norm as most AP fjords are overdeepened and are dominated by advance, as opposed to retreat, features (e.g. see Minzoni et al., 2015, QSR 129, 239-259 and Simms et al., 2011, QSR 30, 1583-1601 for examples). However, it is true that more shallow fjords appear to bear a record of retreat, including what appear to be LIA re-advance and retreat features (see for example Wolfl et al.,2016, Antarctic Science doi:10.1017/S0954102016000262).*

   We have included references to other fjords in the AP, as suggested, to clarify that rapid deglaciation is also recorded in neighboring areas (Lines 488-490). Regarding the work by Wolfl et al. (2016), it actually concludes that the re-advance that caused moraine deposition in Potter Cove occurred between 2.6 and 1.6 cal kyr BP, therefore preceding the LIA.

3. *I am surprised that there is no mention of the Antarctic Peninsula ice core results (Mulvaney et al., 2012, Nature 7414, 141-144 and its bearing on the LIA.*

   We have included this issue in the Introduction (Lines 49-52) and also used this work and references within to expand the discussion on recent rapid warming in the AP (Lines 127-131 and 520-524).

Comments to Reviewer 2

1. *With regard to discussion of Little Ice Age readvances of this system, a reference the authors should add: Christ, A., Talaia-Murray, M., Domack, E., Leventer, A., Lavoie, C., Brachfeld, S., Yoo, K.-C., Gilbert, R., Jeong, S.-M., Wellner, J., 2014. Late Holocene glacial advance and ice shelf growth in Barilari Bay, Graham Land, West Antarctic Peninsula, Geological Society of America Bulletin, doi:10.1130/B31035.1. In particular, take a look at figures 8a, a schematic of the LIA advance in Barilari Bay, just a little to the north of Bourgeois Fjord, and Figure 9, which summarizes southern hemisphere data relevant to the LIA.*

We have used this suggested reference to expand the description of the Little Ice Age events regarding its chronology and spatial impact in the Antarctic Peninsula and the Southern Pacific and Atlantic regions (Lines 127-131). We have also included the information from a recent paper on sedimentation in Marguerite Bay during the Holocene (Peck et al., 2015; Lines 118-123)

2. *My second comment is with regard to lines 110-113 and the discussion of the Bentley et al 2011 paper (not in reference list, but assuming this is QSR, Rapid deglaciation of Marguerite Bay?). Meltwater pulse 1-a is not at 9.6 ka, and my take from the text of Bentley et al 2011 is that the 14.2 ka retreat from the outer shelf is what they suggest might be linked to Meltwater pulse 1-a.*

   We have corrected this mistake with the age of the Meltwater pulse 1-a (Lines 115-117) and included the reference for Bentley et al. (2011) in the reference list.

Other changes

We have added some references to complete the introductory and discussion sections.

Some corrections on a series of parameters in the data acquisition have been made in the Methodology section

We have changed the term 'boulder' for the more generic 'clast', since we are not implying a specific clast size. The term is changed both in the manuscript and in Figure 7.